Power and Performance Trade-off in DS-CDMA Receivers Based on Adaptive LMS-MMSE Multi-user Detector

Qingsheng Wang
University of Natal
2003

Submitted in fulfillment of the academic requirements for the degree of MScEng in the School of Electrical, Electronic and Computer Engineering, University of Natal, South Africa, June 2003

ABSTRACT

Third generation cellular communication systems based on CDMA techniques have shown great scope for improvement in system capacity. Over the last decade, there has been significant interest in DS-CDMA detectors. The conventional detector, the optimal detector and a number of sub-optimal multi-user detectors (MUD) have been extensively analyzed in the literature. Recently, the reduction of power consumption in DS-CDMA systems has also become another important consideration in both system design and in implementation. In order to support wireless multimedia services, all CDMA-based systems for third generation systems have a large bandwidth and a high data rate, therefore the power consumed by the digital signal processor (DSP) is high. This thesis focuses on power consumption in the adaptive Minimum Mean Square Error (MMSE) detector which is based on the Least Mean Square (LMS) algorithm.

This thesis presents a literature survey on MUD and adaptive filter algorithms. A system model of the quantized LMS-MMSE MUD is proposed and its performance is analyzed. The quantization effects in the finite precision LMS-MMSE adaptive MUD including the steady-state weight covariance, mean square error (MSE) and bit error rate (BER) versus wordlength of data and coefficient are investigated when both the data and filter coefficients are quantized. The effects of wordlength size on power consumption are investigated and the tradeoff between the power consumption and performance degradation and the optimal allocation of bits to data and to LMS coefficients under power constraint is presented.

PREFACE

The research work in this dissertation was performed by Qingsheng Wang, under the supervision of Professor Fambirai Takawira, at the University of Natal's school of Electrical, Electronic and Computer Engineering. Parts of this dissertation have been presented by the author at the SATNAC'01 conference in Wild Coast, Natal, South Africa. The entire dissertation, unless specifically indicated to the contrary in the text, is the author's own work and has not been submitted in whole or in part to any other university.

As the candidate's supervisor, I have approved this thesis for submission.

Signed: _____ Name: _____ Date: _____

ACKNOWLEDGEMENTS

I would like to give a special thanks to Professor Fambirai Takawira for his help, guidance and patience as my supervisor over the last two years.

Thanks are also owed to Telkom SA, Alcatel SA Telecoms, THRIP and the University of Natal for their sponsorship of the Centre of Excellence in Radio Access Technologies at the School of Electrical, Electronic and Computer Engineering. Without their financial support, this degree would not have been possible.

Thanks also go to Dr. Xu and my postgraduate colleagues at the Centre for providing assistance for the past two years. They have made the past two years an enjoyable and memorable experience.

Finally, I wish to thank my family. I am forever indebted to them for their love, support and encouragement during the period of my study.

Table of Contents

List of Tables & Figures

Chapter 2

Chapter 3

Chapter 4

Chapter 5

List of Symbols

K	Number of users
L	Number of resolvable channel paths.
$s_k[t]$	Spreading sequence of the k^{th} user
b_k	The data bits of the k^{th} user.
P	The total number of symbols transmitted by each user
L	Number of resolvable channel paths.
$s_k[t]$	Spreading sequence of the k^{th} user
T_c	The chip duration
f_c	The carrier frequency in Hertz
A_k	The k^{th} user's transmitted amplitude
θ_k	Phase shift of the k^{th} user's carrier frequency.
$r(t)$	Received signal.
$\beta_{k,l}$	Attenuation factor of the k^{th} user's l^{th} path
$\tau_{k,l}$	The propagation delay
$n(t)$	The complex zero mean additive white Guassian noise
$\mathbf{r}$	The input sample vector
$\mathbf{S}$	The sampled spreading sequence matrix
$\mathbf{C}$	The sampled user's channel coefficient
$\mathbf{b}$	Vector of the data bits for all users
$\mathbf{n}$	Noise samples vector
$\mathbf{y}_k$	The output of the matched filter
$\mathbf{R}$	The cross-correlation matrix of users' spreading sequences
$\mathbf{z}$	Gaussian random vector with zero mean
$\boldsymbol{\sigma}$	The variance of additive white Guassian noise

$\hat{b}_k$	Hard decision for the k^{th} user
$\rho_{i,k}$	The correlation value between the users' spreading sequences
$E[\overline{\eta}_k]$	The average optimal near-far resistance
$d_{k,\min}$	Minimum distance between two multi-users signals that differ in the Received signal.
η_k	The optimal asymptotic multi-user efficiency
ε	The error vector between the transmitted data and hard decision.
$\left[\mathbf{R}^{-1}\right]_{p,K}$	The diagonal element of $\mathbf{R}^{-1}$ corresponding to the p^{th} bits of k^{th} user
$\mathbf{W}$	The linear map of the MMSE detector
β_k	The k^{th} user interferer to the decision statistic of the desired user 1
$\mathbf{L}$	The linear map of the Polynomial Expansion detector
w_i	The Polynomial coefficients for Polynomial Expansion detector
$\mathbf{F}$	The lower triangular matrix
$\mathbf{M}$	The coefficients of post-combining MMSE detector
$\nabla(t)$	The gradient vector
μ	The step-size parameter of LMS algorithm
P_r	The power of input signal
γ	The forgetting factor.
$e(p)$	The error between the desired signal and its estimates
$\mathbf{w}_{fixed}$	Fixed components of coefficients of the adaptive MMSE detector
$\mathbf{x}_{k,l}(p)$	Adaptive components of coefficients of the adaptive MMSE detector
$\Delta\mathbf{w}_k$	The difference between the actually computed filter coefficients and optimal filter coefficients
λ_{max}	The maximum eigenvalue
$\mathbf{z}_k(p)$	The decision variable
$M_{vv^H\|\mathbf{b}_k(p)}$	The covariance matrix of the vector v
λ_i	The eigenvalues of the matrix $M_{vv^H\|\mathbf{b}_k(p)}$

$d_{k,l}(p)$	The reference signal
Q_d	A quantizer for all the data
Q_c	A quantizer for all the coefficients
δ_c^2	The variance of complex white noise from Q_c
δ_d^2	The variance of complex white noise from Q_d
$\phi_{k,l}(p)$	The noise for quantization of channel coefficients
$\varphi(p)$	The noise for quantization of input data
$\kappa_{k,l}(p)$	The noise for quantization of the output of the filter
$\vartheta_{k,l}(p)$	The noise for quantization of decision variable
$\hbar_{k,l}(p)$	The noise for quantization of filter coefficients
$\mathbf{M}_{\hbar(P)}$	The coefficients error covariance of finite precision CS- LMS-MMSE MUD.
Δ_c	Granularity of the quantizers
$\mathbf{M}_{\Delta_{l'}}$	The coefficients error covariance of finite precision FS- LMS-MMSE MUD.
∂	noise variance consisted in the decision variable
N_u	The duration that the LMS algorithm updata.
ω	Power consumption per logic gate
λ	Power consumption per table lookup
P_{T/N_u}	Total power consumption in the finite precision LMS-MMES MUD during each update iteration
$H_T(f)$	The Transmit filer response
$H_C(f)$	The Channel response
$H_R(f)$	The receive filter response
f_s	The sampling rate
$\mathbf{F}_M$	The coefficients of the expander
$\mathbf{y}_{\exp}$	The output of the expander
$\lvert S(e^{j\omega})\rvert$	The magnitude responsen of ideal lowpass filter
$\mathbf{D}_M$	The interpolation

$\mathbf{y}_{Low}$	The output of the interpolation
$\mathbf{E}_S$	The signal subspace
$\mathbf{E}_n$	The noise subspace
$\mathbf{V}$	The input covariance matrix of infinite precision CS- LMS-MMSE MUD
$\mathbf{V}_{r'}$	The input covariance matrix of the finite precision CS-LMS-MMSE MUD
$\mathbf{V}_{(FS)}$	The input covariance matrix of infinite precision FS-LMS-MMSE MUD
$\mathbf{V}_{r'(FS)}$	The input covariance matrix of the finite precision FS-LMS-MMSE MUD

List of Acronyms

MUD	Multiuser Detector
DS-CDMA	Direct Sequence Code Division Multiple Access
AWGN	Additive White Gaussian Noise
BER	Bit Error Rate
TDMA	Time Division Multiple Access
ISI	Inter-Symbol Interference
MAI	Multiple-Access Interference
TACS	Total Access Communication System
NMT	Nordic Mobile Telephone
AMPS	Advanced Mobile Phone Service
GSM	Global System for Mobile Communication
PDC	Personal Digital Cellular
UMTS	Universal Mobile Telecommunication System
TIA	Telecommunications Industry Association
WLL	Wireless Local Loop
LMS	Least Mean Square
FS	Fractionally Spaced
CS	Chip Spaced
SNR	Signal to Noise Ratio
RLS	Recursive Least Square
PE	Polynomial Expansion
MF	Matched Filter
SIR	Signal Interference Ration
MMSE	Minimum Mean Square Error
BAMUD	Blind Adaptive Multiuser Detector
PIC	Parallel Interference Cancellation
SIC	Successive Interference Cancellation
DE	Decorrelating Detector
MSE	Mean Square Error
HDR	High Density Recording
BPSK	Binary Phase Shift Keying
MMF	Mobil Music Polyphonic
FEC	Forward Error Correction
MLS	Mobil Location System

Appendix A:

Coefficients error covariance matrix of the finite precision LMS-MMSE Multiuser detector.

The derivation is based on the nonlinear technique that is presented in [63] to provide the more accurate predictions. The coefficients error covariance matrix is given as:

$$\begin{aligned}\mathbf{M}_{\hbar(P+1)} = \mathbf{M}_{\hbar(P)} &+ E\{\hbar(p)Q_c\{[\mu e'(p)](\mathbf{r}(p)+\varphi(p))^T(p)/\hbar(p)\} \\ &+ E[Q_c\{[\mu e'(p)](\mathbf{r}(p)+\varphi(p))\}\hbar^T(p)/\hbar(p)] \\ &+ E[Q_c\{[\mu^2 e'^2(p)](\mathbf{r}(p)+\varphi(p))(\mathbf{r}(p)+\varphi(p)^T)\}/\hbar(p)]\end{aligned} \tag{A1}$$

It would be desirable to apply the analysis directly to above equations. However, it is not possible to obtained analytical expressions for expectations of nonlinear functions of nonlinear foundations. Therefore, Bermudez and Bershad have made an approximation of a stochastic recursion with one less quantizer [63], and have proved that the asymptotic behaviors are identical and the transient behaviors are very similar. According to this, equation (A1) can be approximated as:

$$\begin{aligned}\mathbf{M}_{\hbar(P+1)} = \mathbf{M}_{\hbar(P)} &+ E\{Q_c[\mu e(p)]\mathbf{r}(p)\hbar(p)/\hbar(p)\} \\ &+ E\{Q_c[\mu e(p)]\mathbf{r}(p)\hbar^T(p)/\hbar(p)\} \\ &+ E\{Q_c[\mu^2 e'^2(p)][\mathbf{r}(p)\mathbf{r}(p)^T]\}/\hbar(p)]\end{aligned} \tag{A2}$$

To determine a recursive equation for $\mathbf{M}_{\hbar(P)}$, the conditional expectations in (A2) are evaluated and then averaged over $\hbar(p)$. In performing the expectations, the moments of order greater than two are neglected. With the approximations [63]:

$$\begin{aligned}\mathbf{M}_{\hbar(P+1)} = \mathbf{M}_{\hbar(P)} &+ \mu E[E[Q_c'[\mu e(p)]/\hbar(p)]]E[\hbar(p)\hbar^T(p)]\mathbf{R}_r \\ &+ \mu E[E[Q_c'[\mu e(p)]/\hbar(p)]]E[\hbar(p)\hbar^T(p)]\mathbf{R}_r \\ &+ E[E[Q_c^2[\mu e(p)]/\hbar(p)]]\mathbf{R}_r\end{aligned} \tag{A3}$$

Firstly, in order to evaluated the first two terms in (A3), $Q'[y]$ is determined. As shown in Fig. A1:

$$\begin{aligned} Q'[y] &= u(-y-\Delta)+\Delta\delta\left(y+\frac{\Delta}{2}\right) \\ &+\Delta\delta\left(y-\frac{\Delta}{2}\right)+u(y-\Delta) \end{aligned} \tag{A4}$$

Where $u(*)$ and $\delta(*)$ are the unit step and Dirac delta functions [78], respectively. For y is a zero mean Gaussian input variable:

$$E[Q'[y]] = \frac{1}{\sigma_y\sqrt{2\pi}}\int_{-\infty}^{\infty} Q'[y]e^{-\frac{y^2}{2\sigma_y^2}}dy \tag{A5}$$

Then substituting (A4) into (A5) with $y=\mu e(p)$, conditioned on $\hbar(p)$, yields:

$$E[Q'[\mu e(p)]\,|\,\hbar(p)] = 1+\sqrt{\frac{2}{\pi}}\frac{\Delta_C}{\mu\varepsilon_{e|\hbar(p)}}e^{\frac{-\Delta_c^2}{8\mu^2\delta^2_{\varepsilon|\hbar(p)}}} - erf\left(\frac{\Delta_c}{\sqrt{2\delta_{\varepsilon|\hbar(p)}}}\right) \tag{A6}$$

Then, the first two terms can be written as:

$$\begin{aligned} &E[E[Q'[\mu e(p)]\,|\,\hbar(p)]]E[\hbar(p)\hbar^T(p)]\mathbf{R}_r \\ &= E[Q'[\mu e(p)]E[\hbar(p)\hbar^T(p)]\mathbf{R}_r \\ &= \left[1+\sqrt{\frac{2}{\pi}}\frac{\Delta_C}{\mu\varepsilon_e}e^{\frac{-\Delta_c^2}{8\mu^2\delta_c^2}} - erf\left(\frac{\Delta_c}{\sqrt{2\mu\varepsilon_c}}\right)\right]E[\hbar(p)\hbar^T(p)]\mathbf{R}_r \end{aligned} \tag{A7}$$

where $erf(x)=\frac{2}{\pi}\int_0^x e^{-t^2}dt$.

Now, to evaluate the last term in (A3), first define (Fig A1):

$$\begin{aligned} Q^2[y] &= y^2u(-y-\Delta)+\Delta^2u\left(-y-\frac{\Delta}{2}\right)-\Delta^2u\left(-y-\Delta\right) \\ &+\Delta^2u\left(y-\frac{\Delta}{2}\right)-\Delta^2u\left(y-\Delta\right)+y^2u(y-\Delta) \end{aligned} \tag{A8}$$

With zero-mean Gaussian $y=\mu e(p)$ conditioned on $\hbar(p)$. Then:

$$\begin{aligned} &E[Q_c^2[\mu e(p)]/\hbar(p)] \\ &= \sqrt{\frac{2}{\pi}}\frac{1}{\mu\varepsilon_{e|\hbar(p)}}\left\{\Delta^2\int_{\frac{\Delta}{2}}^{\Delta}e^{-\frac{t^2}{2\mu^2\varepsilon_{e|\hbar(p)}}}dt+\int_{\Delta}^{\infty}t^2e^{-\frac{t^2}{2\mu^2\varepsilon_{e|\hbar(p)}}}dt\right\} \end{aligned} \tag{A9}$$

Again approximating $\varepsilon_{c|\hbar(p)}$ by its mean to averaging (A9) over $\hbar(p)$ yields:

$$
\begin{aligned}
&E[Q_c^{\,2}[\mu e(p)]] \\
&= \left(\frac{\Delta_C}{\mu\varepsilon_c}\right)^2 \left[erf\left(\frac{\Delta_c}{\sqrt{2}\mu\varepsilon_e}\right) - erf\left(\frac{\Delta_c}{2\sqrt{2}\mu\varepsilon_c}\right)\right] + 1 \\
&+ \sqrt{\frac{2}{\pi}}\left(\frac{\Delta_c}{\mu\varepsilon_e}\right) e^{\frac{-\Delta_c^2}{2\mu^2\varepsilon_r^2}} - erf\left(\frac{\Delta_c}{\sqrt{2}\mu\varepsilon_c}\right)
\end{aligned}
\tag{A10}
$$

Therefore, from (A7) and (A9), the expression of the coefficients error covariance matrix is obtained. This is given by (3.80).

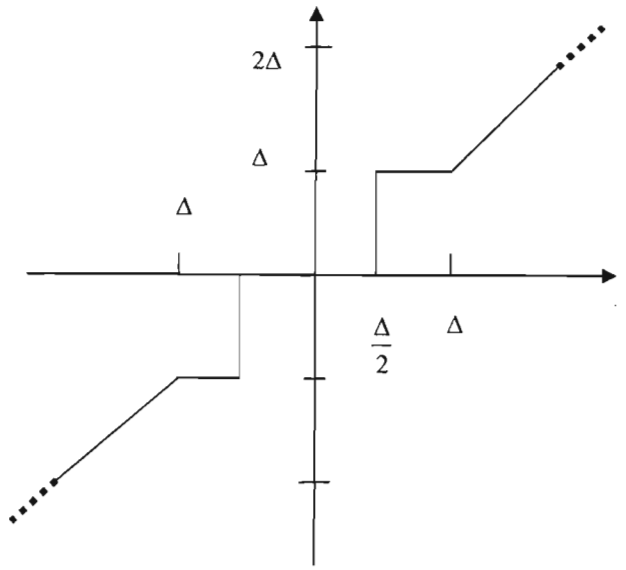

Figure A1. Quantizer model.

Appendix B:

BER of the finite precision LMS-MMSE detector

The BER is calculated by the error function Q:

$$Q(x) = \int_{x}^{\infty} \frac{1}{\sqrt{2\pi}} \exp\left(-\frac{\mu^2}{2}\right) d\mu.. \tag{B1}$$

The received signal of the detector is:

$$\mathbf{r} = \mathbf{SCAb} + \mathbf{n}. \tag{B2}$$

The quantized received signal $\mathbf{r}'$ pass through the adaptive filter with quantized filter coefficients $w'_{k,l}(p)$, which the optimal coefficients is (see chapter 3):

$$\mathbf{W}(opt) = \mathbf{S}\left\{\mathbf{SS}^T + E\left(\sigma^2\left(E[\mathbf{CAAC}^H]\right)^{-1}\right)\right\}^{-1}, \tag{B3}$$

then the output is:

$$y_{k,l}(p) = w'^T_{k,l}(p)\mathbf{r}'. \tag{B4}$$

From figure 3.3, the decision variable of the finite precision LMS-MMSE MUD for all the paths can be written as:

$$\begin{aligned} z'_{k,l}(p) &= Q_d[z_{k,l}(p)] \\ &= Q_d[c'_{k,l}(p)y'_{k,l}(p)] \\ &= Q_d\{c'_{k,l}(p)Q_d[w'^T_{k,l}(p)\mathbf{r}']\} \end{aligned} \tag{B5}$$

By using the relations defined in equation 3.49 that the quantized value can be treated as the original plus the quantization noise. Therefore, in the steady state, the decision variable for the k^{th} user and l^{th} path of the finite precision LMS-MMSE MUD $z'_{k,l}(p)$ can be mathematically written as (condition on $\mathbf{b} = 1$):

$$
\begin{aligned}
z'_{k,l}(p) = {} & c_{k,l}(p)(\mathbf{SCA})w^T{}_{k,l}(opt) + c_{k,l}(p)\mathbf{n}w^T{}_{k,l}(opt) \\
& + c_{k,l}(p)(\mathbf{SCA})\hbar^T{}_{k,l}(p) + c_{k,l}(p)\mathbf{n}\hbar^T{}_{k,l}(p) \\
& + c_{k,l}(p)\varphi_{k,l}(p)w^T{}_{k,l}(opt) + c_{k,l}(p)\varphi_{k,l}(p)\hbar^T{}_{k,l}(p) \\
& + c_{k,l}(p)\kappa_{k,l}(p) + (\mathbf{SCA})w^T{}_{k,l}(opt)\phi_{k,l}(p) + \phi_{k,l}(p)\mathbf{n}w^T{}_{k,l}(opt). \\
& + \phi_{k,l}(p)(\mathbf{SCA})\hbar^T{}_{k,l}(p) + \phi_{k,l}(p)\mathbf{n}\hbar^T{}_{k,l}(p) \\
& + \phi_{k,l}(p)\varphi_{k,l}(p)w^T{}_{k,l}(opt) + \phi_{k,l}(p)\varphi_{k,l}(p)\hbar^T{}_{k,l}(p) \\
& + \phi_{k,l}(p)\kappa_{k,l}(p) + \vartheta_{k,l}(p).
\end{aligned}
\tag{B6}
$$

It should be noted that all the noise in (B6) are zero mean and uncorrelated each other. Also, all the quantization noise is independent of the corresponding input. Consequently, all the terms in (B6) are uncorrelated each other, and all the terms that consist of noise are zero mean. Therefore, the mean value of the decision variable is:

$$
\begin{aligned}
\overline{z}'_{k,l}(p) &= E[z'_{k,l}(p) \mid \mathbf{b} = 1] \\
&= c_{k,l}(p)\mathbf{SCA}w_{k,l}(opt)
\end{aligned}
\tag{B7}
$$

and the variance of the decision variable is:

$$
\delta^2_{z'} = E[(z'_{k,l}(p) - \overline{z}'_{k,l}(p))^2 \mid \mathbf{b} = 1]. \tag{B8}
$$

Insert the equation (B7) into (B8), yields:

$$
\delta^2_{z'} = E[(z'_{k,l}(p) - c_{k,l}(p)\mathbf{SCA}w^T{}_{k,l}(opt))^2 \mid \mathbf{b} = 1]. \tag{B9}
$$

Then, insert equation (B6) into (B9) the variance of the decision variable is given by:

$$
\begin{aligned}
\delta^2_{z'} = E[& c_{k,l}(p)\mathbf{n}w^T{}_{k,l}(opt) \\
& + c_{k,l}(p)(\mathbf{SCA})\hbar^T{}_{k,l}(p) + c_{k,l}(p)\mathbf{n}\hbar^T{}_{k,l}(p) \\
& + c_{k,l}(p)\varphi_{k,l}(p)w^T{}_{k,l}(opt) + c_{k,l}(p)\varphi_{k,l}(p)\hbar^T{}_{k,l}(p) \\
& + c_{k,l}(p)\kappa_{k,l}(p) + (\mathbf{SCA})w^T{}_{k,l}(opt)\phi_{k,l}(p) + \phi_{k,l}(p)\mathbf{n}w^T{}_{k,l}(opt). \\
& + \phi_{k,l}(p)(\mathbf{SCA})\hbar^T{}_{k,l}(p) + \phi_{k,l}(p)\mathbf{n}\hbar^T{}_{k,l}(p) \\
& + \phi_{k,l}(p)\varphi_{k,l}(p)w^T{}_{k,l}(opt) + \phi_{k,l}(p)\varphi_{k,l}(p)\hbar^T{}_{k,l}(p) \\
& + \phi_{k,l}(p)\kappa_{k,l}(p) + \vartheta_{k,l}(p)|^2 \ \mathbf{b} = 1]
\end{aligned}
\tag{B10}
$$

It should be noted that in equation (B10), all the terms are zero mean. It presents no cross-product. Also, all the quantization noises $\phi_{k,l}(p)$, $\kappa_{k,l}(p)$, $\varphi_{k,l}(p)$, $\vartheta_{k,l}(p)$ are independent of its corresponding input of quantizers and each other, therefore, all the terms in equation are independent of each other. All the quantization noises are defined as follow (chapter 3):

$$
\begin{aligned}
c'_{k,l}(p) &= c_{k,l}(p) + \phi_{k,l}(p) \\
\mathbf{r}'(p) &= \mathbf{r}(p) + \varphi_{k,l}(p) \\
y'_{k,l}(p) &= y_{k,l}(p) + \kappa_{k,l}(p) \\
z'_{k,l}(p) &= z'_{k,l}(p) + \vartheta_{k,l}(p) \\
w'_{k,l}(p) &= w_{k,l}(opt) + \hbar_{k,l}(p)
\end{aligned}
\qquad \text{(B11)}
$$

The following table gives the variances of each term:

	Mean	Variance
$c_{k,l}(p)\mathbf{n}w^T_{k,l}(opt)$	0	$c_{k,l}(p)c^T_{k,l}(p)w_{k,l}(opt)w^T_{k,l}(opt)\delta_n^2$
$c_{k,l}(p)(\mathbf{SCA})\hbar^T_{k,l}(p)$	0	$c_{k,l}(p)c^T_{k,l}(p)(\mathbf{SCA})(\mathbf{SCA})^{-1}E[\hbar_{k,l}(p)\hbar^T_{k,l}(p)]$
$c_{k,l}(p)\mathbf{n}\hbar^T_{k,l}(p)$	0	$c_{k,l}(p)c^T_{k,l}(p)\delta_n^2 E[\hbar_{k,l}(p)\hbar^T_{k,l}(p)]$
$c_{k,l}(p)\varphi_{k,l}(p)w^T_{k,l}(opt)$	0	$c_{k,l}(p)c^T_{k,l}(p)w_{k,l}(opt)w^T_{k,l}(opt)\delta_d^2$
$c_{k,l}(p)\varphi_{k,l}(p)\hbar^T_{k,l}(p)$	0	$c_{k,l}(p)c^T_{k,l}(p)\delta_d^2 E[\hbar_{k,l}(p)\hbar^T_{k,l}(p)]$
$c_{k,l}(p)\kappa_{k,l}(p)$	0	$c_{k,l}(p)c^T_{k,l}(p)\delta_d^2$
$(\mathbf{SCA})w^T_{k,l}(opt)\phi_{k,l}(p)$	0	$w_{k,l}(opt)w^T_{k,l}(opt)(\mathbf{SCA})(\mathbf{SCA})^{-1}\delta_d^2$
$\phi_{k,l}(p)\mathbf{n}w^T_{k,l}(opt)$	0	$w_{k,l}(opt)w^T_{k,l}(opt)\delta_n^2\delta_d^2$
$\phi_{k,l}(p)(\mathbf{SCA})\hbar^T_{k,l}(p)$	0	$(\mathbf{SCA})(\mathbf{SCA})^{-1}E[\hbar_{k,l}(p)\hbar^T_{k,l}(p)]\delta_d^2$
$\phi_{k,l}(p)\mathbf{n}\hbar^T_{k,l}(p)$	0	$E[\hbar_{k,l}(p)\hbar^T_{k,l}(p)]\delta_n^2\delta_d^2$
$\phi_{k,l}(p)\varphi_{k,l}(p)w^T_{k,l}(opt)$	0	$w_{k,l}(opt)w^T_{k,l}(opt)\delta_d^2\delta_d^2$
$\phi_{k,l}(p)\varphi_{k,l}(p)\hbar^T_{k,l}(p)$	0	$E[\hbar_{k,l}(p)\hbar^T_{k,l}(p)]\delta_n^2\delta_d^2$
$\phi_{k,l}(p)\kappa_{k,l}(p)$	0	$\delta_d^2\delta_d^2$
$\vartheta_{k,l}(p)$	0	δ_d^2

Table B1. The variances of each term in equation (B10).

Recalling the equation (3.74) in chapter 3:

$$
\mathbf{M}_{\hbar(p)} = E[\hbar_{k,l}(p)\hbar^T_{k,l}(p)], \qquad \text{(B12)}
$$

The total variance of the decision variable is given as:

$$\begin{aligned}\delta_{z'}^2 = c_{k,l}(p)c^T{}_{k,l}(p)\{M_{h(p)}[(\mathbf{SCA})(\mathbf{SCA})^{-1} + \delta_n^2 + \delta_{il}^2] \\ + w_{k,l}(opt)w^T{}_{k,l}(opt)[\delta_n^2 + \delta_{il}^2] + \delta_{il}^2\} \\ + M_{h(p)}[\delta_{il}^2(\mathbf{SCA})(\mathbf{SCA})^{-1} + \delta_{il}^2\delta_n^2 + \delta_{il}^2\delta_{il}^2] \\ + \delta_{il}^2\{w_{k,l}(opt)w^T{}_{k,l}(opt)[(\mathbf{SCA})(\mathbf{SCA})^{-1} + \delta_{il}^2 + \delta_n^2] + \delta_{il}^2\} \\ + \delta_{il}^2\end{aligned} \tag{B13}$$

Thus the signal-to-interference ratio of the decision variable is given by the following expression:

$$SNR = \frac{\overline{z}'_{k,l}(p)^2}{\delta_{z'}^2}. \tag{B14}$$

Finally the expression for the bit error rate of the finite precision LMS-MMSE MUD is given by the following expression:

$$\begin{aligned}BER &= Q\{SNR\} \\ &= Q\{\frac{\overline{z}'_{k,l}(p)^2}{\delta_{z'}^2}\}.\end{aligned} \tag{B15}$$

Reference:

[1] Craig Michael Teuscher "*Low Power Receiver Design for Portable RF Applications: Design and Implementation of an Adaptive Multiuser Detector for an Indoor, Wideband CDMA Application*" PhD thesis, University of California, Berkeley, 1994.

[2] F. Swarats, P. V. Rooyan, I. Oppermann and M. P. Lotter, " *CDMA Techniques for Third Generation Mobile Systems*" Kluwer Academic Publishers, Boston/Dordrecht/London, 1999.

[3] Shimon Moshavi, Bellcore "Multiuser Detection for DS-CDMA Communications", *IEEE Communications Magazine*, pp 124-136, October 1996.

[4] D. V. Sarwate and M. B. Pursley, "Crosscorrelation Properties of Pseudorandom and Related Sequence", *Proc. IEEE*, vol. 68,NO. 5, pp. 593-619, May 1980.

[5] R. Kohno, "Pseudo-Noise Sequence and Interference Cancellation Techniques for Spread Spectrum Systems", *IEICE Trans. Commun.*, vol. J74-B-1, no. 5, pp. 1083-1092 May 1991.

[6] J. M. Holtzman, "CDMA Power Control for Wireless Network", *Third Generation Wireless Information Networks,* D.G. Goodman and S. Nanda, eds., Norwell, MA: Kluwer, pp 299-311, 1992.

[7] V. K. Garg, K. Smolik. JJ. E. Wilkes, "*Applications of Code-Division Multiple Access (CDMA) in Wireless/Personal communications*", Upper Saddle River, NJ: prentice Hall, 1996.

[8] J. C. Liberti, " *Spatial Processing for High Tier Wireless Systems*", Bellcore Pub. IM-558, Sept 1996.

[9] S. Verdu, " Minimum Probability of Error for Asynchronous Gaussian Multiple Access", *IEEE Trans. IT.*, vol IT-32, no. 1, pp. 85-96, Jan. 1986.

[10] Benjamin M. Zaidel, Shamai, and Hagit Messer. "Performance of Linear MMSE Multiuser Detection Combined with A Standard IS-95 Uplink" *Wireless Network 4*, pp.429-44, 1998.

[11] Dao Sheng Chen, Sumit Roy. "An Adaptive Multi-use Recriver for CDMA System" *IEEEE Journal Selected Areas in Communications*, Vol. 12, No. 5, pp. 808-815, June 1994.

[12] Aditya Dua, "*Multiuser Detection in DS-CDMA Systems: A Review*" SPANN Lab, IIT Bombay, Department of Electrical Engineering Indian Institute of Technology.

[13] R. Lupas and S. Verdu, "Near-Far Resistance of Multiuser Detection in Asynchronous Channels", *IEEE Trans. Commun.*, vol. 38, no 4, pp. 496-508, April 1990.

[14] S. Moshavi, "*Survey of Multiuser Detection for DS-CDMA Systems*", Bellcore Pub., IM-555, Aug 1996.

[15] S. Verdu, " *Multiuser Detection*", Cambridge University Press 1998.

[16] S. Verdu, " Minimum Probability of Error for Asynchronous Multiple Access Communication Systems ", *IEEE Military Communication Conf.*, pp. 213-219, 1983.

[17] J, G. Proakis, "*Digital Communications*", 2nd edition., New York: McCraw-Hill, 1989.

[18] Kohno, R. Hatori, M & Imai, H, " Cancellation Techniques of co-channel Interference in Asynchronous Spread Spectrum Multiple Access Systems", *Electronics and Communications in Japan*, vol. 66-A, no. 5, pp. 20-29, 1983.

[19] R. Lupas and S. Verdu, " Linear Multiuser Detectors for Synchronous Code Division Multiple Access Channels", *IEEE Trans on Information Theory*, vol. 35, no. 1, pp. 123-136, April 1989.

[20] S. Verdu, "Multiuser Detection", *Advances in statistical Signal Processing*, vol. 2, Signal Detection pp. 369-409, JAI Press: Greenwich, CT , 1993.

[21] R.Lupas-Colaszewski.S. Verdu, "Asymptotic efficiency of linear multiuser detectors", Proc. *25th Conf. on Decision and control*, Athens, Greece, pp. 2094-2100, Dec 1986.

[22] A. Duel-Hallen, K. Holtzman, Z. Zvonar, " Multiuser detection for CDMA systems", *IEEE Pers. Commun.*, vol. 2, no. 2, pp. 46-58, Apr 1995.

[23] S. Moshavi, " *Multistage linear Detectors for DS-CDMA Communications*", PHD thesis, Dept. Elec. Eng., City University. New York, NY, Jan 1996.

[24] A, J. Viterbi, " Very Low Rate Convolutional Codes for Maximum Theoretical Performance of Spread-Spectrum Multiple Access Channels", *IEEE JSAC,* vol. 8, no. 4, pp. 641-649, May 1990.

[25] R. Kohno et al., "Combination of an Adaptive Array Antenna and a Canceller of Interference for Direct Sequence Spread Spectrum Multiple Access Systems", *IEEE JSAC,* vol. 8, no. 4, pp. 675-682, May 1990.

[26] M. K. Varanasi, B. Aazhang, "Multistage Detection in Asyncronous Code Division Multiple Access Communications", *IEEE Trans, Commun.*, vol. 38, no.4, pp.509-519, Apr 1990.

[27] P. Patel , J. Holtzman, "Performance Comparison of a DS/CDMA system Using a Successive Interference Cancellation Scheme and a Parallel IC Scheme under Fading", *Proc. ICC'94*, New Orleans, LA, pp. 510-514, May 1994.

[28] R. M. Buehrer, B. D. Woener, "Analysis of Adaptive Multistage Interference Cancellation for CDMA Using an Improved Gaussian Approximation", *Proc. IEEE MILCOM'95*, San Diego, CA, pp. 1195-1199, Nov 1995.

[29] D. Divsalar, M. Simon, " *Improved CDMA Performance Using Parallel Interference Cancellation*", JAP pub. 95-21, Oct. 1995.

[30] T. R. Giallorenzi, S. G. Wilson, " Decision Feedback Multiuser Receivers for Asynchronous CDMA Systems", *Proc. IEEE MILCOM'93*, Houston, TX, pp. 1677-1682, Dec 1993.

[31] Chazi-Moghadam, V & Mistafa, K, " A CDMA Interference Canceling Receiver with an Adaptive Blind Array", *IEEE Journal on Selected Areas in Communications*, vol. 16, no. 8, pp. 1542-1549, Oct 1998.

[32] Xue, G, Weng, J, Le-Ngoc, T & Tahar, S, " Adaptive Multistage Parallel Interference Cancellation for CDMA", *IEEE Journal on Selected Areas in Communications*, vol. 17, no. 10, pp. 1815-1827, Oct 1999.

[33] G. W. Stewart, "*Introduction to Matrix Computations*", New York: Academic, 1973

[34] A. Duel-Hallen, "A Family of Multiuser Decision-Feedback Detectors for Asynchronous Code Division Multiple Access Channels", *IEEE Trans. Commun.*, vol. 43, no. 2/3/4, pp. 421-434, Feb/Mar/Apr 1995.

[35] M. Latva-aho, M. j. Juntti, " LMMSE Detection for DS-CDMA Systems in Fading Channels", *IEEE Trans. on Commun.*, vol. 48, no. 2, pp. 194-199, Feb 2000.

[36] P. Van Rooyan, I. Oppermann " DS-CDMA Performance with Maximum Ratio Combining and Antenna Arrays", *Wireless Networls, The Journal of Mobile Communication, Computation and Information.* Vol. 4, no. 6, pp. 479-489, Oct 1998.

[37] Liu. H, Li. K, " A Decorrelating Rake Receiver for CDMA Communication Over Frequency-Selective Fading Channels", *IEEE Trans on communication*, vol. 47, no, 7, pp. 1036-1045, July 1999.

[38] Ulukus, S, Yates, R D, " A Blind Adaptive Decorrelating Detector for CDMA Systems", *IEEE Journal on Selected Areas in Communications*, vol. 16, no. 8, pp. 1530-1541, Oct 1998.

[39] Sawahashi, M, Miki, Y, Andoh, H and Higuchi, K, " Serial Canceller Using Channel Estimation by Pilot Symbols for DS-CDMA", *Technical report of the IEICE, RCS95-50*, vol. 12, no. RCS95-50, pp. 43-48, July 1995.

[40] Sawahashi, M, Miki, Y, Andoh, H and Higuchi, K, " Poilt Symbol-Assisted Coherent Multistage Interference Canceller for DS-CDMA Mobile Radio", *IEE Electronics Letter*, vol. 32, pp. 301-302, Feb 1996.

[41] Kawabe, M, Sato, S, Sugimoto, H & Fukasawa, " Interference Cancellation System Using Estimation of Propagation Parameters", *Proc. JTC-CSCC'94*, Japan, pp. 173-178, 1994.

[42] Patel, P & Holtzman, J, " Analysis of a Simple Successive Interference Cancellation Scheme in a DS/CDMA system", *IEEE Journal on Selected Areas in Communications*, vol.12, no. 5, pp. 796-807, June 1994.

[43] Soong, A, C, K and Krzymien, W, A, "A Novel CDMA Multiuser Interference Cancellation Receiver with Reference Symbol Aided Estimation of Channel Parameters", *IEEE Journal on Selected Areas in Communications*, Vol.14, no.8, pp. 1536-1547, Oct 1996.

[44] Fawer, U and Aazhang, B, " A Multiuser Receiver for Code Division Multiple Access Communications Over Multipath Channel", *IEEE Transaction on Communications*, vol. 43, no, 2/3/4, pp. 1556-1565, Feb/Mar/Apr 1995.

[45] Poor, H, V and Wang X, " Code-aided interference suppression for DS-CDMA communications- part 2: Parallel Blind Adaptive Implementations", *IEEE Transactions on Communications*, vol. 45, no. 9, Sep 1997.

[46] Simon Haykin. " *Adaptive Filter Theory*", Prentice-Hall, Englewood Cliffs, New Jersey, 1986.

[47] Z. Xie, R. T. Short, C. K. Rushforth, " A Family of Sub-optimum Detectors for Coherent Multiuser Communications", *IEEE JSAC*, vol. 8 no. 4, pp. 683-690, May 1990.

[48] B. Widrow, "Adaptive filter ", in *Aspect of Network and System Theory*, R. Kalman and N. DeClaris, Eds. New York: Holt, Rinehart, and Winston, pp. 563-587, 1971.

[49] Latva-aho, " Bit Error Probability Analysis for FRANES WCDMA Downlink Receiver", *IEEE Trans on Vehicular Technology*, vol. 47, no. 4, Nov 1998.

[50] Oppermann, I, Van Rooyen P & Vucetic B, "Effect of Sequence Selection on MAI Suppression in Limited Spreading CDMA Systems", *Wireless Network*, vol. 4, no. 4, pp. 471-478, 1998.

[51] John G. Proakis, "*Digital Communication*", McGraw-Hill International edition, 1989.

[52] Ungerboeck G, "Theory on the Speed of Convergence in Adaptive Equalizers for Digital Communication", *IBM J. Res. Devel.*, vol. 16, pp. 546-555, 1972.

[53] J. R. Treichler, "Transient and Convergence Behavior of the Adaptive line enhancer", *IEEE Trans. Acoust., Speech, Signal Processing*, vol. ASSP-27, pp.53-62, Feb 1979.

[54] M. J. Barrett, "Error Probability for Optimal and Suboptimal quardratic Receivers in Rapid Rayleigh Fading Channels", *IEEE J. Select. Areas Commun.*, vol. 5, no. 2, pp. 302-304, Feb 1987.

[55] Juntti. M, "*Multiuser Demodulation for DS/CDMA Systems in Fading Channels*", PHD Thesis, University of Oulu, 1998.

[56] Juntti. M, J & Latva-aho. M, "Bit Error Probability Analysis of Linear Receiver for CDMA Systems in Frequency-Selective Fading Channels", *IEEE Transactions on Communications*, vol. 47, no. 12, pp. 1788-1792.

[57] A. P. Chandrakasan, R. W. Brodersen, "Minimizing Power Consumption in Digital CMOS Circuits", *IEEE Proceedings*, vol. 83, pp. 498-523, April 1995.

[58] K. K.Parhi, "Algorithm Transformation Techniques for Concurrent Processors," IEEE Proceedings, vol. 77, pp. 1879{1895, Dec. 1989.

[59] C. Caraiscos , B. LIU, "A Roundoff Error Analysis of the LMS Adaptive Algorithm", *IEEE Transactions in Acoustics, Speech, and Signal Processing*, vol. ASSP-32, NO. 1, pp. 34-41, Feb 1984.

[60] R. Gupta, A. O. Hero, "Power Versus Performance Tradeoff for Reduced Resolution LMS Adaptive Filter. *IEEE Transactions on Signal Processing*, vol. 48, no. 10, pp. 2772-2784.

[61] Guilford. J, Das, P, " The Use of the Adaptive Lattice Filter for Narrowband Jammer Rejection in DS Spread Spectrum Systems", *Rensselaer Polytechnic Institute*, Unpublished.

[62] S. U. H. Qureshi," Adaptive Equalization", *proceedings of the IEEE* 73(9), pp. 1349-1387, Sep 1985.

[63] J. Carlos M. Bermuddez, N. j. Bershad, " A nonlinear Analytical Model for the Quantized LMS Algorithm-The Arbitrary Step Size Case", *IEEE Transactions on Signal Processing*, vol. 44, no. 5, pp. 1175-1183, May 1996.

[64] B. Widrow *et al.*, "Stationary and Nonstationary Learning Characteristics of the LMS Adaptive Filter", *Proc. IEEE*, vol. 64, pp. 1151-1162, Aug 1976.

[65] R. D. Gitlin, J. E. Mazo, M. G. Taylor, "On the Design of Gradient Algorithms for Digitally Implemented Adaptive Filters," *IEEE Trans. Circuit Theory*, vol. CT-20, pp. 125-136, Mar. 1973.

[66] J. Carlos M. Bermuddez, N. j. Bershad, " A nonlinear Analytical Model for the Quantized LMS Algorithm-The Power-of-two Step Size Case", *IEEE Transactions on Signal Processing*, vol. 44, no. 5, pp. 2895-2900, May 1996.

[67] Oliver Yuk-Huang Leung, Chung-Wai Yue, Chi-ying Tsui and Roger S. K. Cheng, " Reducing Power Consumption of Turbo Code Decoder Using Adaptive Iteration with Vaiable Supply Voltage", *Dept. Electrical and Electronic Eng., The HK University of Science and Technology.*

[68] Chi-ying Tsui, Roger S. K. Cheng and Curtis Ling, " Using Transformation to Reduce Power Consumption of IS-95 CDMA Receiver", *Submitted to International Symposium on Low Power Electronics and Design*, 1999.

[69] D. Singh, M. Pedram, S. Rajgopal, and T. J. Mozdzen, " Power Conscious CAD Tools and Methodologies: A Perspective", *Proceedings of the IEEE*, vol. 83, no. 4 pp. 570-593, Apr 1995.

[70] Honing M. L, Madhow U and Verdu S, " Blind Adaptive Multiuser Detection", *IEEE Transactions on Information Theory*, vol. 41, no. 4, pp944-960, July 1995.

[71] G. ling, F., and Proakis, J. G., " Fractionally-Spaced Equalizers Based on Singular-Value Decomposition", *Proc, Int. Conf., Acoust., Speech, Signal Processing*, New York, 25. D.4.10, April 1988.

[72] G. ling, F., and Proakis, J. G., "Applications of Fractionally-Spaced Decision-Feed-back Equalizers to HF Fading Channels", *Proc. MILCOM*, San Diego, Calif., Oct 1988.

[73] Ling F., " On the convergence Speed of Fractionally-Spaced Equalizer Using Intersymbol Interpolation", *Proc. Int. Conf. Commun. Tech.*, Nanjing, China, Nov 1987.

[74] T. J. Lim, Y. Gong, and B. Farhang-Boroujeny, " Convergence Analysis of Chip- and Fractionally Spaced LMS Adaptive Multiuser CDMA Detectors", *IEEE Transaction on Signal Processing*, vol. 48, no. 8, pp. 2219-2227, Aug 2000.

[75] T. J. Lim and Roy, S, "Adaptive Filter in Multiuser CDMA Detection", *Wireless Network*, vol. 4, no. 4, pp.304-318, 1998.

[76] Nesper O and Ho. P, "A Reference Symbol Assisted Interference Cancellation Hybrid Receiver for an Asynchronous DS/CDMA Systems", *Proc. IEEE International Symposium on Personal, Indoor and Mobile Radio Communications*, Taipei, Taiwan, pp. 108-112, Oct 1996.

[77] Claes Tidestav "The Multivariable Decision feedback Equalizer: Multiuser Detection and Interference Rejection" PHD Thesis, Uppsala University, 1999.

[78] A. V. Oppenheim and R. W. Schafer, Discrete-Time Signal Processing. Englewood Cliffs, NJ: Prentice-Hall, 1989.

Chapter 1
Introduction

1.1 Introduction

Cellular mobile communication systems are one of the fastest growing areas in digital wireless communications today. The earliest cellular communication systems include the Total Access Communication System (TACS) in the United Kingdom, Nordic Mobile Telephone (NMT) and the Advanced Mobile Phone Service (AMPS). The common feature of these communication systems is that they employ analog technology, and are called first generation systems. The most fatal disadvantage of first generation systems is that they only covered a small percentage of the service area, therefore the systems capacity is small, beside this, the power consumption in the mobile terminals is high.

Second generation cellular communication systems have thus been developed based on digital technology. The standards for the second cellular generation system include:

- Global System for Mobile Communication (GSM) (Europe, Africa & Asia)
- The IS-54 and IS-95 (United States)
- Personal Digital Cellular (PDC) (Japan)

The main disadvantage of second generation cellular communication systems is that they only offer voice and SMS services, thus they obviously can not satisfy the requirements of future mobile communication systems. Future mobile communication systems (third generation) have to have:

- High flexibility
- Large system capacity

- Low power consumption
- Easy implementation
- Multi service
- Multi QoS

The spread spectrum code division multiple access (CDMA) scheme is playing a vital role in third generation communication systems (3G).

1.2 Code Division Multiple Access System

The wideband CDMA that forms the basis of (Universal Mobile Telecommunication System) UMTS 3G networks was developed originally by Qualcomm. CDMA is characterized by high capacity and small cell radius, employing spread-spectrum technology and a special coding scheme. CDMA was adopted by the Telecommunications Industry Association (TIA) in 1993. In May 2001 there were 35 million subscribers on CDMA systems worldwide and over 35 countries have either commercial or trial activity ongoing. There are already 43 Wireless Local Loop (WLL) systems in 22 countries using CDMA technology, whilst worldwide resources are being devoted to roll out third-generation CDMA technology, including Multi-Carrier (cdma2000 1xMC and HDR in 1.25 MHz bandwidth), and 3xMC in 5 MHz.

CDMA is a multiple access scheme, where users transmit their information using the entire allocated bandwidth simultaneously, with their signals modulated by a unique spread sequence. The spread spectrum CDMA system has several attractive features when compared to other multiple access systems:

- All the CDMA users use the same frequency, therefore, the frequency reuse factor is 1.
- The CDMA receivers are able to exploit the multipath fading by the use of the Rake receiver.
- All the spread signal of the CDMA system has low power level therefore it has a low probability of being intercepted.
- All the CDMA mobile terminals and base stations are on the same frequency, therefore it is easy to handoff between the different base stations.

Like the second generation communication systems, CDMA systems also have their disadvantages. One of the major drawbacks of a CDMA system is the near-far problem, where the signal from a user with weak transmitted power is overwhelmed by a user with a strong transmitted power. The traditional way of minimizing the near-far problem is by the use of power control, making the received signal from different users arrive at the receiver with equal power levels.

Another major drawback of the CDMA system is called multiple access interference (MAI). MAI is always present when the cross-correlation matrix of the users' spreading sequences is not zero. The conventional way to mitigate MAI is through the design of spreading sequences with good cross-correlation properties, ideally, if the spreading sequences were all orthogonal, then the MAI will be completely removed. However, it is obviously impossible to design spreading sequences that maintain orthogonality over all possible delays since the channels contain some degree of asynchronism.

The technical solution of the near-far problem and MAI is the use of a multiuser detector (MUD), which was first proposed in 1986 by Verdu. This had a significant impact in the area of spread spectrum, since following his work many MUDS for CDMA system were proposed. Here, information about multiple users is used jointly to better detect each individual user. The utilization of multi-user detection algorithms has the potential to provide significant additional benefits for a DS-CDMA system. However, an optimal multiuser detector has been shown to have a complexity that is exponential in terms of the number of users, therefore, a number of sub-optimal multi-user detectors have been developed. There are two main classes of sub-optimal multi-user detectors: linear multi-user detectors and subtractive interference cancellation multi-user detectors.

One of the most popular sub-optimal multi-user detector is the Linear Minimum Mean Square (MMSE) multi-user detector [47]. The standard approach of this detector is to minimize the mean square error between the training data and filter output. The inversion of a matrix is needed to compute the optimal filter coefficients, and this operation greatly increases the complexity of computation. Thus, the adaptive MMSE multi-user detector has been developed. The adaptive implementation of the MMSE detector greatly reduces the computational requirements of the MMSE detector, since the matrix inversion in the computation of the optimal coefficients can be avoided.

The Least Mean Square (LMS) algorithm is one of the most commonly used adaptive algorithms. However, the implementation of this algorithm in hardware needs the use of finite number of bits. The finite precision LMS-MMSE detector can be viewed as an infinite precision LMS-MMSE detector implemented with the insertion of quantizers in the data path and in the detector coefficients path. In addition, the finite precision implementation of the detector can effectively reduce the power consumption in the detector, this is significant since low power implementation has become an important aspect in communication systems.

1.3 Motivations and Original Contribution

As power consumption in CDMA systems has become an important aspect, and the implementation in hardware requires finite wordlengths, there is a need for the finite precision implementation of the adaptive LMS-MMSE detector. However, the finite precision implementation of the LMS-MMSE detector can also degrade the performance of the system. Several publications have discussed the tradeoff between power consumption and performance in a simple LMS algorithm, however, no work has been done in determining the tradeoff between power consumption and performance in the finite precision LMS-MMSE detector. The focus of this dissertation is on the analysis of the finite precision effects and the power consumption in the LMS-MMSE detector. In addition to this, the relationship between power consumption and performance in the finite precision LMS-MMSE detector is also presented.

The original contributions made in this dissertation are as follows:

- The analysis of quantization effects in the finite precision chip-spaced (CS) LMS-MMSE detector. (Chapter 3).
- The convergence analysis of the finite precision fractionally spaced (FS) LMS-MMSE detector. (Chapter 5).
- An analysis of the tradeoff between power consumption and performance in the finite precision LMS-MMSE detector. (Chapter 4)

The following publication has been published:

Wang Q S and F. Takawira " Quantization Effects in Adaptive LMS-MMSE Multi-User Detector". *SATNAC 2001*, pp. 198-201, Wild Coast Sun, KwaZulu Natal, South Africa. (2001) *[Conference proceedings]*

1.4 Dissertation Outline

This chapter has given an overview of digital wireless communication systems and of CDMA systems. The motivation and original contributions of this research are also presented. In Chapter 2, the DS-CDMA system used in this dissertation is given. In addition to this, Chapter 2 presents an overview of DS-CDMA detectors in both the fading and non-fading channel. These are the conventional detector, the optimal multiuse detector, linear and non-linear multiuser detectors, blind adaptive multiuser detector and training-based adaptive multiuser detectors.

Chapter 3 presents an analysis of the quantization effects in the finite precision LMS-MMSE detector. The system model of the finite precision LMS-MMSE detector with the sampling rate equal to the chip rate is given. The analysis in this chapter includes 1) the mean coefficients error, 2) mean coefficients error covariance matrix, 3) the mean square error and 4) the bit error rate. Computer simulation results are presented alongside the analysis results to verify the validity of the analysis.

Chapter 4 presents the power consumption of the finite precision LMS-MMSE detector. Following this, the tradeoff between the power consumption and performance of the finite precision LMS-MMSE detector is analyzed.

In Chapter 5, the convergence behavior of the finite precision LMS-MMSE detector is investigated when the sampling rate is much higher than the chip rate. The mean coefficient error covariance matrix and mean square error are also presented in this chapter. Finally, Chapter 6 presents conclusions of this dissertation and further work is suggested.

Chapter 2
Multiuser Detectors

2.1 Introduction

Although multiuser detection is expected to play a major role in enabling high performance adaptive receivers for next-generation wireless applications, most existing systems do not yet incorporate these advanced techniques. Three primary explanations are offered for this present situation [1]:

1) Developments in the field are relatively recent in origin.
2) Questions persist about the complexity of multiuser algorithms.
3) Low power implementations have only recently become feasible.

This chapter reviews the literature in single-user detection and multiuser detection. Multiuser detection is the basis for the system design and analysis presented in subsequent chapters. There are two important classes of multiuser detectors described, both of which achieve significant performance gains over conventional, single-user detection.

The chapter is organized as follows. Section 2.2 presents the signal model that will be used in this chapter. Section 2.3 is a review of the conventional detector. Following this, Section 2.4 presents the linear and non-linear multiuser detectors (MUD) in a non-fading channel, whilst Section 2.5 presents the MUD in fading channels. Section 2.6 is a review of the adaptive MUD. Finally Section 2.7 concludes this chapter.

2.2 DS-CDMA Signal model

A standard asynchronous DS-CDMA system model with K users and L propagation paths will be considered. Fig. 2.1 is the block diagram of a DS-CDMA system. The modulation scheme used is BPSK with bit duration T and chip duration $T_c = T/N$, where N is an integer called the processing gain. Each user $k \in \{1,...,K\}$ is assigned a discrete-time signature waveform $s_k[t]$ that has unit energy. Independent, binary antipodal data streams $b_k = \{-1,+1\}$ modulate these signature waveforms. The spread data streams can be mathematically written as:

$$x(t) = \sum_{p=0}^{P-1} b_k(p)\, s_k(t - pT), \tag{2.1}$$

where P denotes the total number of symbols transmitted by each user. The spread data streams are then converted to a higher frequency by multiplying them with a carrier. Thus the transmitted signal for the k^{th} user is given by:

$$x(t) = \sum_{p=0}^{P-1} A_k b_k(p) s_k(t - pT)\cos(2\pi f_c t), \tag{2.2}$$

where A_k denote the amplitude of the k^{th} user's carrier frequency.

The received baseband signal at the receiver is a sum of all users' baseband signals, plus an additive white Gaussian noise (AWGN). The received signal $r(t)$ can be expressed as follows:

$$r(t) = \sum_{p=0}^{P-1}\sum_{k=1}^{K}\sum_{l=1}^{L} A_k b_k(p) s_k(t - pT - \tau_{k,l}) c_{k,l}(t) + n(t), \tag{2.3}$$

where $\tau_{k,l}$ represents the propagation delay, and $c_{k,l}(t)$ is the channel fading coefficients. $n(t)$ is the complex zero mean additive white Guassian noise, with a two-sided power spectral density of $N_0/2$ W/Hz.

The received signal is sampled at a rate of $1/T_s$. The sampling rate may be greater or equal to the chip rate, and the received discrete-time signal can be obtained and written in matrix form as follows [2]:

$$\mathbf{r} = \mathbf{SCAb} + \mathbf{n}, \tag{2.4}$$

where the matrices and vector used in equation (2.4) are defined as follows:

- $\mathbf{r} = [\mathbf{r}^{\mathrm{T}}(0),...,\mathbf{r}^{\mathrm{T}}(P-1)]$ is the input sample vector,

  $\mathbf{r}^{\mathrm{T}}(p) = [r(T_s(pSN+1)),...,r(T_s(pSN+SN))]$, where S is the number of samples per chip, and N the number of chips per symbol.

- $\mathbf{S} = [\mathbf{S}^0,...,\mathbf{S}^{P-1}]$ is the sampled spreading sequence matrix with:

  $\mathbf{S}^p = [\mathbf{s}_{1,1}^{(p)},...,\mathbf{s}_{1,L}^{(p)},...\mathbf{s}_{K,L}^{(p)}]$

  $\mathbf{s}_{k,l}^{(p)} = [0_{pSN+\tau_{k,l}}, \mathbf{s}_k^{\mathrm{T}}, 0_{SN(P-p-1)+\tau_{k,l}}]$

  $\mathbf{s}_k = [s_k(0),...,s_k(T_s(SN-1))]^{\mathrm{T}}$,

- $\mathbf{C} = \mathrm{diag}[\mathbf{C}^{(0)},...,\mathbf{C}^{(P-1)}]$ is the channel coefficient matrix with:

  $\mathbf{C}^{(p)} = \mathrm{diag}[\mathbf{C}_1^{(p)},...,\mathbf{C}_K^{(p)}]$

  $\mathbf{C}_k^{(p)} = [c_{k,l}^{(p)},...,c_{K,L}^{(p)}]^{\mathrm{T}}$,

- $\mathbf{A} = \mathrm{diag}[\mathbf{A}^{\mathrm{T}}(0),...,\mathbf{A}^{\mathrm{T}}(P-1)]$ is the total received energies matrix with:

  $\mathbf{A}(p) = \mathrm{diag}[A_1,...,A_K]$,

- $\mathbf{b} = [\mathbf{b}^{\mathrm{T}}(0),...,\mathbf{b}^{\mathrm{T}}(P-1)]^{\mathrm{T}}$ is the data vector with:

  $\mathbf{b}(p) = [b_1(p),...b_K(p)]$,

and $\mathbf{n}$ is the channel noise vector.

In the case of a non-fading channel, there is only one propagation path, and the received discrete-time signal can be written as:

$$\mathbf{r} = \mathbf{SAb} + \mathbf{n}, \tag{2.5}$$

2.3 The Conventional Detector

One of the main attractions of the conventional detector is its low computational complexity. However, the conventional detector does not use any information concerning other users, therefore the performance of this detector is severely degraded because of the effect of multiple access interference (MAI).

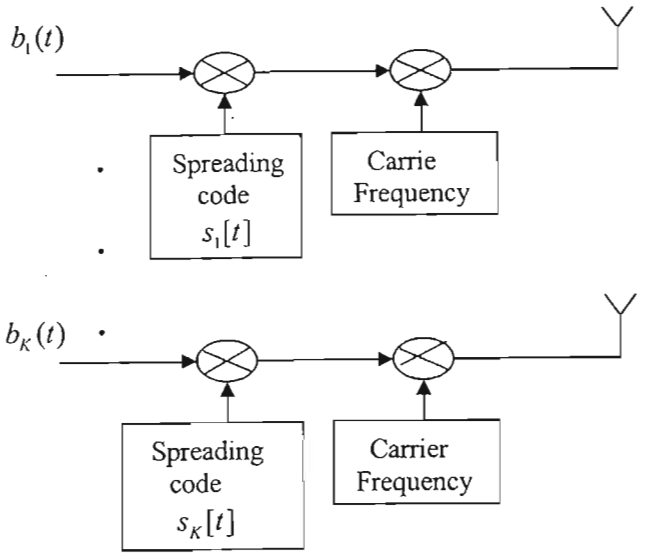

Figure 2.1: Block diagram of DS-CDMA transmitters.

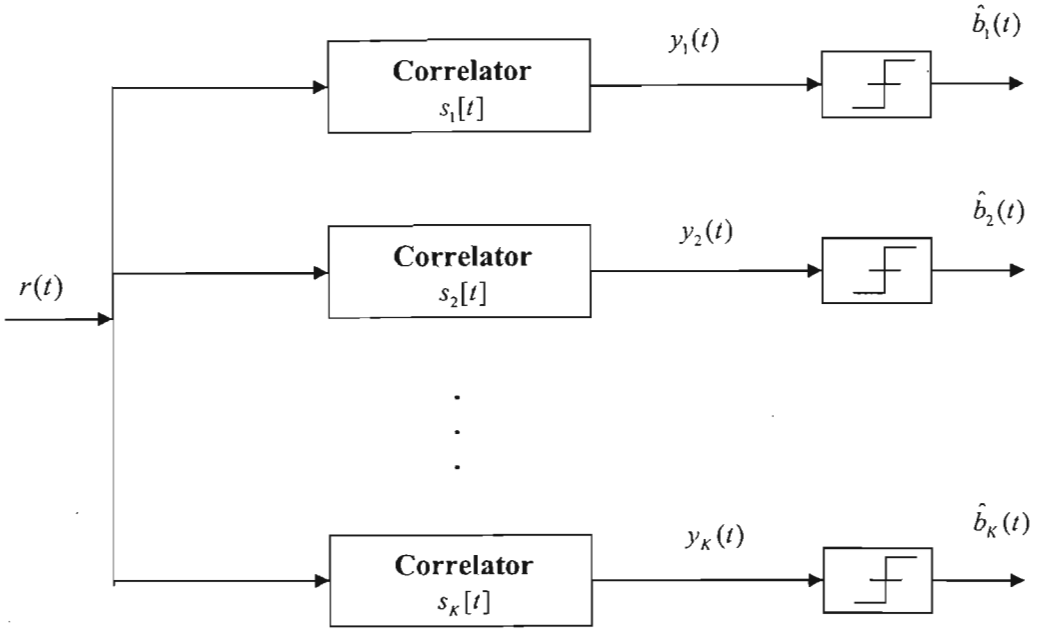

Figure 2.2. The conventional DS-CDMA detector.

In this Section we look at the conventional detector (Fig. 2.2), and the effect of MAI [3]. The system model used in this Section is described in Section 2.2. As shown in Fig. 2.2, the

conventional detector, also known as the matched filter, correlates the desired user's spreading sequence with the received signal. The outputs of the matched filter are then sampled at the bit rate and these sampled outputs are then used as the decision statistics. The decision statistics of the conventional detector in a non-fading channel can be mathematically written as follows:

$$\begin{aligned} \mathbf{y}_k &= \mathbf{S}^T\mathbf{r} \\ &= \mathbf{S}^T\mathbf{SAb} + \mathbf{S}^T\mathbf{n} \\ &= \mathbf{RAb} + \mathbf{S}^T\mathbf{n} \\ &= \mathbf{RAB} + \mathbf{z} \end{aligned}, \tag{2.6}$$

where $\mathbf{R}$ is the cross-correlation matrix that defined as:

$$\mathbf{R} = \mathbf{S}^T\mathbf{S}. \tag{2.7}$$

and $\mathbf{z}$ is a Gaussian random vector with zero mean and a covariance matrix equal to $\sigma^2\mathbf{R}$, where σ^2 is the noise variance, i.e. $\sigma^2 = N_0/2$.

In the case of a fading channel, the channel parameters $\mathbf{C}$ must be estimated, and a variety of strategies can then be applied to obtain reliable channel estimates. Hence the decision statistics of the conventional detector in a fading channel is given by:

$$\begin{aligned} \mathbf{y}_k &= \mathbf{S}^T\mathbf{C}^H\mathbf{r} \\ &= \mathbf{C}^H\mathbf{S}^T\mathbf{SCAb} + \mathbf{S}^T\mathbf{C}^H\mathbf{n} \end{aligned}. \tag{2.8}$$

The final "hard" decisions of the transmitted information are given by:

$$\hat{\mathbf{b}}_k = sign(\mathbf{y}_k). \tag{2.9}$$

It is clearly shown in Fig. 2.2, that the strategy of the detector comes straight from single user designs, where each branch detects one user's information without consideration of the existence of other users. Therefore, the performance of this detector depends highly on the properties of the correlation between the spreading sequences. In order to achieve optimal detection, the correlation between the same user's spreading sequences are required to be much higher than the correlation between the different user's spreading sequences. In other words, the autocorrelation must be much large than the cross-correlation. The correlation value between the spreading sequences is defined as [3]:

$$\rho_{i,k}(\tau) = \frac{1}{T}\int^T s_i[t]s_k[t+\tau]dt, \tag{2.10}$$

In equation (2.10), if $i = k$, then the correlation value $\rho_{k,k}(\tau = 0) = 1$, which presents the autocorrelations of the k^{th} user's spreading sequence. In the case of $i \neq k$, the cross-correlation value of different uses' spreading sequences is $0 \leq \rho_{i,k}(\tau) < 1$. Assuming $\mathbf{C} = \mathbf{I}$, the output of the k^{th} user's matched filter for a particular bit interval can be written as [4]:

$$\begin{aligned} y_k &= \frac{1}{T}\int r(t)s_k[t]dt \\ &= A_k b_k + \sum_{\substack{i=1 \\ i\neq k}}^{K} \rho_{i,k} A_i b_i + \frac{1}{T}\int n(t)s_k[t]dt. \end{aligned} \tag{2.11}$$

The first term in the right hand side of equation (2.11) is the data stream of the k^{th} desired user. The second term is the correlation with all other users, giving rise to MAI. The existence of MAI has a significant impact on the performance and capacity of the conventional detector. This emphasizes the need for low cross- correlations between the spreading sequences, otherwise, the MAI term will dominate the output of the matched filter. The MAI also increases with the number of active users in the system, and is susceptible to power variation amongst users. In other words, users with larger amplitudes can interfere with weak users. Hence the overall effect of MAI on system performance increases, especially when user's signals arrive at the detectors at different amplitudes [3]. Such a situation arises when the transmitters have different distances to the receiver, known as the near-far problem.

MAI can cause a high bit error rate (BER) and poor system capacity, with much work being done on mitigating the effect of MAI. Research has been focused on the following aspects [4, 5, 6, 7, 8]:

- **Spreading Sequence Design.** As can be seen from equation (2.11), if $\rho_{i,k} = 0$, in other words, if the spreading sequences were all orthogonal, then there would be no MAI effect in the outputs of the matched filter. However, it is not possible to design spreading sequences that are orthogonal over all possible delays because in practice most channels contain some degree of asynchronies. The most possible and effective way is to look for the spreading sequences that have as low a cross-correlation as possible. This approach is focused on the design of spreading sequences with low cross-correlation.

- **Power Control.** The near-far problem can be overcome by using power control to ensure that all users' signals arrive at the receiver with the same amplitude. Power control can be implemented by two different strategies. One strategy is called "open loop power control", that is, the mobile unit detects the power level it receives from the base station and then adjusts its transmitted power to be inversely proportional to the power level received from the base station. The other strategy is called "closed loop power control", that is, the base station sends power control instructions to the mobile units.
- **Sectored Antennas.** These directed antennas can focus on a certain angle range of coverage, eliminating the affects of users in different sectors. The direction of the antennas can be fixed or adjusted dynamically.
- **FEC Codes.** The design of forward error correction (FEC) codes allows acceptable error rate performance at lower signal-to-noise ratio levels.

It can be concluded that the conventional detector will perform optimally in a synchronous system with orthogonal spreading sequences and perfect power control. It does not take into account any other users in the system, therefore it is not robust with respect to fading channels, asynchronism and spreading sequences with substantial cross-correlation. In order to mitigate MAI effectively, a number of multiuser detectors have been developed.

2.4 Multiuser Detector in AWGN Channel

Multiuser detection (MUD), also known as Co-Channel Interference Suppression is a technique that can greatly improve the performance and capacity of a CDMA communications system. As discussed in Section 2.3, the increase in MAI not only affects the performance of detectors, but also limits the system capacity. With MUD, it has become possible to reduce or filter out the MAI, enhancing both the performance and capacity.

The optimal multiuser detector was first proposed and analyzed by Verdu in 1986 [9]. Based on the criterion of maximum likelihood estimation, he proposed a cost function, the maximization of which leads to the jointly optimum demodulation of all users. Optimal multiuser detectors require joint estimation of channel parameters and data symbols [10, 11], and so is far too complex for practical implementation, and hence several sub-optimal multiuser detectors have been proposed.

There are two important classes of sub-optimal multiuser detectors. The first class is called "linear multiuser detectors" [12]. These detectors apply a linear mapping (transformation) to the soft output of the conventional detector to produce a new set of outputs. This new set of outputs is treated as the decision statistic and is used to make a decision on the transmitted bits. Popular linear multiuser detectors are: the Decorrelating Detector, the Minimum Mean Square Error (MMSE) detector and the Polynomial Expansion Detector. The second class of sub-optimal multiuser detectors is called "subtractive interference cancellation detectors". Such detectors estimate the interference and then subtract it out. Some examples of subtractive interference cancellation detectors are Successive Interference Cancellation, Parallel Interference Cancellation and Decision Feedback Detectors. Starting with the optimal multiuser detector, a review of these multiuser detectors is presented.

The detection problem in an asynchronous channel is more complicated than in a synchronous channel [13]. In a synchronous channel, the bits of each user are aligned in time, the detection only focus on one bit interval independent of the others. However in most practical implementations, the channel is asynchronous, so there is an overlap between bits of different intervals, thus, the decision can not simply focus on one bit interval only, rather the decision problem must be framed over the whole message [13]. More details of the asynchronous channel are introduced in [14].

2.4.1 Optimal Multiuser Detectors

The optimal multiuser detector is also known as the maximum-likelihood sequence (MLS) detector. An optimal MUD consists of a bank of matched filters, each matched filter decoding one user, follow by a maximum-likelihood sequence estimator, see Fig. 2.3. The function of the maximum-likelihood sequence estimator is to estimate the most likely transmitted sequences $\mathbf{b}$, which maximizes the probability that $\mathbf{b}$ was transmitted, given that $\mathbf{r}$ was received [3]. The probability used here is called "joint a posteriori probability". It can be mathematically written as [3].

$$\mathbf{b} = \arg \max_{\mathbf{b} \in \{-1,+1\}^k} P(\mathbf{b}|\mathbf{r}). \tag{2.12}$$

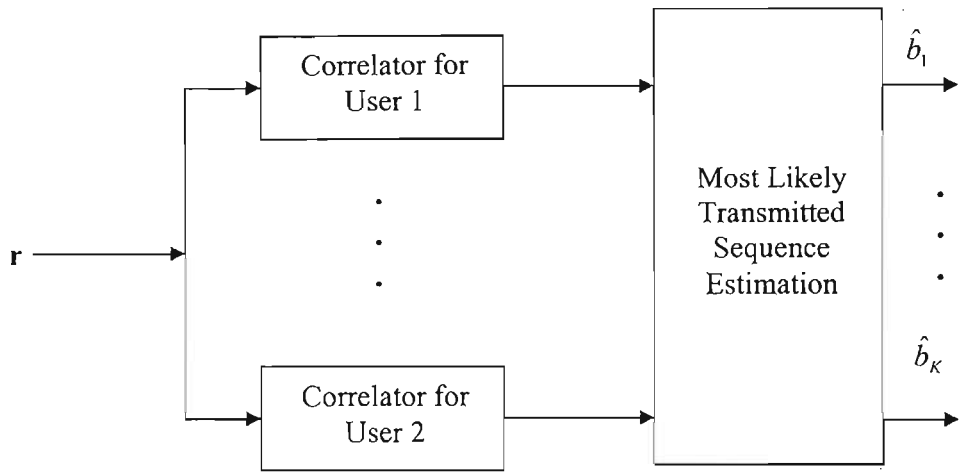

Figure 2.3. Block diagram of optimal multiuser detector.

It is important to expand the analysis of equation 2.12, since it yields the optimal near-far resistance parameter, the best bit error rate (BER) and optimal asymptotic multiuser efficiency [15]. The average optimal near-far resistance in a synchronous DS-CDMA system with random spreading sequences is given by [15]:

$$E[\overline{\eta}_k] = [1 - \frac{K-1}{N}], \tag{2.13}$$

and in a symbol-asynchronous and chip- asynchronous DS-CDMA system, the average near-far resistance is:

$$E[\overline{\eta}_k] = [1 - \frac{2K-2}{N}]. \tag{2.14}$$

The lower bound of the minimum BER with the optimal MUD is given by [15]:

$$P_k(\sigma) \geq 2^{1-w_{k,\min}} Q(\frac{d_{k,\min}}{\sigma}). \tag{2.15}$$

where $w_{k,\min}$ is the smallest possible weight of the error vector $\boldsymbol{\varepsilon} = \mathbf{b} - \hat{\mathbf{b}}$, and $d_{k,\min}$ is one half of the minimum distance between two users' signals that differ in the k^{th} bit.

The optimal asymptotic multiuser efficiency is given by [15]:

$$\eta_k = \min_{\substack{\varepsilon \in \{-1,0,1\} \\ \varepsilon_k = 1}} \frac{1}{A_k^2} \varepsilon^T \mathbf{ARA} \varepsilon . \tag{2.16}$$

If there are K users in the system and each user transmits P symbols, then there are 2^{PK} possible $\mathbf{b}$ vectors with $\mathbf{b} = \{-1, +1\}$. It is obvious that an exhaustive search for all possible $\mathbf{b}$ vectors is impossible for practical implementation. However, the optimal multiuser detector can be implemented for a DS-CMDA system by using a bank of matched filters followed by Viterbi algorithm [16]. This method parallels the use of the Viterbi algorithm to implement MLS detection in channels corrupted by inter-symbol interference [16,17]. The two important properties of MLS detector are:

- Although it becomes possible for a DS-CDMA system to be implemented using the Viterbi algorithm in an MLS detector, unfortunately the number of states in the Viterbi algorithm still grows exponentially with the number of users. Therefore, the overall complexity of MLS detector is still too high to implement in a practical system, especially when the number of users and size of transmitted messages are large.
- Another property of the MLS detector is that the detector requires knowledge of spreading sequences, received amplitudes and phases for all users to be detected. However, those values are not known in a practical system a-priori, therefore they must be estimated [3].

Because of these properties, the MLS detector may be implemented only in situations where a small number of users are to be detected. However, a realistic DS-CDMA system has a relatively large number of active users, the property of exponential complexity in the number of users makes the cost of this detector too high. Therefore a number of sub-optimal multiuser detectors, which offer good performance versus complexity tradeoffs, have been developed.

2.4.2 Linear Multiuser detector

Linear MUD techniques apply a linear mapping to the soft output of the chip-matched filters to reduce the MAI. The result of the linear transformation is known as the decision variable

and is used to make a decision on the transmitted bits. Although some linear MUD, such as MMSE multi-use detector can be implemented adaptively, the MUD still fall under the category of one-shot detectors. The general structure of linear MUD is illustrated in Fig. 2.4. In the following, the three most popular linear MUDs are reviewed.

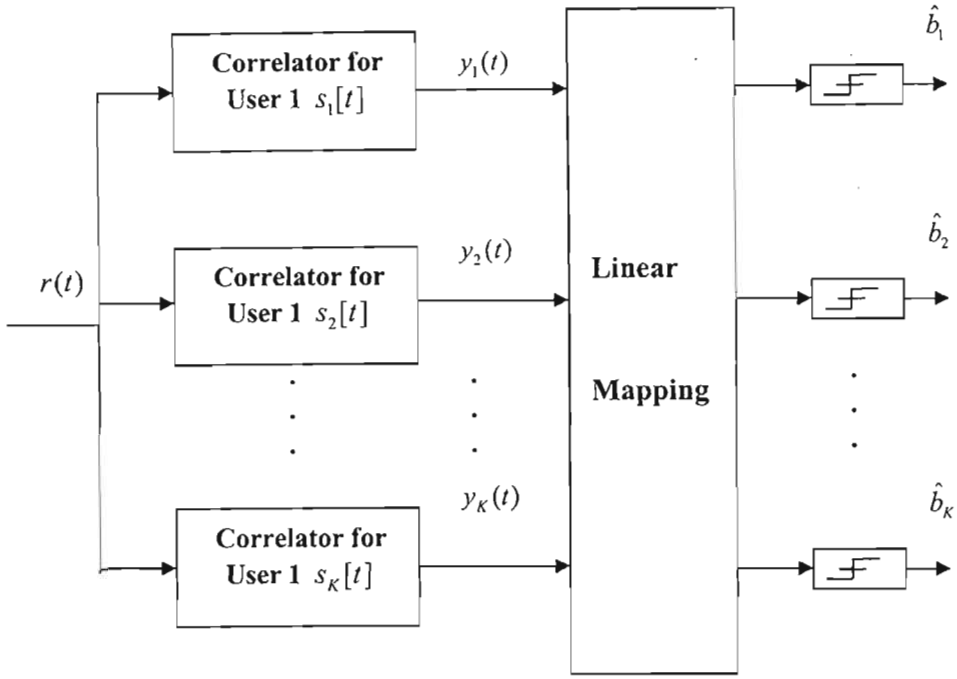

Figure 2.4 The structure of linear multiuser detector.

2.4.2.1 The Decorrelating Detector

The decorrelating detector applies the inverse of the correlation matrix of users' spreading sequences to the soft outputs of the matched filter, with the modified soft outputs of the matched filter referred to as the decision variable.

The discussion begins with the case of a non-fading channel. As shown in Fig. 2.5, the soft output of the matched filter bank can be written as (as discussed in Section 2.3):

$$\mathbf{y} = \mathbf{RAb} + \mathbf{z}. \tag{2.17}$$

In order to see the affect of the MAI, (2.17) is rewritten without consideration of the noise:

$$\mathbf{y} = \mathbf{RAb}\,, \tag{2.18}$$

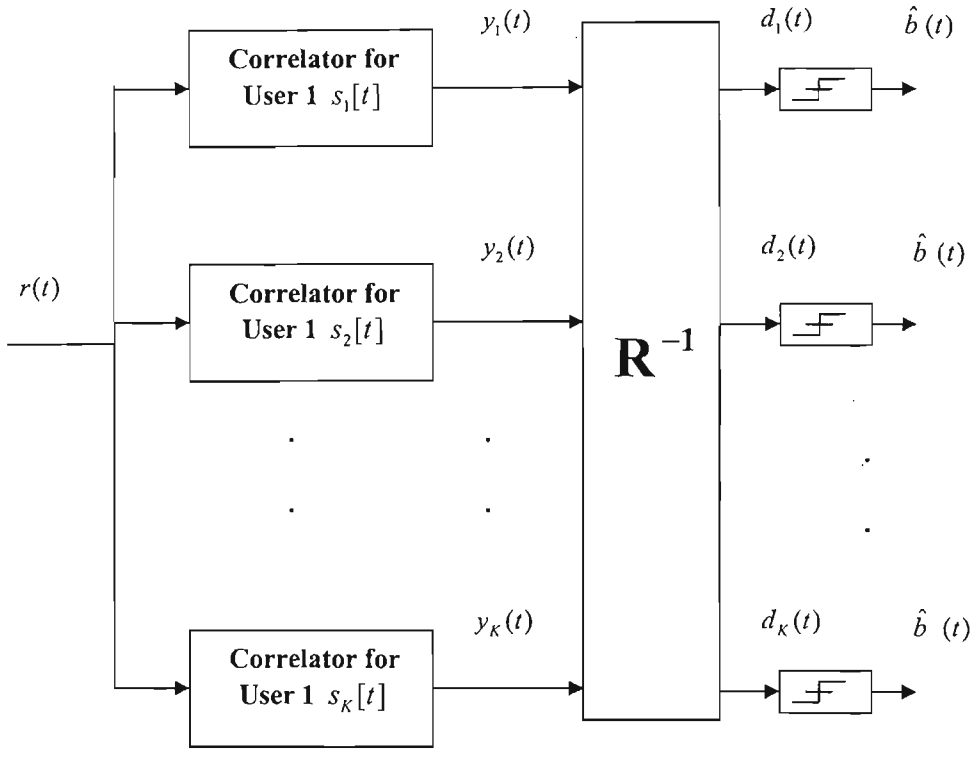

Figure 2.5. The decorrelating DS-CDMA detector.

then the decision variable can be written as [15]:

$$\begin{aligned}\mathbf{R}^{-1}\mathbf{y} &= \mathbf{R}^{-1}\mathbf{RAb} \\ &= \mathbf{Ab}\end{aligned}\,. \tag{2.19}$$

It is followed by:

$$\begin{aligned}\hat{b}_k &= \text{sign}(\mathbf{R}^{-1}\mathbf{y}) \\ &= \text{sign}(\mathbf{R}^{-1}\mathbf{RAb}) \\ &= \text{sign}(\mathbf{Ab}) \\ &= b_k\end{aligned}\,. \tag{2.20}$$

Now, bringing back the noise and premultiplying the outputs of a bank of matched filter with $\mathbf{R}^{-1}$, results in:

$$\begin{aligned}\mathbf{R}^{-1}\mathbf{y} &= \mathbf{R}^{-1}\mathbf{R}\mathbf{A}\mathbf{b} + \mathbf{R}^{-1}\mathbf{z} \\ &= \mathbf{A}\mathbf{b} + \mathbf{R}^{-1}\mathbf{z}\end{aligned} \tag{2.21}$$

As shown in (2.20), the decorrelating detector perfectly decodes the desired user's transmitted bits, as long as the signature waveforms are independent and $\mathbf{R}$ can be inverted.

Furthermore, if we compare (2.19) and (2.21), it clearly shows that the decorrelating detector completely eliminates the MAI, the decision only being affected by the Gaussina noise.

If a set of spreading sequences is given, the BER of the p^{th} bit of the k^{th} user of the decorrelating detector is given as [15]:

$$probability(\hat{b}_k(p) \neq b_k(p)) = Q\left(\frac{A_k}{\sigma[\mathbf{R}^{-1}]_{P.K}}\right). \tag{2.22}$$

where $[\mathbf{R}^{-1}]_{P.K}$ is the diagonal element of $\mathbf{R}^{-1}$,corresponding to the p^{th} bit of the k^{th} user.

The decorrelating detector was first proposed in [18], and analyzed by Lupas and Verdu in [13, 19]. There are some attractive features of the decorrelating detector [13, 19, 20]:

- The decorrelating detector removes the affects of MAI completely, therefore, the detector does not have to estimate or control the received amplitudes and the detection of the desired user can be implemented independently of other users.
- The computational complexity of the decorrelating detector is better than that of the optimal detector. The complexity is linear in the number of users.
- When the energies of all users are not known at the receiver, it corresponds to the maximum likelihood sequence detector. In other words, it yields the joint maximum likelihood sequence estimation of the users' transmitted bits and their received amplitudes.
- Both performance and system capacity of the decorrelating detector have been shown to be much better than those of the conventional detector [17]. The decorrelating detector also has stronger resistance to the near-far problem than that of conventional detector.

The major disadvantage of the decorrelating detector is that, it enhances the noise by the term $\mathbf{R}^{-1}\mathbf{z}$, in other words, the decorrelating detector completely eliminates the affect of the MAI at the expense of enhancing the noise, particularly when the signal-to-noise ratio is low, because $\mathbf{R}^{-1}$ is always greater or equal to 1 for each bit [21]. Despite this disadvantage, the decorrelating detector has been shown to outperform the conventional detector, and has lower computational complexity than the optimal detector.

Another drawback of the decorrelating detector is that, in order to successfully demodulate the transmitted bits, detector needs to invert the matrix $\mathbf{R}$, this increases the computational complexity and makes the detector difficult to implemented in real time. The problem becomes more serious when users use long spreading sequences, because the correlation matrix changes in each bit interval, therefore the computations of the correlation matrix have to be repeated frequently.

In order to avoid the problem of computing the inverse of a large matrix, several sub-optimal approaches have been proposed [3]. A number of algorithms have also been introduced [22], which can be implemented together with the decorrelating detector to avoid computing the matrix inversion.

2.4.2.2 The MMSE Multiuser Detector

The structure of the MMSE detector is shown in Fig. 2.6. The MMSE detector is a linear detector that applies the linear mapping $\mathbf{W}$ to the outputs of the matched filter, resulting:

$$\mathbf{d} = \mathbf{W}^T\mathbf{y}. \tag{2.23}$$

The optimal solution of the linear mapping $\mathbf{W}$ is derived by finding the linear mapping that can minimize the mean square error between the transmitted bits and the output of the linear MUD [15], this can be mathematically written as:

$$MSE_{\min} = \min E\left[\left\|\mathbf{b} - \mathbf{W}^T\mathbf{y}\right\|^2\right], \tag{2.24}$$

then the optimal solution of linear mapping $\mathbf{W}$, is given as:

$$\mathbf{W} = [\mathbf{R} + \sigma^2\mathbf{A}^{-2}]^{-1}, \tag{2.25}$$

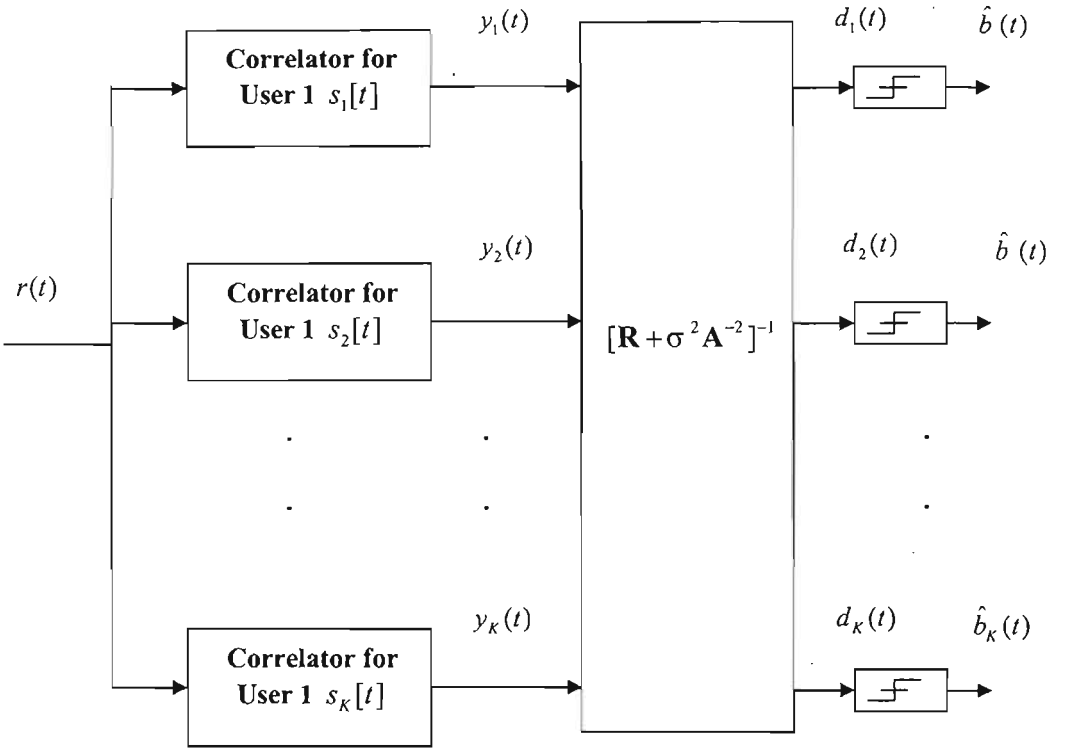

Figure 2.6. The minimum mean square error multiuser detector.

The optimal solution of the linear mapping $\mathbf{W}$, given by (2.25), yields the maximum output signal-to-interference ratio of any linear transformation [15]:

$$\text{SIR}=A_k^2\mathbf{s}_k^T\,\mathbf{å}^{-1}\,\mathbf{s}_k\,, \tag{2.26}$$

Where $\mathbf{å}$, the interference covariance matrix:

$$\mathbf{å}=\sigma^2\mathbf{I}+\sum_{k=2}^{K}A_k^2\mathbf{s}_k\mathbf{s}_k^T\,, \tag{2.27}$$

denotes the covariance matrix of the interference. The probability of error can be written as [15]:

$$P_1^w(\sigma)=2^{1-K}\sum_{b_2,\ldots,b_K\in\{-1,+1\}^{K-1}}Q\left(\frac{A_1}{\sigma}\frac{(\mathbf{W}^T\mathbf{R})_{11}}{\sqrt{(\mathbf{W}^T\mathbf{R}\mathbf{W}^T)_{11}}}\left(1+\sum_{k=2}^{K}\xi_k b_k\right)\right), \tag{2.28}$$

where the leakage coefficient ξ_k is the contribution of the k^{th} user interferer to the decision statistic of the desired user1, and is given by [15]:

$$\beta_k = \frac{B_k}{B_1}, \qquad B_k = A_k(\mathbf{W}^T\mathbf{R})_{1k}. \tag{2.29}$$

As can be seen from equation (2.25), the MMSE MUD not only inverts the correlation matrix $\mathbf{R}$, but also takes the background noise σ^2 into account. As the background noise goes to zero, the performance of the MMSE MUD converges to that of the decorrelating detector. The MMSE MUD decouples the desired user and completely eliminates MAI without the enhancement of background noise, therefore, the MMSE MUD provides better performance than the decorrelating detector.

Unfortunately, like the decorrelating detector, the MMSE detector also faces the task of matrix inversion, increasing the computational complexity of the detector. Another disadvantage is that the MMSE detector requires the estimation of the received amplitudes and the performance of the MMSE detector depends on the powers of the interfering users [3], causing some loss of resistance to the near-far problem.

Most of the sub-optimal approaches for implementing the decorrelating detector are also applicable to the MMSE detector, since both the MMSE detector and the decorrelating detector face the task of matrix inversion. However, the most important property of the MMSE detector is that it can be implemented adaptively to avoid matrix inversion. When implemented adaptively, the linear mapping $\mathbf{W}$ converges to the optimal solution through adaption, and suppresses all the interference from other users and the background. The MMSE detector has been widely used because of this property.

2.4.2.3 The Polynomial Expansion Detector

The Polynomial Expansion (PE) detector, introduced in [23], aims to efficiently implement different linear detectors. The detector does not actually perform matrix inversion, but approximates the desired inverse matrix by a polynomial expansion of the correlation matrix, thus, it can be used to achieve the performance levels of both the decorrelating and the MMSE detector. The polynomial coefficients can be computed using some adaptive algorithms. The PE detector applies the polynomial expansion in $\mathbf{R}$ to the matched filters output $\mathbf{y}$. The linear mapping of the PE detector is [3]

$$\mathbf{L} = \sum_{i=0}^{P} w_i \mathbf{R}^i , \tag{2.30}$$

and the decision variable is given by:

$$\mathbf{d} = \mathbf{L}\mathbf{y} , \tag{2.31}$$

Polynomial coefficients w_i $(i = 0,1,...,P)$ can be chosen to optimize the performance when $\mathbf{R}$ and P are given.

The PE detector can approximate the decorrelating and MMSE detector, therefore it has the benefits of both of these two detectors. Beside this, the PE detector also has some advantages over the decorrelating detector and MMSE detector. Firstly, the PE detector has low computational complexity, secondly, it has a relatively simple structure, with the complexity of the structure increasing linearly with the number of the users and number of stages. Finally, the PE detector does not have to estimate the received amplitudes or phases.

2.4.3 Nonlinear Multiuser Detectors

Nonlinear multiuser detectors utilize feedback to reduce MAI in the received signal. The detectors separately estimate the MAI contributed by each user and then subtract out some or all of the MAI, therefore the detectors are called "Subtractive Interference Cancellation detectors". These detectors are implemented with multiple stages and can be broken down into three classes. The categories are not disjoint and a particular implementation of sub-optimal detectors may use a combination of the three classes.

2.4.3.1 Successive Interference Cancellation Detectors

The Successive Interference Cancellation (SIC) detector takes a serial approach to interference cancellation [24, 25]. Each stage of this detector makes a decision, regenerates, and cancels out one direct sequence user from the received signal, so that the remaining users see less MAI in the next stage. The SIC detector is shown in Fig. 2.7.

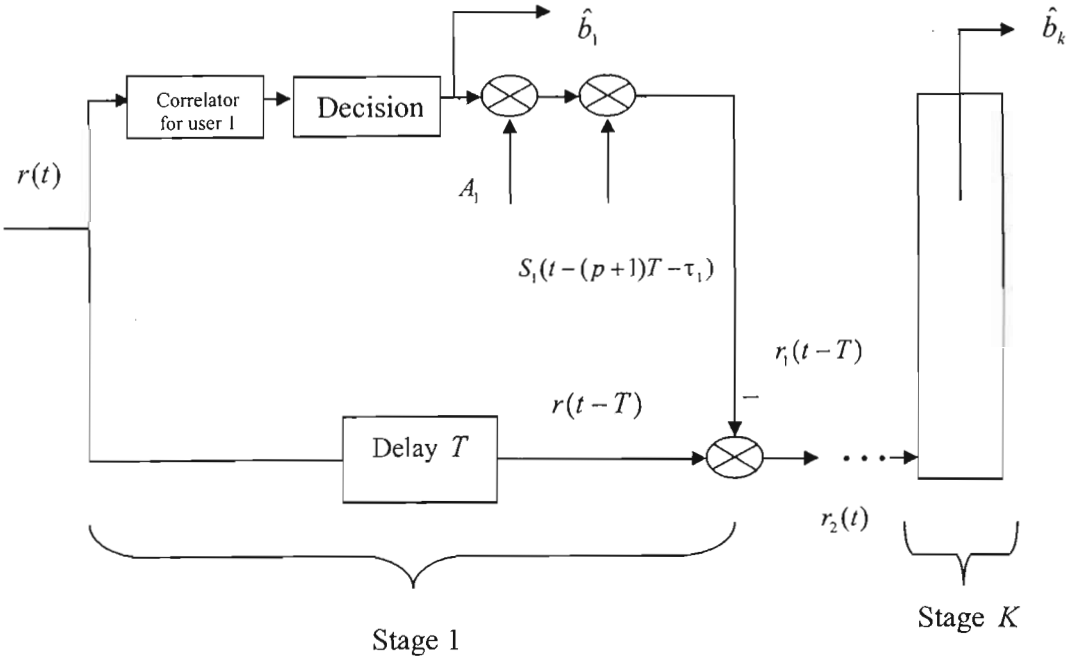

Figure 2.7 Successive interference cancellation (SIC) detectors.

The SIC detector is preceded by a stage which ranks the users in descending order of received power. As can be seen from the diagram, in the first stage, the SIC detector will detect the strongest signal and make the hard decision on this signal for the strongest user, then the detector will regenerate the received signal for this strongest user and subtract it out from the total received signal. A "cleaner" version of the received signal is thus obtained. This process is repeated in a multistage structure [3]. The multistage SIC detector comprises of K stages in series, where K is the number of active users in the system. At the k^{th} stage, the detector takes the cleaned output of the $k-1$ stage as the input of the k^{th} stage, then yields one additional data decision on the k^{th} strongest signal and gives a "cleaner" received signal for next stage.

As discussed before, The SIC detector is preceded by a stage which ranks users in descending order of received power, therefore, the strongest user will not benefit from any MAI reduction; the weakest user will, however, see a huge reduction in its MAI. The SIC detector offers significant performance improvements over the conventional detector, especially when disparity amongst received power levels is large. Also, compared with the conventional detector, the SIC detector only requires a limited additional hardware.

It is intuitively clear that the one of the disadvantage of the SIC detector is that its performance is extremely sensitive to initial bit estimates [3]. If the initial bit estimates are not reliable, then even if the timing, amplitude and phase are perfectly estimated, there is still a big degradation in the performance. Therefore, it is crucial that the data estimates of at least the strong users are reliable. The SIC detector also causes a few difficulties in implementation. First, each stage of cancellation requires one bit delay. Second, when the power profile changes, the sorting operation needs to be performed again, leading to an increase in the complexity of the detector.

2.4.3.2 Parallel Interference Cancellation Detectors

The SIC detector estimate and subtracts out all of the MAI for each user in series. In contrast to the SIC detector, the parallel interference cancellation (PIC) detector estimates and subtracts out all of the MAI for each user in parallel. One stage of a PIC detector is shown in Fig. 2.8. Like the decorrelating or the MMSE detectors, the initial bit estimates, y_k, are typically derived from a conventional detector (the conventional detector is not shown in Fig. 2.8), then the estimated bits y_k are scaled by received power level estimates and re-spread by signature codes. The sum of all the signals of interfering users for each user [3] creates its complete MAI estimate. Subtracting out those complete MAI from the received signal yields the cleaned received signal for each user. These signals are then passed through a second bank of matched filters to produce a new set of decision variables. This process can be repeated for multiple stages, where each stage inputs the bit estimates of the preceding stage and produces a new set of estimates at the output. The multistage PIC structure was introduced in [26] and numbers of papers have investigated PIC detection utilizing soft decisions, such as [27, 28, 29]. PIC and SIC detectors are analyzed and compared in [27], and the SIC detector is found to perform better than the PIC detector in a non-power-controlled channel, however, the performance of the PIC detector is better than that of the SIC detector in a power controlled channel.

Like the SIC detectors, the performance of the PIC detector is severely affected by incorrect initial bit estimates and wrong received power estimates. Thus, several variations on the PIC detector has been developed in order to improve its performance, such as replacing the first matched filters bank (the first matched filters bank is not shown in Fig. 2.8) by a

decorrelating detector to avoid too many incorrect initial bit estimates, improving performance. Another variation on the PIC detector has been developed in [30], using the already detected bits at the output of the current stage to detect the remaining bits in the same stage. Other variations on the PIC detector such as its adaptive implementation can be found in [31,32].

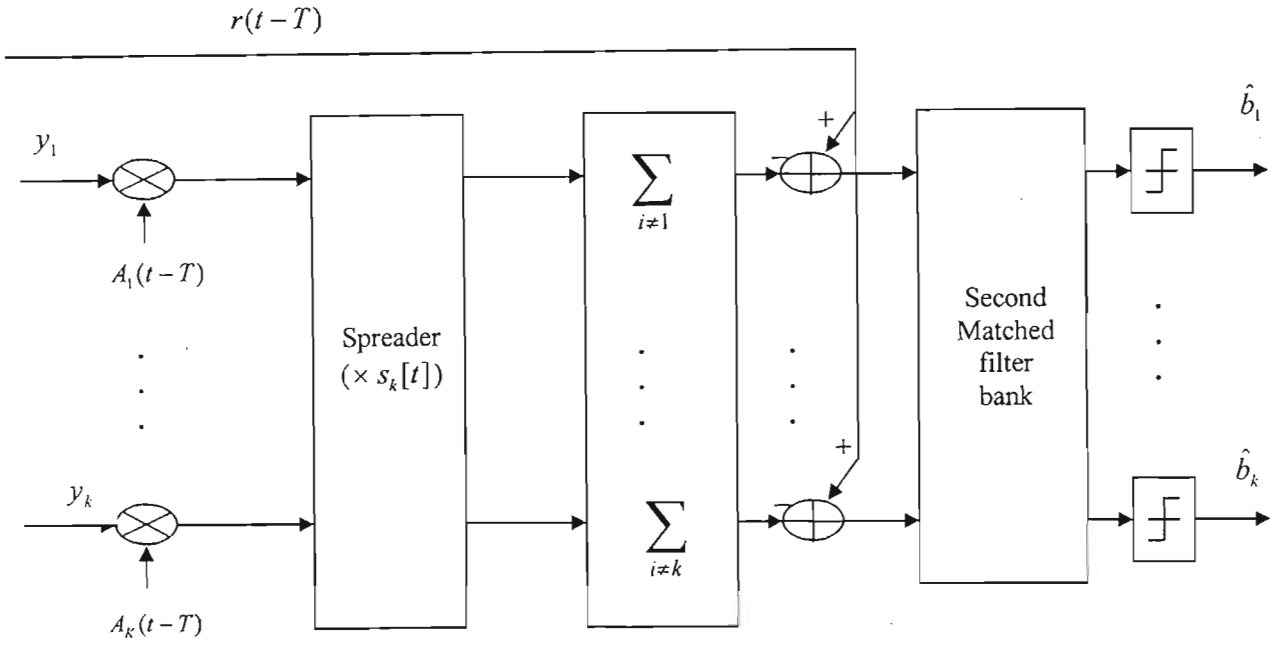

Figure 2.8 One stage of a parallel Interference cancellation detector.

2.4.3.3 Decision Feedback Detectors

The decision feedback detector performs linear pre-processing followed by a structure of SIC detection. The linear operation partially decorrelates the users without enhancing noise, and the SIC operation makes a decision and subtracts out the interference from one additional user at a time, in descending order of strength.

This detector is based on the white noise channel model, which is widely used in single user detection theory. A noise-whitening filter applied in the first stage is obtained from the Cholesky decomposition [33] of the correlation matrix $\mathbf{R}$. The Cholesky decomposition expresses a matrix as the product of a lower triangular and an upper triangular matrix therefore $\mathbf{R}$ can be written as:

$$\mathbf{R} = \mathbf{F}^{\mathrm{T}}\mathbf{F}, \tag{2.32}$$

where $\mathbf{F}$ is the lower triangular matrix, then the matrix, and $(\mathbf{F}^T)^{-1}$ is used as the coefficient of the whitening filter for the noise that is existing in the signal.

Under some assumption [34], the decision feedback detector provides the maximum signal-to-interference ratio and eliminates all MAI. However, it is obvious that the decision feedback detector faces the calculation of the Cholesky decomposition and also needs to invert the matrix. Another disadvantage is that the decision detector has to estimate the received signal amplitudes. A detailed analysis can be found in [35], including a comparison between the decision feedback detector and the decorrelating detector.

2.5 Multiuser Detectors in a Fading Channel

2.5.1 The RAKE Receiver

MAI and fading are the two major factors limiting the performance of mobile wireless communication systems. In Section 2.4, the elimination of MAI through MUDs in CDMA systems has been discussed. However, one of the main advantages of CDMA systems is the ability to use multiple signals that arrive at the receivers with different time delays. This phenomenon is called multipath fading.

The presence of a multipath channel greatly increases the complexity of a multiuser detector. Without multipath, the spreading codes can be selected carefully, in order to minimize the cross-correlation between user signals. In other words, without multipath, the selected optimum code can be an orthogonal code that completely eliminates MAI. A single-user correlation receiver then performs optimally. However, with the presence of a multipath channel, the system cannot guarantee that the received signals are orthogonal at the receiver. This is because after passing the multipath fading channel, desired spreading codes become random and time varying, therefore the cross-correlation between user signals also become channel-dependent.

Certain receiver structures can decode the multipath components separately, e.g. in a fading environment the receiver can use the unfaded components to recover the transmitted signal.

The receiver structure, which takes the multipath components into account, is called a RAKE receiver. The details of the Rake receiver can be found in [35].

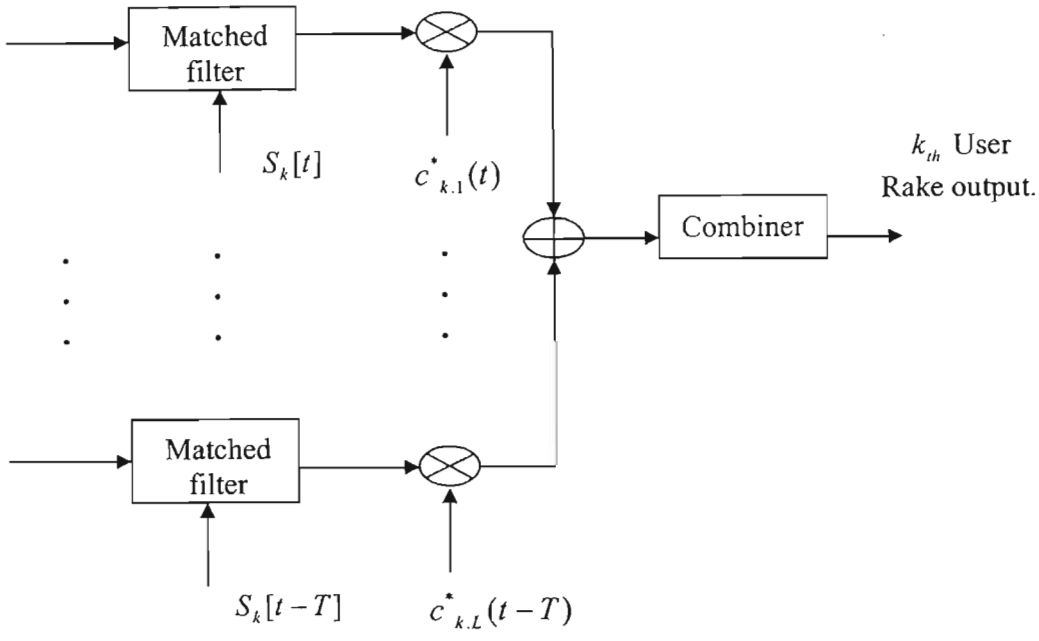

Figure 2.9 Block diagram of the RAKE matched filters for the k^{th} user.

All the multiuser detectors discussed above, including linear and non-linear MUDs, can be extended to multipath fading channels by replacing the matched filters bank by a bank of RAKE matched filters, one for each user. The block diagram of the RAKE matched filters for the k^{th} user is shown in Fig. 2.9.

The RAKE receiver for the k^{th} user consists of L fingers (branches), corresponding with the number of multipath. The RAKE receiver can detect the received signals with different delays separately, and those signals are then combined at the combiner.

Several techniques have been introduced to improve the performance of multiuser detectors over multipath fading channels. A popular technique used for this combination is a diversity technique, called maximum ratio combining [36]. In maximum ratio combining each signal branch is multiplied by a factor which is proportional to the signal amplitude. That is, branches with strong signal become stronger, and weak signals become weaker. Another

technique is to combine the signals from multiple diversity branches, called equal gain combining (EGC). Its performance is almost as good as maximum ratio combining, and it is less complex in terms of signal processing. Sub-optimal implementation of the RAKE filter requires channel coefficient estimation, with the errors of estimation directly degrading receiver performance.

In linear MUDs, such as the decorrelating detector and the MMSE detector, the multipath combining can either happen before the multiuser filtering or after the multiuser filtering, resulting in a post-combining MUD or pre-combining MUD [2], respectively as shown in Fig. 2.10.

Several multiuser detectors used in a fading channel will be introduced in this Section. Rayleigh fading is assumed, throughout.

2.5.2 Decorrelating Detector

Recalling the (2.21), in non-fading AWGN channel, the decision variables of the decorrelating detector are formed by multiplying the outputs of the matched filters by the inverse cross-correlation matrix of the spreading sequences. Therefore the decision variables of the decorrelating detector in non-fading AWGN channel can be written as:

$$\begin{aligned} \mathbf{R}^{-1}\mathbf{y} &= \mathbf{R}^{-1}\mathbf{R}\mathbf{A}\mathbf{b} + \mathbf{R}^{-1}\mathbf{z} \\ &= \mathbf{A}\mathbf{b} + \mathbf{R}^{-1}\mathbf{z} \end{aligned} \quad . \tag{2.33}$$

Now, looking at the decorrelating detector in a multipath fading channel, the decision variables are formed by multiplying the outputs of the matched filters by the inverse cross-correlation matrix of the spreading sequences. Followed by multipath combining, the decision process can be written as:

$$d_k = \mathbf{C}^H\mathbf{R}\mathbf{C}\mathbf{A}\mathbf{b} + \mathbf{C}^H\mathbf{R}^{-1}\mathbf{z}) . \tag{2.34}$$

Liu .H and Li .K [37] have analyzed the performance of the decorrelating detector in a fading channel. In [38], performance differences of pre-combining and post-combining decorrelating detector in known channels have been compared.

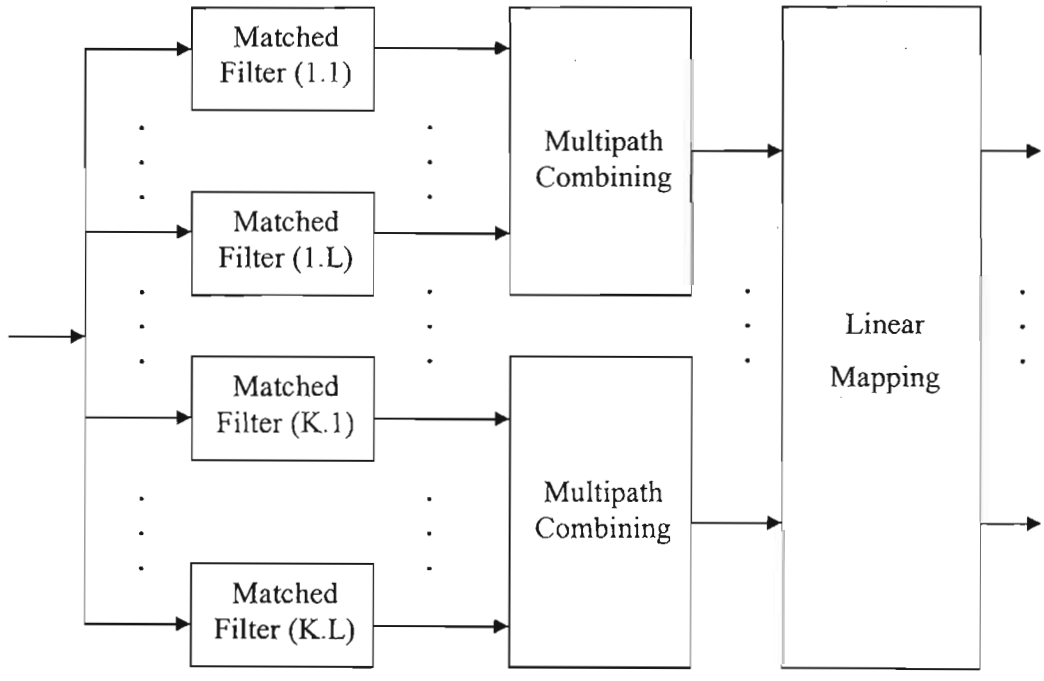

(a) Post-Combining multiuser detector.

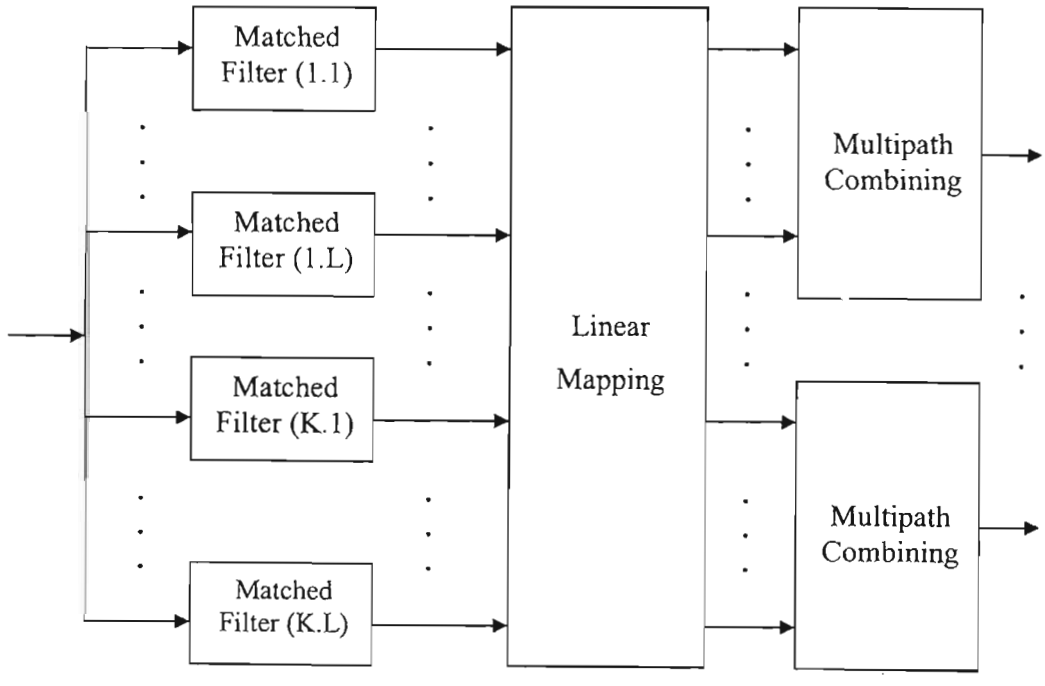

(b) Pre-Combining multiuser detector.

Figure. 2.10. The structures of linear multiuser detector in multipath fading channel.

2.5.3 MMSE Detector

If the multipath combining takes place before the multiuser detection, then it is easy to show that the post-combining MMSE detector is given by [2]:

$$\mathbf{M} = \mathbf{SCA}(\mathbf{AC}^H\mathbf{S}^T\mathbf{SCA} + \sigma^2\mathbf{I})^{-1}. \tag{2.35}$$

It can be seen from (2.35) that the optimal filter coefficients of the post-combining MMSE detector in fading channels depend on the channel coefficient for all users and all paths. The decision variable (the output of the post-combining MMSE detector) can be written as:

$$\mathbf{d} = (\mathbf{AC}^H\mathbf{S}^T\mathbf{SCA} + \sigma^2\mathbf{I})^{-1}(\mathbf{SCA})^H\mathbf{r}, \tag{2.36}$$

The possible way to eliminate the dependence on the fading channel is to implement the MMSE detector as the pre-combining MMSE detector. The pre-combining MMSE detector is given by [2]:

$$\mathbf{W} = \mathbf{S}(\mathbf{S}^T\mathbf{S} + \sigma^2\mathbf{H}^{-1})^{-1}, \tag{2.37}$$

where

$$\begin{aligned} \mathbf{H} &= diag[A_1^2\mathbf{H}_{C1},\ldots,A_K^2\mathbf{H}_{CK}], \\ \mathbf{H}_{Ck} &= daig[E[|c_{k,1}|^2],\ldots,E[|c_{k,L}|^2]]. \end{aligned} \tag{2.38}$$

Therefore the output of the pre-combining MMSE detector can be written as:

$$\mathbf{d} = (\mathbf{S}^T\mathbf{S} + \sigma^2\mathbf{H}^{-1})^{-1}\mathbf{Sr}, \tag{2.39}$$

Assuming the channel is a non-fading AWGN channel, in other words, all the non-zero elements in **C** are equal to 1, then it is clearly seen from (2.35) and (2.37), that the post-combining and pre-combining MMSE detectors are exactly same.

2.5.4 Successive Interference Cancellation Detectors

In Section 2.4.3.1, the SIC detector in non-fading AWGN channel is reviewed. However, to implement the SIC detector in a fading channel using the Rake matched filters to perform the users strength estimation, not only requires information on the users' spreading sequence,

timing and amplitude, but also requires the information on the channel fading. Similarly to the SIC detector in a non-fading channel, the detector process in fading channel can also be repeated in multistage structure, where the multistage SIC detector comprises of K stages in series, where K is the number of active users in the system. At the k^{th} stage, the detector takes the cleaned output of the $k^{th}-1$ stage as the input of the k^{th} stage, then yields one additional data decision on the k^{th} strongest signal, and gives a "cleaner" received signal for next stage. In each stage, the SIC detector performs the following steps:

1. Detects the strongest signal in the stage using the Rake matched filter.
2. Make a hard decision for the strongest user in the stage.
3. Regenerates an estimation of the received signal detected in step 2 for use, using the knowledge of its spreading sequence, time, amplitude and fading coefficients.
4. Subtract out the received signal estimated in step 3 from the total input signal at the stage.

The SIC detector repeats the four steps above until all the users' information has been detected. The SIC detector in a fading channel was presented in [39], and the analysis of the SIC detector in a fading channel can be found in [41, 42, 43].

2.5.5 Parallel Interference Cancellation

The PIC detector in a fading channel uses the output of the first Rake matched filter bank as the initial bit estimates. In order to implement the PIC detector in a fading channel, the detector needs the channel fading coefficients, the propagation delay of the paths of the interfering users and all the other information introduced in Section 2.4.3.2. Using this information, the PIC detector sums up all the input signals except those of the user of interest, which create the complete MAI estimation for the user of interest. Subtracting out this estimated MAI from the received signal, results feed into the second Rake matched filters bank, which yields the decision variable for the user of interest. In [40, 44], the performance of the PIC detector in a fading channel was analyzed.

2.6 Adaptive Multiuser Detection

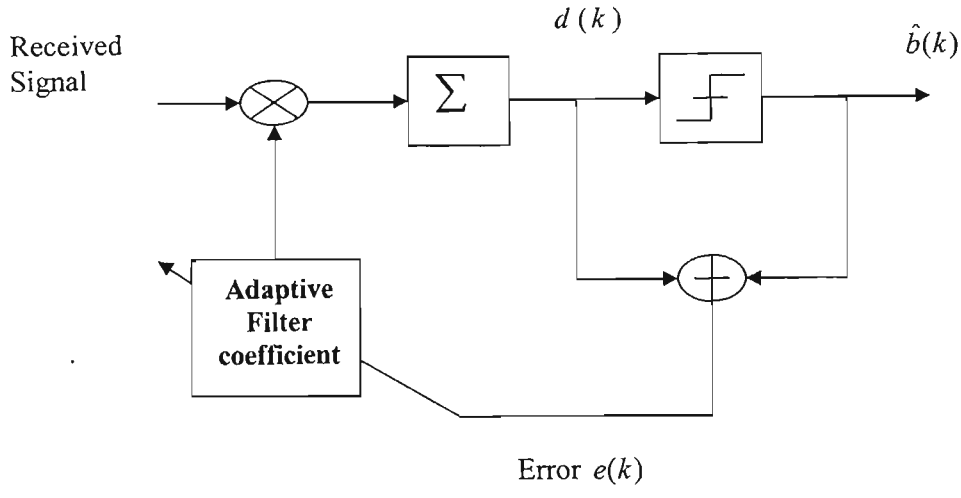

Figure 2.11 Block diagram of an adaptive multiuser detector.

The linear multiuser detection techniques discussed earlier all have significant computational complexity. Adaptive techniques have thus been introduced in many cases to achieve these linear transforms. MMSE detection is very attractive from an implementation perspective and has the following attractive characteristics [2]:

- MMSE criterion results in a convex cost function, which ensures global convergence for iterative algorithms.
- The MMSE detector provides an excellent approximation to the optimal receiver.
- A number of algorithm exist, these algorithms include Least Mean Square (LMS) algorithm and Recursive Least Squares (RLS) algorithm.

The adaptive multiuser detector continuously updates the filter coefficients in order to minimize the MMSE between the output $d(k)$ and the desired signal $\hat{b}(k)$. Fig. 2.11 is a block diagram of an adaptive multiuser detector. The minimum mean square error between the output $d(k)$ and the desired signal $\hat{b}(k)$ can be mathematically written as:

$$MSE_{\min} = \min E\left[\left\|\hat{b}(k) - y(k)\right\|^2\right]. \tag{2.40}$$

When the adaptive multiuser detector is implemented adaptively, the detector eliminates all the effects of interference regardless of whether it is MAI or inter-symbol interference (ISI). Most of the existing adaptive algorithms require training symbols /sequences, an exception is the blind adaptive multiuser detector.

2.6.1 The Blind Adaptive Multiuser Detectors

The adaptive multiuser detector requires the adaptive filter coefficients to be adapted by the use of training symbols. The disadvantage of this detector is that when the system conditions change, the training symbols have to be re-sent to guarantee the performance.

The blind adaptive multiuser detector (BAMUD) eliminates the need for training symbols, as the only information required at the receiver in order to adapt the filter coefficients is the desired user's spreading sequences and timing information. The goal of training-based adaptive multiuser detectors is to minimize the mean square error between the output $y(k)$ and the desired signal $\hat{b}(k)$, rather than do this, the blind adaptive multiuser detector minimizes the mean output energy (MOE), which has been shown to be equivalent to minimizing the MSE. The major difference between the MOE and MSE is that minimizing the MOE does not require the training sequence. More detailed studies about the BAMUD can be found in [45].

2.6.2 Adaptive Algorithms

Implementations of adaptive MMSE multiuser detection require the use of adaptive algorithms that are able to adapt the filter coefficients to their optimal value. Various adaptive algorithms have been developed for implementation in the adaptive process. In this Section, two of the most important adaptive algorithms are described. The Least Mean Square (LMS) adaptive algorithm is introduced firstly, followed by the Recursive Least Squares (RLS) algorithm.

2.6.2.1 LMS Adaptive Algorithms

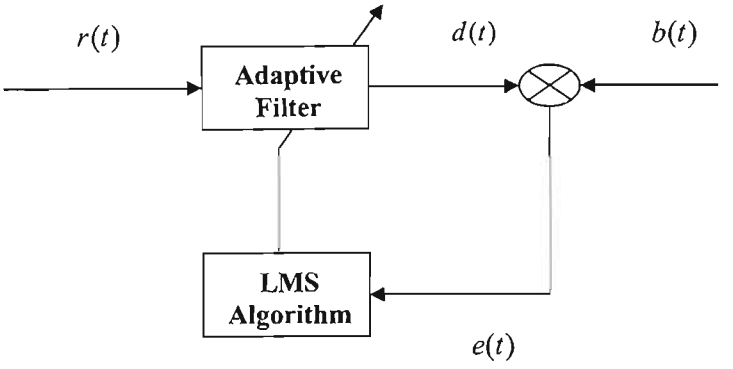

Figure 2.12 Block diagram of the LMS adaptive algorithm

The LMS adaptive algorithm is one of the most commonly used algorithms because of its low computational complexity. Its basic approach is to use the method of steepest descent to iteratively adapt the filter coefficients to the optimal solution. Because the mean squared error performance surface is a quadratic function of the filter coefficients, by using the method of steepest descent, a minimum value of $E[|e(t)|^2]$ can be obtained. According to the method of steepest descent, the filter coefficients are updated as follows:

$$\mathbf{W}(t+1) = \mathbf{W}(t) - \mu\nabla(t), \tag{2.41}$$

where $\mathbf{W}(t)$ is the vector of the adaptive filter coefficients, $\nabla(t)$ is the gradient vector and μ is a positive parameter that controls the rate of convergence, called step-size parameter. However, in practice, it is not possible to find the true gradient vector at the receiver, therefore an approximation is required. The approach taken in the LMS algorithm for approximating the gradient vector is to use a gradient estimate of the instantaneous squared error [46]:

$$\begin{aligned}\nabla(t) &= \frac{\partial e(t)^2}{\partial \mathbf{W}(t)} \\ &= e\frac{\partial(b(t) - y(t))}{\partial \mathbf{W}(t)}\end{aligned} \tag{2.42}$$

It should be noted that the desired signal $b(t)$ is independent of the filter coefficients, therefore the approximation of the gradient vector can be written as [46]:

$$\nabla(t) = -e(t)\mathbf{r}. \tag{2.43}$$

Substituting (2.43) into (2.41), the complete LMS adaptive algorithm is formed:

$$\mathbf{w}(t+1) = \mathbf{w}(t) + \mu e(t)\mathbf{r}, \tag{2.44}$$

where

$$e(t) = b(t) - \mathbf{w}^H \mathbf{r}. \tag{2.45}$$

Convergence speed is an important performance measurement in an adaptive system. As can be seen from the LMS update equation (2.44), the step-size parameter μ plays an important role in determining the convergence speed, therefore the step-size parameter μ must be chosen carefully, it cannot be too larger or too small. If μ is too large, the adaptation process can be unstable, and the filter coefficients may never converge to the optimal MMSE solution. However, if the step-size parameter μ is chosen to be too small, then the filter coefficients may converge to the optimal MMSE solution too slowly to cope with the changing signal statistics. It has been shown that in order to guarantee filter coefficient convergence to the optimal value, the step-size parameter μ has to satisfy:

$$0 < \mu < \frac{2}{N * P_r}, \tag{2.46}$$

where N is the length of the filter coefficients and P_r is the power of input signal. It seems obviously that the step-size parameter should be chosen as:

$$\mu = \frac{2}{N * P_r} \tag{2.47}$$

However, the large step-size used to provide fast convergence speed will cause the filter coefficient to wind around the optimal solution and this phenomenon will introduce excess Mean Square Error (MSE) into the system. In an adaptive system, the total MSE is given by the following equation:

$$MSE_{\text{total}} = MSE_{\min} + MSE_{\text{excess}}, \tag{2.48}$$

Where MSE_{excess} represents the MSE due to the filter coefficients not being optimal, and MSE_{min} is the MSE for the optimal filter coefficient.

There are two reasons for the LMS adaptive algorithm being popular: firstly, the LMS adaptive algorithm has relatively low computational complexity. Secondly, low power implementation of CDMA detector becomes more and more important, the LMS adaptive algorithm also gains popularity as it is well suited to low power implementations. However, the major drawback of this algorithm is its relatively slow convergence speed. A detailed analysis of the LMS adaptive algorithm can be found in many literature sources.

2.6.2.2 RSL Adaptive Algorithms

Compared with the LMS algorithm, the RSL algorithm has faster convergence speed. The RSL algorithm is based on the well know least squares method and the filter coefficients update equation can be written as [46]:

$$\mathbf{w}(t) = \mathbf{w}(t-1) + \frac{\mathbf{p}(t-1)\mathbf{r}(t)}{\alpha(t)} e(t) \tag{2.49}$$

where:

$$\mathbf{p}(t) = \frac{1}{\gamma}[\mathbf{p}(t-1) - \frac{\mathbf{p}(t-1)\mathbf{r}(t)}{\alpha(t)} \mathbf{r}^T(t)\mathbf{p}(t-1)] \tag{2.50}$$

and

$$\begin{aligned} e(t) &= y(t) - \mathbf{r}^T(t)\mathbf{w}(t-1) \\ \alpha(t) &= \gamma + \mathbf{r}^T(t)\mathbf{p}(t-1)\mathbf{r}(t) \end{aligned} \tag{2.51}$$

$\mathbf{p}(t)$ is essentially a recursive way of computing the inverse matrix $[\mathbf{r}^T(t)\mathbf{r}(t)]$, γ is referred as the forgetting factor, and should be within the range of $[0, 1]$.

As mentioned above, one of the advantages of the RLS algorithm is its fast convergence speed, however, from the RLS filter coefficients update equation, it can be seen that the major disadvantage of the RLS algorithm is its high computational complexity, due to matrix inversion. Another drawback is that, unlike the LMS algorithm, the RLS algorithm is sensitive to roundoff errors and finite precision effects, therefore it is not suitable for low power implementation.

2.7 Summary

This chapter has presented a review of MUDs in both non-fading and fading channels. The MAI, fading and multipath are major factors, limiting the capacity and performance of existing wireless mobile communication systems. The existence of MAI has a significant impact on the capacity and performance of the conventional detector. In addition, the presence of strong users exacerbates the MAI of the weaker users, known as the near-far problem. Much research has done to eliminate those problems, resulting in the design of multiuser detection.

Unlike the conventional detector, in multiuser detection, all the information on spreading sequences and timing of multiple users is used to detect each individual user. Although the optimal multiuser detector provides huge gains compared to the conventional detector in performance and system capacity, the major drawback of this detector is that its computational complexity is exponential with the number of users in the system, making the optimal multiuser detector too complex to implement in practical DS-CDMA systems. Therefore, after Verdu proposed the optimal multiuser detector, a number of sub-optimal multiuser detectors have been developed. It has been shown that sub-optimal multiuser detectors offer a good performance versus complexity tradeoff. Most of the sub-optimal multiuser detectors fall into two categories: Linear and non-linear (subtractive interference cancellation) detectors (see Fig. 2.13).

Linear multiuser detectors include decorrelating detectors, minimum mean squared error detectors and polynomial expansion detectors. Linear multiuser detectors apply a linear mapping to the output of the matched filter bank to remove the MAI seen by each user.

The decorrelating detector applies the inverse of the correlation matrix to the output of the matched filter bank. The desirable feature of this detector is that it can be implemented without knowing the received amplitudes.

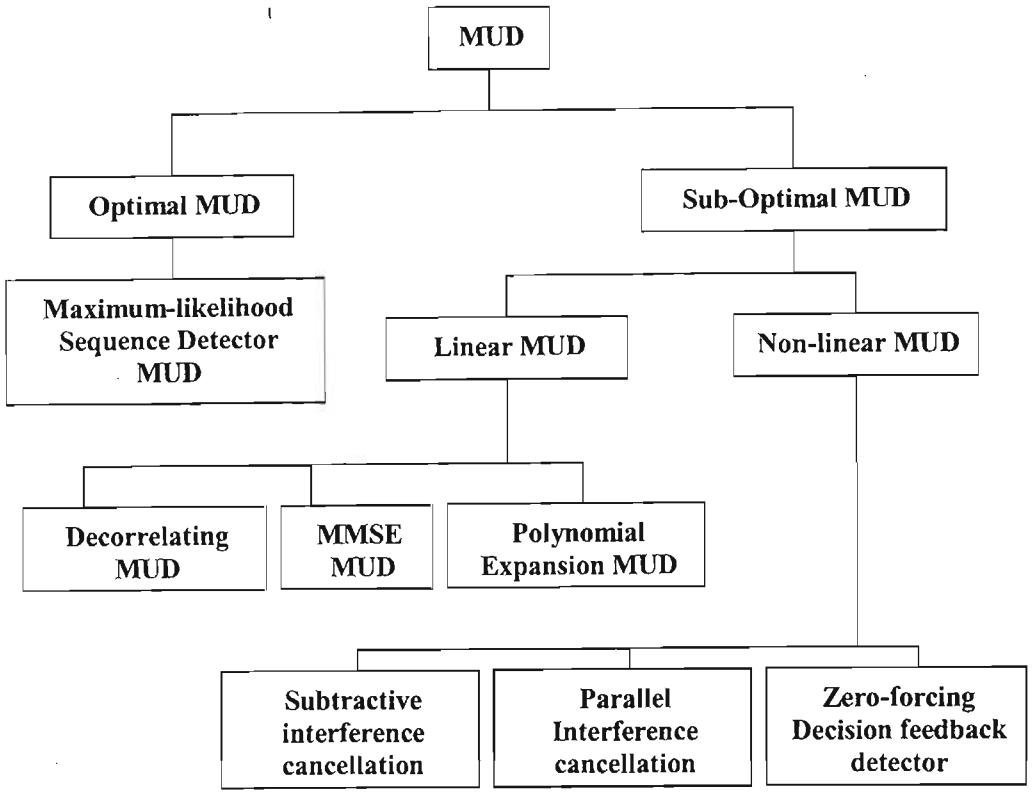

Figure 2.13 The categories of MUDs.

The minimum mean square error detector applies a modified inverse of the correlation matrix to the output of the matched filter bank. Generally, the minimum mean square error detector provides better bit error rate performance than the decorrelationg detector. However, one of the drawbacks of this detector is that it requires an estimation of the received powers. Both the decorrelating detector and the minimum mean square error detector need to compute the cross-correlation matrix. This become very difficult when the codes are long or time-varying, because then the cross-correlations changes with each bit.

The polynomial expansion detector applies a polynomial expansion in the correlation matrix to the output of the matched filter bank. Its most important advantage is that it can approximate either the decorrelating detector or minimum mean square error detector. This detector does not require an estimation of the received amplitudes. The detector can also be easily implemented with long codes.

Non-linear multiuser detectors include the subtractive interference cancellation, parallel interference cancellation and Zero-forcing Decision feedback detectors. Those detectors attempt to estimate and subtract off the MAI. The bit decision used to estimate the MAI can be either a hard or soft decision. Soft decisions provide a joint estimate of data and amplitude and therefore are easier to be implemented, whilst hard decision schemes perform better than the soft decision schemes only when reliable channel estimates can be achieved.

The subtractive interference cancellation detector takes a serial approach to subtracting out the MAI, first making the decision according to the strongest user, then regenerating, and canceling out the strongest user. Thereby a partial clean signal is obtained. This partial clean signal then goes to the next stage, and the process is repeated until all the direct sequence users are canceled out.

In contrast, the parallel interference cancellation detector estimates and subtracts all of the MAI for each user in parallel. The performance of subtractive interference cancellation detector is better than the performance of parallel interference cancellation detectors in a fading channel.

Generally, the parallel interference cancellation detector requires more hardware, and the subtractive interference cancellation detector faces the problem of large delays and power reordering. There are also some subtractive interference cancellation combined with the linear preprocessing, detectors such as the Zero-forcing Decision feedback detector.

The major disadvantage of nonlinear detectors is that their performance is sensitive to the estimation of the received amplitude. An imperfect estimation of the received amplitude can significantly degrade the performance.

Multiuser detectors are currently being researched further, in order to develop a system that can provide good performance as well as low cost. This has drawn more and more attention from researchers and holds much promise for improving DS-CDMA system capacity.

Chapter 3
Finite Precision LMS-MMSE Adaptive Multiuser Detectors

3.1 Introduction

The conventional approach to reception in CDMA systems is to neglect multiple-access-interference (MAI) and inter-symbol-interference (ISI). This imposes tight limits on the system capacity due to interference, even if strict power control is used. A more efficient way to detect different users in a CDMA system is based on multiuser detection. An optimal multiuser detector requires the joint estimation of channel parameters and data symbols, so optimal multiuser detectors are far too complex for practical implementations and hence several sub-optimal multiuser detectors have been proposed.

One of the most popular sub-optimal multiuser detectors is the linear Minimum Mean Square Error multiuser detector [47]. This detector optimally trades-off the attenuation of the non-orthogonal inter-user interference for additive noise enhancement. The standard approach of this detector is to minimize the mean square error between the training data and filter output which requires knowledge of all of the users in the channel, and the channel fading parameters. This information requirement is certainly too stringent for practical applications. The inversion of a matrix is needed to compute the optimal filter coefficients, which greatly increases the complexity of computation. In order to overcome these difficulties, the adaptive MMSE multiuser detector has been developed and investigated by many researchers.

In this chapter, an LMS adaptive filter is used in the MMSE multiuser detector. The LMS algorithm was first introduced by Widrow [48], and coefficients of the filter are iteratively

computed using this LMS adaptive algorithm. Such implementation greatly reduces the computational requirements of the MMSE detector, since the matrix inversion inherent in the computation of the optimal coefficients can be avoided.

The LMS algorithm is one of the most commonly used adaptive algorithms. However, the implementation of this algorithm in hardware needs the use of finite length of bits. The finite precision LMS-MMSE adaptive MUD can be considered as an infinite precision LMS-MMSE adaptive MUD implemented with quantizers in the data path and in the detector coefficients' path. The function of the quantizers is to reduce the wordlength of the coefficients and data. Reducing the wordlength of the bits can both reduce the complexity of the detector, and the power consumption. However, it also causes degradation in the performance. This chapter will look at the finite precision effects in the LMS-MMSE multiuser detector. The analysis of weight error covariance, mean square error (MSE) and bit error rate (BER) will be presented together with the simulation results. In the next chapter, the relationship between the performance and power consumption will be investigated.

The rest of this chapter is organized as follows: In Section 3.2, a brief overview of the adaptive LMS-MMSE MUD is presented. Following this, the system model of a modified LMS-MMSE MUD, which is a finite precision LMS-MMSE MUD, is presented in Section 3.3. The analysis of weight error covariance, MSE and BER for the finite precision LMS-MMSE MUD are also presented in Section 3.3, whilst Section 3.4 presents a review of the slowdown phenomenon. Section 3.5 presents the results, and finally Section 3.6 concludes the chapter.

3.2 The Adaptive MMSE MUD.

As discussed in chapter 2, MUDs in multipath channels can be classified into two categories: pre-combining and post combining MUDs. A post-combining MUD depends on the channel coefficients of all users, and the training signals have to be adapted as the channel changes, therefore, it has severe tracking problems in a fast fading channel. The pre-combining MMSE MUD assumes that the channel fading coefficients are either known or estimated. It only depends on the average channel profiles of the users, therefore, the adaptive

implementation of the pre-combining MMSE MUD has significant advantage when compared to a post-combining MMSE MUD.

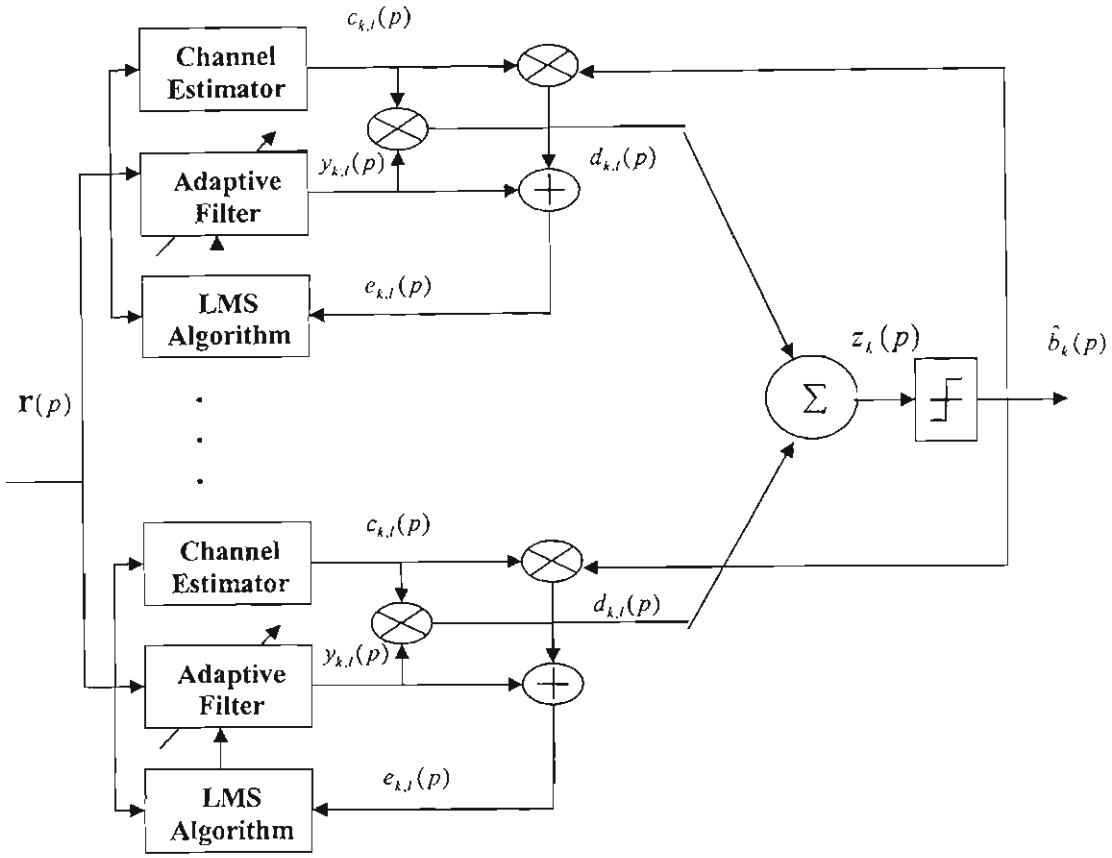

Figure 3.1 Block diagram of the adaptive LMS-MMSE MUD.

3.2.1 System Model

Fig. 3.1 presents the block diagram of the adaptive LMS-MMSE MUD [2]. $\mathbf{r}(p)$ represents the received signal in the p^{th} bits interval. Assuming the considered DS-CDMA system consists of K users in a fading channel with L propagation paths, the received signal can then be written as (the complete description of the signal model can be found in Chapter 2):

$$\mathbf{r} = \mathbf{SCAb} + \mathbf{n}, \tag{3.1}$$

where **S** , **C** and **A** are the matrices of the users' spreading sequences, channel fading coefficients and user's amplitude respectively, and **n** , **b** and **r** are the vectors of the noise samples, users' transmitted bits and received signal respectively. It can be seen from the diagram, that the adaptive pre-combining MMSE MUD does not require additional training sequences, since the product of decisions made by the conventional detector $\hat{b}_k(p)$ and the known or estimated channel fading coefficients can usually be used as the training sequences to train the adaptive filter coefficients.

3.2.2 The Optimal Solution for the MMSE MUD.

The optimal filter coefficients of the post-combining MMSE MUD are obtained through minimizing the following cost function:

$$\mathbf{J} = E[|\mathbf{b} - \hat{\mathbf{b}}|^2]. \tag{3.2}$$

Therefore the optimal filter coefficients of post-combining MMSE MUD are [45]:

$$\mathbf{M} = \mathbf{SCA}(\mathbf{AC}^H\mathbf{S}^T\mathbf{SCA} + \sigma^2\mathbf{I})^{-1}. \tag{3.3}$$

Unlike the Post-combining MMSE detector, the pre-combining MMSE detector selects its weighting coefficients in order to minimize the mean square of the difference between the data amplitude product vector **h** and its estimate. The data amplitude product vector **h** is defined as follows [3, 49, 50]:

$$\mathbf{h} = \mathbf{CAb} \tag{3.4}$$

and

$$\hat{\mathbf{h}} = \mathbf{W}^T\mathbf{r} \tag{3.5}$$

is its estimation. Therefore, the cost function of the pre-combining MMSE MUD can be written as:

$$\mathbf{J} = E[\| \mathbf{h} - \hat{\mathbf{h}} |^2]. \tag{3.6}$$

Combining (3.4), (3.5) and (3.6) together, the expression for the optimal filter coefficients of the pre-combining MMSE MUD is given by:

$$\mathbf{W} = \mathbf{S}\left\{\mathbf{SS}^T + E\left(\sigma^2\left(E[\mathbf{CAAC}^H]\right)^{-1}\right)\right\}^{-1}. \tag{3.7}$$

3.2.3 The LMS-Based MMSE MUD

The received signals are fed into the LMS-MMSE MUD with filter coefficients $\mathbf{w}_{k,l}(n)$, and the output of the *lth* branch for the *nth* symbol is given by:

$$y_{k,l}(p) = \mathbf{w}^{H}{}_{k,l}(p)\mathbf{r}(p). \tag{3.8}$$

Either channel fading coefficients $c_{k,l}(p)$ are known or are estimated. The hard decisions of the LMS-MMSE MUD are given by:

$$\hat{b}_k(p) = \text{sign}\left(\sum_{l=1}^{L} c_{k,l}(p) y_{k,l}(p)\right). \tag{3.9}$$

It is not possible to calculate the optimal filter coefficients of the pre-combining MMSE MUD directly because of its computational complexity. An adaptive filter, based on the iteratively solving the optimization problem, is used. The most widely used method is the estimation of the gradient of the error function, which provides the steepest descent on the MSE error surface [46, 51]. Thus the filter coefficients are updated by:

$$\mathbf{w}_{k,l}(p+1) = \mathbf{w}_{k,l}(p) + \mu e_{k,l}(p)\mathbf{r}(p), \tag{3.10}$$

Where the error $e_{k,l}(p)$ between the desired signal and its estimates is given by:

$$e_{k,l}(p) = d_{k,l}(p) - \mathbf{w}_{k,l}{}^{H}\mathbf{r}(p). \tag{3.11}$$

It should be noted that in the adaptive version of the MMSE MUD, the filter coefficient could be decomposed into two components: the fixed and adaptive components. This can be mathematically expressed as (see Fig. 3.2):

$$\begin{aligned} \mathbf{w}_{k,l}(p) &= \mathbf{w}_{fixed} + \mathbf{w}_{adaptive} \\ &= \mathbf{s}_{k,l}^{T} + \mathbf{x}_{k,l}(p) \end{aligned} \tag{3.12}$$

where the $\mathbf{w}_{fixed}$ component is given by:

$$\mathbf{w}_{fixed} = \mathbf{s}_{k,l}^{T} = [0_{pSN+\tau_{k,l}}, \mathbf{s}_k^{\mathrm{T}}, 0_{SN(P-p-1)-\tau_{k,l}}]^{T} \tag{3.13}$$

This gives the fixed spreading sequence for users with the delay $\tau_{k,l}$, and performs the function of the correlators. The adaptive component $\mathbf{x}_{k,l}(p)$ can be updated as shown in the following equations:

$$\begin{aligned} x_{k,l}(p+1) &= x_{k,l}(p) + \mu e_{k,l}(p)\mathbf{r}(p) \\ e_{k,l}(p) &= d_{k,l}(p) - y_{k,l}(p) \end{aligned}, \tag{3.14}$$

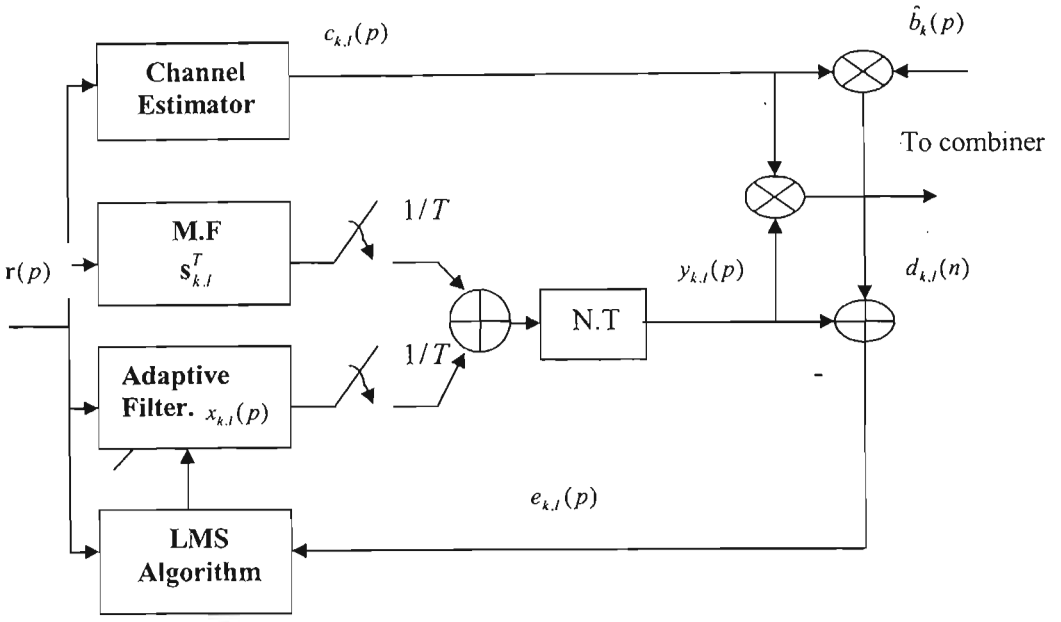

Figure 3.2. One receiver path in the adaptive LMS-MMSE MUD.

The error, $e_{k,l}(p) = d_{k,l}(p) - y_{k,l}(p)$, produced by the difference between the estimate and training signals, is used to update the filter coefficients. As shown in Fig. 3.2, in pre-combining LMS-MMSE MUDs, the training signals $d_{k,l}(n)$ are the product of the channel coefficients estimates and data symbols, this is given by:

$$d_{k,l}(p) = c_{k,l}(p)\hat{b}_k(p), \tag{3.15}$$

In this system model, in order to make the analysis of the LMS-MMSE MUD mathematically tractable, additive white Gaussian noise and the users' transmit bits are assumed to have the following properties [46]:

- The users' transmitted bits are statistically, independent of the previous bits and the next bits, as shown by:

$$E[\mathbf{b}(p)\mathbf{b}^H(p-1)] = 0, \tag{3.16}$$

- The sample vector of the received signals is statistically uncorrelated with all past bits of the training sequence, as shown by:

$$E[\mathbf{r}(p)d_k^{H}(p-1)]=0, \tag{3.17}$$

- The training sequences are dependent on the corresponding sample vector and channel information, but statistically uncorrelated with the past training sequences.

- The mean value of additive white Gaussian noise is zero, and is statistically independent of the users' transmitted bits, as shown by:

$$\begin{aligned} E[\mathbf{n}]&=0 \\ E[\mathbf{b}\mathbf{n}^{H}]&=0 \end{aligned}, \tag{3.18}$$

3.2.3.1 Convergence Properties of the LMS-Based MMSE MUD

This section gives a brief review of the convergence properties of the LMS-MMSE detector [51]. The convergence behavior has drawn great interest both in practice and in theory because it determines the number of reference signals required. Recalling the LMS algorithm update equation and assuming that $l=1$, then l can be dropped off from the update equation:

$$\mathbf{w}_k(p+1)=\mathbf{w}_k(p)+\mu e_k(p)\mathbf{r}(p), \tag{3.19}$$

Define the difference between the computed filter coefficients and the optimal filter coefficients is given by $\Delta\mathbf{w}_k$:

$$\Delta\mathbf{w}_k(p)=\mathbf{w}_k(p)-\mathbf{w}_{opt}, \tag{3.20}$$

then the update equation for $\Delta\mathbf{w}_k$ can be written as [46]:

$$\Delta\mathbf{w}_k(p+1)=(\mathbf{I}-\mu\mathbf{r}(p)\mathbf{r}^{H}(p))\Delta\mathbf{w}_k(p). \tag{3.21}$$

Now, define:

$$\mathbf{V}=E[\mathbf{r}(p)\mathbf{r}^{H}(p)]. \tag{3.22}$$

Under the condition that $\Delta\mathbf{w}_k(p)$ is independent of $\mathbf{r}(p)$, then the expectation of (3.21) together with (3.22), gives the expression for the updating equation for $\Delta\mathbf{w}_k$:

$$E[\Delta\mathbf{w}_k(p+1)] = E[\mathbf{I} - \mu\mathbf{V}]E[\Delta\mathbf{w}_k(p)]. \tag{3.23}$$

It is clearly seen that the step-size parameter is one of the major factors affecting the convergence speed of the LMS algorithm. If the step-size parameter is chosen to be too small, then the adaptation is slow, however, the excess MSE will also be small after adaptation. In contrast, if the step-size parameter is large, then the convergence speed is relatively fast, at the expense that the excess MSE is large after adaptation. However, when the LMS algorithm is implemented in the pre-combining MMSE MUD, the step-size parameter can be set more freely, since the pre-combining MMSE MUD does not require the tracking of the channel fading coefficients, but has to satisfy the condition described in (3.24) to ensure that the filter coefficients converge to the optimal solution [46, 52].

$$0 < \mu < \frac{2}{\lambda_{\max}}, \tag{3.24}$$

where $\lambda_{\max}$ is the maximum eigenvalue of the matrix $\mathbf{V}$. However, quite often, the step-size parameter is set as:

$$\mu = \frac{\mu'}{\mathbf{r}^H(p)\mathbf{r}(p)}, \tag{3.25}$$

where $0 < \mu' < 1$. The LMS adaptive algorithm with this step-size parameter is also called the normalized LMS algorithm.

Another important factor that affect the convergence of the LMS-MMSE MUD is the spreading range of the eigenvalues of the correlation matrix $\mathbf{V}$ [53]. If the correlation matrix $\mathbf{V}$ is spread widely, this is when the ratio of $\lambda_{\max}$ to $\lambda_{\min}$ is large, the convergence speed of the LMS algorithm will be slow. In contrast, if the ratio of $\lambda_{\max}$ to $\lambda_{\min}$ is small, the step-size parameter can be chosen so that the convergence speed of the LMS algorithm can be relatively fast.

3.2.3.2 BER of the LMS-Based MMSE MUD

The performance of the pre-combining MMSE MUD is analyzed in a known channel to obtain the average bit error probability, based on the characteristic function method presented in [54]. The output of the filter for the l^{th} path and k^{th} user is given by:

$$y_{k,l}(p) = \mathbf{w}_{k,l}^{H}(p)\mathbf{r}(p). \tag{3.26}$$

Therefore, after maximum ratio combining, the decision variable of the pre-combining MMSE MUD can be written as:

$$\mathbf{z}_k(p) = \mathbf{c}_k^{H}(p) y_k(p), \tag{3.27}$$

In order to derive the BER expression, the vector $\mathbf{c}_k(p)$ for the k^{th} user is assumed to be a complex Gaussian vector with zero mean.

$$\mathbf{c}_k(p) = [c_{k,1}(p),...,c_{k,L}(p)], \tag{3.28}$$

and

$$y_k(p) = [y_{k,1}(p),...,y_{K,L}(p)]. \tag{3.29}$$

Now define [3]:

$$\mathbf{Q} = \begin{pmatrix} \mathbf{0}_L & \mathbf{I}_L \\ \mathbf{I}_L & \mathbf{0}_L \end{pmatrix}. \tag{3.30}$$

and

$$\nu = [\mathbf{c}_k^{T}(p), \mathbf{y}_k^{T}(p)]^{T}, \tag{3.31}$$

then (3.27) can be written by using (3.30) and (3.31), and the decision variables have the new form [55, 56]:

$$z_k(p) = \nu^{H}\mathbf{Q}\nu. \tag{3.32}$$

Since the vector $\mathbf{c}_k(p)$ for the k^{th} user is Gaussian and the output vector of the filter $y_k(p)$ conditioned on the data symbol $\mathbf{b}_k(p)$ is also a complex Gaussian random vector, the BER for user k conditioned on the data symbol, can be written as [55, 56]:

$$P(error \mid \mathbf{b}_k(p)) = \sum_{\substack{i=1 \\ \lambda_i<0}}^{2L} \prod_{\substack{j=1 \\ j\neq i}}^{2L} \frac{\lambda_i}{\lambda_i - \lambda_j}. \tag{3.33}$$

where λ_i, $i=1, 2,..., 2L$ are the eigenvalues of the matrix $M_{\nu\nu^H|\mathbf{b}_k(p)}\mathbf{Q}$, and $M_{\nu\nu^H|\mathbf{b}_k(p)}$ is the covariance matrix of the vector ν, given by:

$$M_{\nu\nu H|\mathbf{b}_k(p)} = \begin{pmatrix} M_{\mathbf{c}_k(p)} & M_{\mathbf{c}_k(p)\mathbf{y}_k^H(p)|\mathbf{b}_k(p)} \\ M_{\mathbf{c}_k^H(p)\mathbf{y}_k^H(p)|\mathbf{b}_k(p)} & M_{\mathbf{y}_k(p)|\mathbf{b}_k(p)} \end{pmatrix}. \tag{3.34}$$

Finally, the bit error probability of the *kth* user of the pre-combining MMSE MUD in a fading channel is given by [3]:

$$P_k = \frac{1}{2^{PK-1}} \sum_{\substack{\bar{\mathbf{b}}(p)\in\{-1,1\}^{PK-1} \\ b_k=1}} P\{error\,|\,\bar{\mathbf{b}}(p)\}. \tag{3.35}$$

To derive the expression for the BER of the adaptive LMS-MMSE MUD, a simpler approximation would be to assume that the distribution of the k^{th} user's decision variable has a gaussian distribution.

According to the Wiener Filter solution, the optimal filter coefficients of the adaptive LMS-MMSE MUD can be written as:

$$\mathbf{w}_{opt} = \boldsymbol{\alpha}_k \mathbf{V}^{-1}. \tag{3.36}$$

where:

$$\mathbf{V} = E[\mathbf{r}(p)\mathbf{r}^H(p)]. \tag{3.37}$$

and the correlation function $\boldsymbol{\alpha}_k$ for the user of interest is defined as:

$$\boldsymbol{\alpha}_k = E[\mathbf{r}(p)b_k]. \tag{3.38}$$

For the adaptive LMS-MMSE MUD, the relationship between the output signal-to-noise ration (SNR) and minimum MSE are always satisfied by the following condition [51]:

$$SNR = \frac{1\text{-}MSE_{\min,k}}{MSE_{\min,k}}. \tag{3.39}$$

Therefore the expression for the BER of the k^{th} user can be written as:

$$BER_k = Q\left(\frac{1\text{-}MSE_{\min,k}}{MSE_{\min,k}}\right). \tag{3.40}$$

where Q is given by:

$$Q(x) = \int_{x}^{\infty} \frac{1}{\sqrt{2\pi}} \exp\left(-\frac{u^2}{2}\right) du \,. \tag{3.41}$$

The relationship presented in (3.40) also holds when there is residual inter-symbol interference (ISI). The minimum MSE that can be achieved by the detector for the k^{th} user can be written as:

$$MSE_{\min,k} = 1 - \boldsymbol{\alpha}_k^H \mathbf{V}^{-1} \boldsymbol{\alpha}_k \,. \tag{3.42}$$

Equation (3.42) represents the minimum MSE that can be achieved by the k^{th} user's adaptive filter, however, when a misadjustment occurs, the total MSE at the output of the k^{th} user is given by the following expression [47]:

$$MSE_k = 1 - \mathbf{w}_k^H \boldsymbol{\alpha}_k - \boldsymbol{\alpha}_i^H \mathbf{w}_k + \mathbf{w}_k^H \mathbf{V} \mathbf{w}_k \,. \tag{3.43}$$

When infinite training symbols are used, MSE_k can be written as follows [46, 51]:

$$\begin{aligned} MSE_k &= MSE_{\min,k} + MSE_{exc,k} \\ &= MSE_{\min,k} \left(1 + \sum_{i=1}^{P} \frac{\mu\lambda_i}{2 - \mu\lambda_i}\right). \end{aligned} \tag{3.44}$$

Thus the BER expression for the LMS-MMSE detector in a non-fading channel is given by the following expression:

$$BER = Q\left(\frac{1\text{-}MSE_k}{MSE_k}\right). \tag{3.45}$$

In a fading channel, the average BER can be calculated under the conditional that the channel fading coefficients are non-time varying. The average BER under this condition can be obtained as follows:

$$BER = E\left(Q\left(\frac{1 - MSE_k}{MSE_k}\right)\right). \tag{3.46}$$

3.3 Finite Precision LMS-MMSE MUD

3.3.1 Introduction

There have been many strategies developed to reduce power consumption over the last decade, these include reduction of clock speed and data rate, parallelization and pipelining of operations, differential encoding of data [57, 58], sign-magnitude algorithm and reduction of voltage. This dissertation looks at the widely used adaptive LMS-MMSE MUD, where the strategy used for power reduction is to reduce the number of bits used to represent data and digital filter coefficients in the LMS-MMSE MUD. Reducing the number of bits used to represent data and coefficients can reduce the complexity of the detectors, and therefore, the power consumption is reduced. This strategy can be implemented with any hardware constructions and can also be easily adjusted in real time.

However, reducing the number of bits used to represent data and digital filter coefficients can degrade the performance of the system. Previous publications have studied the finite precision effects on the behavior of the LMS adaptive algorithm. However, so far, no work has been done on performance analysis of the finite precision LMS-MMSE detector, as measured by the adaptive filter coefficients convergence rate, steady state MSE and BER.

3.3.2 System Model of the Finite Precision LMS-MMSE MUD

The finite precision LMS-MMSE MUD can be viewed as an infinite precision LMS-MMSE MUD, implemented with separate uniform scalar quantizers in the data and filter coefficient paths. The detector adapts the coefficients of the LMS-MMSE MUD using the received signals together with the error signals obtained by subtracting the soft output from the reference signals. Fig. 3.3 shows the block diagram of the finite precision LMS-MMSE MUD in the multipath fading channel, with two different quantizers for data and coefficients, respectively.

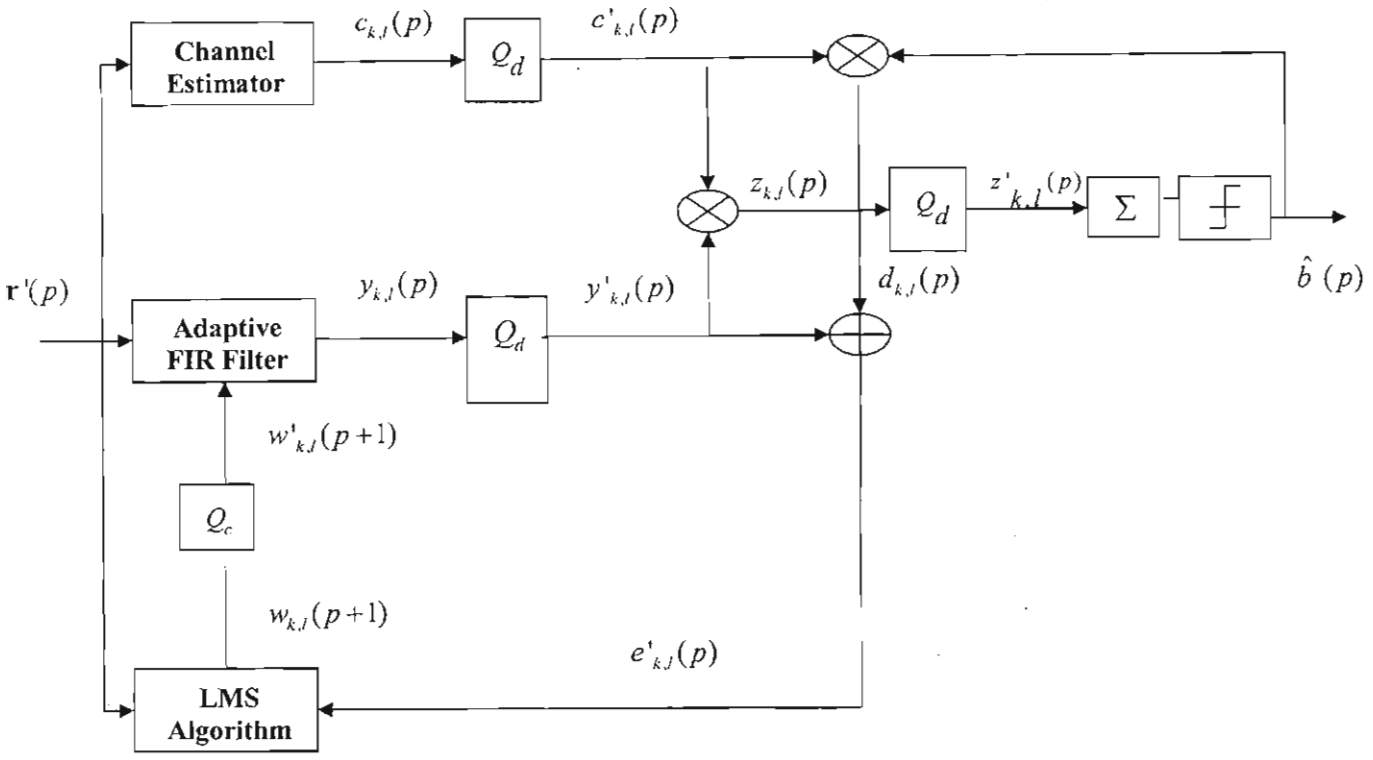

Figure 3.3 Finite precision LMS-MMSE MUD (one branch).

The unprimed and primed symbols are used to represent quantities of infinite and finite precision, respectively. Some important notations are also present below:

$\mathbf{r}(p) = [r(p),...,r(p-N+1)]$: The received signal vector with length N equals to the number of filter taps.

$y_{k,l}(p)$: The output of the filter.

$d_{k,l}(p)$: The reference signal, equal to the product of the estimated channel coefficients and data symbols.

$z_{k,l}(p)$: The decision variable before quantization, which is formed by the product of the output of the l^{th} detector path and the estimated channel coefficients.

$w_{k,l}(p)$: The adaptive coefficient of a N-taps FIR filter.

$c_{k,l}(p)$: The complex coefficients of the fading channel.

$e_{k,l}(p)$: The error signal produced by the difference between the filter output and the reference signals.

Q_d : The quantizer for all the data.

Q_c : The quantizer for the coefficients.

The value of the input signals of the LMS-MMSE MUD is assumed to have been properly scaled to lie between –1 and +1. The quantizers Q_c and Q_d are allocated B_c bits plus sign and B_d bits plus sign, respectively, and will add the complex white quantization noise to both the data and the coefficients. The noise variance of the quantizer Q_c is given by [59]:

$$\delta_c^2 = (\frac{1}{12}) * 2^{-2B_c} . \tag{3.47}$$

and for quantizer Q_d:

$$\delta_d^2 = (\frac{1}{12}) * 2^{-2B_d} . \tag{3.48}$$

The above two equations represents the variances of the quantization noise when the quantizers are allocated B_c bits plus sign and B_d bits plus sign, respectively. In each quantization operation, the quantizer will introduce an additional noise to its input sequences. Therefore, the quantized values can be looked as the summation of the non-quantized value and quantization noise, as shown by:

$$\begin{aligned} c'_{k,l}(p) &= c_{k,l}(p) + \phi_{k,l}(p) \\ \mathbf{r}'(p) &= \mathbf{r}(p) + \varphi(p) \\ y'_{k,l}(p) &= y_{k,l}(p) + \kappa_{k,l}(p) \\ z'_{k,l}(p) &= z'_{k,l}(p) + \vartheta_{k,l}(p) \\ w'_{k,l}(p) &= w_{k,l}(opt) + \hbar_{k,l}(p) \end{aligned} \tag{3.49}$$

where $\phi_{k,l}(p)$, $\varphi(p)$, $\kappa_{k,l}(p)$ and $\vartheta_{k,l}(p)$ are the noise caused by the operation of quantization of the data. Their elements are assumed to be white sequence, and they are independent of the input signals and each other, with zero mean and variance δ_d^2. $\hbar_{k,l}(p)$ is the zero mean error vector caused by the operation of quantization of the coefficients plus the misadjustment.

As discussed before, the finite precision LMS-MMSE multiuser detector can be considered as an infinite precision LMS-MMSE multiuser detector implemented with insertion of

quantizers in the data path and in the filter coefficients path, then the filter update equation in the finite precision LMS-MMSE MUD can be written following the infinite case. Thus, the coefficients are updated according:

$$w'_{k,l}(p+1) = W'_{k,l}(p) + Q_c\{\mu e'_{k,l}(p)\mathbf{r}'(p)\}. \tag{3.50}$$

and the error $e'_{k,l}(p)$ is given by:

$$e'_{k,l}(p) = d_{k,l}(p) - Q_d[W'^{T}_{k,l}(p)\mathbf{r}'(p)]. \tag{3.51}$$

One should bare in mind that the reference sequence $d_{k,l}(p)$ is already a quantized value, because $d_{k,l}(p)$ is the product of the quantized estimated channel coefficients $c'_{k,l}(p)$ and estimated data symbols $\hat{b}_k(p)$, as shown in Fig. 3.3.

The calculation of the inner product, $Q_d[W'^{T}_{k,l}(p)\mathbf{r}'(p)]$, depends on how the quantization operation is performed [59]. If the quantization operation is performed after the summation of each individual product, which is:

$$Q_d[W'^{T}_{k,l}(p)\mathbf{r}'(p)] = Q_d[\sum_{n=0}^{N-1} w'_{(k,l)}(n,p)\mathbf{r}'(p-n)], \tag{3.52}$$

then the noise added into the inner product $\partial_{k,l}(p)$ has variance δ_d^2. Otherwise, if the quantization has occurred before the summation of each individual product, which is:

$$Q_d[W'^{T}_{k,l}(p)\mathbf{r}'(p)] = \sum_{n=0}^{N-1} Q_d[w'_{(k,l)}(n,p)\mathbf{r}'(p-n)]. \tag{3.53}$$

then the noise added into the inner product has variance $N\delta_d^2$, where N is an integer equal to the number of detector's taps.

In the finite precision LMS-MMSE MUD, the decision variable is formed by the product of the quantized output of the adaptive filter and the quantized channel fading coefficients, therefore, the decision variable can be written mathematically as:

$$z'_k(p) = \sum_{l=1}^{L} c'_{k,l}(p) y'_{k,l}(p). \tag{3.54}$$

Then, the hard decision made by the finite precision LMS-MMSE MUD according to the hard-decision rule is given by:

$$\hat{b}_k(p) = sign(\sum_{l=1}^{L} c'_{k,l}(p) y'_{k,l}(p)). \quad (3.55)$$

3.3.3 Analysis of the Finite Precision LMS-MMSE MUD

The finite precision LMS-MMSE MUD is achieved by reducing the wordlength representing both data and coefficients, and it effectively reduces the power consumption in the digital signal processor. However, the reduction of the wordlength also degrades the performance of the detector. The performance of the finite precision LMS-MMSE MUD is typically characterized by two quantities: the convergence property and the BER. In this section, we consider the convergence property and performance degradation caused by the effects of finite precision. The mean coefficient error analysis of the finite precision LMS-MMSE MUD is considered, weight error covariance and mean square error (MSE) are investigated. In the analysis of mean coefficients error and MSE, the second-order statistical analysis of the real-valued finite-precision LMS algorithm under the assumption of a linear white noise model for the quantization error is performed. Which is referred to as the "standard analysis" [59]. In the analysis of weight error covariance matrix, the nonlinear technique that is presented in [63] is used to provide more accurate predictions. However, in [63], Bermudez and Bershad made the approximation with one less quantizer, since it is not possible to obtain analytical expressions for expectations of nonlinear functions. Bermudez and Bershad have proved that the approximation are identical and the transient behaviors are very similar. Finally, the analysis of the BER of the finite precision LMS-MMSE MUD is presented.

It should be note that when the LMS adaptive algorithm is used in a CDMA detector consisting of adjustable filter coefficients, the sampling rate may be higher or equal to the chip rate, corresponding to the fractionally space (FS) LMS-MMSE MUD and chip-space (CS) LMS-MMSE MUD. In the rest of this chapter, a finite precision chip-space LMS-MMSE MUD will be assumed unless otherwise stated. A more detail presentation of the fractionally space (FS) finite precision LMS-MMSE MUD is presented in chapter 5.

In order to make the analysis of the finite precision LMS –MMSE MUD more tractable, the following assumptions are made [60]:

1. The input data vector $\mathbf{r}(p)$ is independent, Gaussian and over time, the covariance of the input vector is given as:

$$E[\mathbf{r}(p)\mathbf{r}^H(p)] = \mathbf{SCC}^H\mathbf{S}^H + \mathbf{I}\delta_n^2. \tag{3.56}$$

2. The quantization errors of both quantizers Q_d and Q_c are zero mean, white with variances δ_d^2 and δ_c^2.

3. The quantization errors are independent of the input of the quantizers.

4. The step-size μ and the number of bits that are allocated to the data and coefficients by the quantizers satisfies the following conditions:

$$\mu > 0, \quad B_d, B_c \geq 1.. \tag{3.57}$$

5. The reference signal formed by the product of the estimated channel coefficients and data symbols can be expressed as the output of the adaptive filter when the coefficients are optimal plus an additive, zero mean noise $\lambda_{k,l}(p)$, as shown by:

$$d_{k,l}(p) = w_{k,l}^T(0)\mathbf{r}'(p) + \lambda_{k,l}(p). \tag{3.58}$$

In the following the analysis of the mean coefficient error, filter coefficients error covariance matrix, the MSE and the BER for the finite precision LMS-MMSE MUD are based on these assumptions.

3.3.3.1 The Mean Coefficients Error (Mean Convergence) of the Finite Precision LMS-MMSE MUD.

This section investigates the convergence behavior of the finite precision LMS-MMSE MUD. The convergence behavior is of great interest both in practice and in theory, because it determines how long it takes to minimize the MSE, and how many reference symbols are used to train the detector. In [46, 61], the convergence behavior of the infinite precision LMS algorithm has been analyzed.

The analysis of the convergence behavior of the finite precision LMS-MMSE MUD as shown in this section, starts by recalling the finite precision LMS-MMSE MUD update (3.50) and (3.51) which is given again as:

$$w'_{k,l}(p+1) = w'_{k,l}(p) + Q_c\{\mu e'_{k,l}(p)\mathbf{r}'(p)\}. \tag{3.59}$$

and

$$e'_{k,l}(p) = d_{k,l}(p) - Q_u[w'^{T}_{k,l}(p)\mathbf{r}'(p)]. \tag{3.60}$$

Firstly, consider the update equation (3.59), and let $\hbar_{k,l}(p)$ represent the difference between the optimal detector coefficient $w_{k,l}(0)$ and the actual detector coefficient (also see (3.49)):

$$\hbar_{k,l}(p) = w'_{k,l}(p) - w_{k,l}(0). \tag{3.61}$$

Inserting (3.61) into (3.59) yields the detector update equation in a different form, which is given by:

$$\hbar_{k,l}(p+1) = \hbar_{k,l}(p) + Q_c\{\mu e'_{k,l}(p)\mathbf{r}'(p)\}. \tag{3.62}$$

Then, assuming $Q_c\{\mu e'_{k,l}(p)\mathbf{r}'(p)\} = \mu e'_{k,l}(p)\mathbf{r}'(p) + \ell_{k,l}(p)$, where $\ell_{k,l}(p)$ is the quantization noise with zero mean, (3.62) can be written as:

$$\hbar_{k,l}(p+1) = \hbar_{k,l}(p) + \mu e'_{k,l}(p)\mathbf{r}'(p) + \ell_{k,l}(p). \tag{3.63}$$

Secondly, for the error equation (3.60), using assumption (5), the error $e'_{k,l}(p)$ between the reference signal and the output of the filter can be written in a different form as well, as shown by:

$$\begin{aligned} e'_{k,l}(p) &= d_{k,l}(p) - Q_u[w'^{T}_{k,l}(p)\mathbf{r}'(p)] \\ &= w^{T}_{k,l}(0)\mathbf{r}'(p) + \lambda_{k,l}(p) - Q_u[w'^{T}_{k,l}(p)\mathbf{r}'(p)] \end{aligned} \tag{3.64}$$

Assuming the computation of the inner product term $Q_u[W'^{T}_{k,l}(p)\mathbf{r}'(p)]$ is quantized after the summation of each individual product, as shown in (3.52), then (3.64) can be rewritten as:

$$\begin{aligned} e'_{k,l}(p) &= w_{k,l}(opt)\mathbf{r}'^{T}(p) + \lambda_{k,l}(p) - w'^{T}_{k,l}(p)\mathbf{r}'^{T}(p) + \partial_{k,l}(p) \\ &= (w^{T}_{k,l}(opt) - w'^{T}_{k,l}(p))\mathbf{r}'^{T}(p) + \lambda_{k,l}(p) + \partial_{k,l}(p) \\ &= -\hbar_{k,l}(p)\mathbf{r}'^{T}(p) + \lambda_{k,l}(p) + \partial_{k,l}(p) \end{aligned} \tag{3.65}$$

Finally, Substituting (3.65) into (3.63) yields:

$$\begin{aligned} \hbar_{k,l}(p+1) &= \hbar_{k,l}(p) + \mu[-\Delta w'_{k,l}(p)\mathbf{r}'(p) + \lambda_{k,l}(p) + \partial_{k,l}(p)]\mathbf{r}'^{T}(p) + \ell_{k,l}(p) \\ &= (\mathrm{I}-\mu\mathbf{r}'(p)\mathbf{r}'^{T}(p))\,\Delta w'_{k,l}(p) + \mu\lambda_{k,l}(p)\mathbf{r}'^{T} + \mu\partial_{k,l}(p)\mathbf{r}'^{T}(p) + \ell_{k,l}(p) \end{aligned} \tag{3.66}$$

Taking the expectation of (3.66) and using the fact that $\lambda_{k,l}(p)$, $\partial_{k,l}(p)$ and $\ell_{k,l}(p)$ are all of zero mean value yields:

$$E[\hbar_{k,l}(p+1)] = (\mathrm{I}-\mu\mathbf{V}_{\mathbf{r}'\mathbf{r}'^{T}})E[\hbar_{k,l}(p)] \tag{3.67}$$

which is the complete expression for the convergence property of the finite precision LMS-MMSE MUD, where $\mathbf{V}_{\mathbf{r}'\mathbf{r}'^{T}}$ is defined as:

$$\mathbf{V}_{\mathbf{r}'\mathbf{r}'^{T}} = E[\mathbf{r}'(p)\mathbf{r}'^{T}(p)] \tag{3.68}$$

As can be seen from the (3.67), if the step size parameter μ satisfies the following condition:

$$0 < (1-\mu\mathbf{V}_{\mathbf{r}'\mathbf{r}'^{T}}) < 1 \tag{3.69}$$

then the current coefficients error will always be less than the previous coefficients' error, in other words, the filter coefficients will converge to the optimal value.

The convergence of the finite precision LMS-MMSE MUD is analogous to the infinite case. As in the infinite case, the convergence speed is limited by the smallest eigenvalue of $\mathbf{V}_{\mathbf{r}'\mathbf{r}'^{T}}$, and the excess MSE is mainly determined by the biggest eigenvalue of $\mathbf{V}_{\mathbf{r}'\mathbf{r}'^{T}}$ [51]. When the eigenvalues of $\mathbf{V}_{\mathbf{r}'\mathbf{r}'^{T}}$ are widely spread, where the smallest eigenvalue is relatively small, then the (3.69) become:

$$(1-\mu\mathbf{V}_{\mathbf{r}'\mathbf{r}'^{T}}) \Rightarrow 1. \tag{3.70}$$

Therefore, the convergence speed is relatively slow, and the excess MSE is also small. In contrast, if the eigenvalue of $\mathbf{V}_{\mathbf{r}'\mathbf{r}'^{T}}$ is not widely spread, then the convergence speed is relatively fast at the expenses of a larger excess MSE.

The step-size μ is also an important factor that limits the convergence speed of the finite precision LMS-MMSE MUD. If the step-size is too small, then the convergence speed is slow,

however the steady-state coefficients are closer to the optimal value. On the other hand, when the step-size is too large, the convergence speed become faster, but the larger step-size will causes the adaptation process of the coefficients to be unstable.

3.3.3.2 Mean Coefficients Error Covariance Matrix of the Finite Precision LMS-MMSE MUD.

Bermudez and Bershad proposed the nonlinear analysis technique [63], and proved that it gives more accurate predictions. Therefore the analysis in this section is based on the nonlinear technique that is presented in [63]. In the adaptive detectors, the overall MSE at any stage of adaptation is given by [62]:

$$\begin{aligned} MSE &= mse_{\min} + mse_{\text{excess}} \\ &= mse_{\min} + tr[\mathbf{V}\mathbf{M}_h] \end{aligned} \tag{3.71}$$

where $\mathbf{V}$ and $\mathbf{M}_h$ is defined respectively as:

$$\mathbf{V} = E[\mathbf{r}(p)\mathbf{r}^T(p)] \tag{3.72}$$

and

$$\mathbf{M}_h = E[\hbar_{k,l}(p)\hbar^T{}_{k,l}(p)] \tag{3.73}$$

is the coefficients' error covariance matrix. It is clearly seen from (3.71), that in order to derive the expression for the MSE, the solution of the coefficients error covariance matrix must be found first.

In [63], the finite precision LMS adaptive filter has been analyzed, In this section, the finite precision LMS-MMSE is analyzed using the techniques in [63].

The expression for the weight error covariance matrix can be obtained by post-multiplying the update equation of coefficients' error by its transpose and averaging, this yields the expression for the coefficients error covariance matrix, given by:

$$\mathbf{M}_{h(p)} = E[\hbar_{k,l}(p)\hbar^T{}_{k,l}(p)], \tag{3.74}$$

Recalling the update equation of coefficients' error (3.62):

$$\hbar_{k,l}(p+1) = \hbar_{k,l}(p) + Q_c\{\mu e'_{k,l}(p)\mathbf{r}'(p)\}, \tag{3.75}$$

Substituting (3.75) into (3.74) and averaging on the data, yields:

$$\begin{aligned}\mathbf{M}_{\hbar_{k,l}(P+1)} = E\{&[\hbar_{k,l}(p) + Q_c\{\mu e'_{k,l}(p)\mathbf{r}'(p)\}] \\ &[\hbar_{k,l}(p) + Q_c\{\mu e'_{k,l}(p)\mathbf{r}'(p)\}]^T / \hbar_{k,l}(p)\}\end{aligned} \tag{3.76}$$

Writing the filter coefficient in matrix form, so that the subscript k,l can be dropped off, and simplifying (3.76) yields:

$$\begin{aligned}\mathbf{M}_{\hbar(P+1)} = \mathbf{M}_{\hbar(P)} &+ E\{Q_c\{[\mu e'(p)]\mathbf{r}'^T(p)\hbar(p)/\hbar(p)\} \\ &+ E\{Q_c\{[\mu e'(p)]\mathbf{r}'(p)\}\hbar^T(p)/\hbar(p)] \\ &+ E[Q_c\{[\mu^2 e'^2(p)]\mathbf{r}'(p)\mathbf{r}'^T(p)\}/\hbar(p)]\end{aligned} \tag{3.77}$$

Recalling from (3.49) that:

$$\mathbf{r}'(p) = \mathbf{r}(p) + \varphi(p), \tag{3.78}$$

equation (3.77) can be written as:

$$\begin{aligned}\mathbf{M}_{\hbar(P+1)} = \mathbf{M}_{\hbar(P)} &+ E\{\hbar(p)Q_c\{[\mu e'(p)](\mathbf{r}(p) + \varphi(p))^T(p)/\hbar(p)\} \\ &+ E[Q_c\{[\mu e'(p)](\mathbf{r}(p) + \varphi(p))\}\hbar^T(p)/\hbar(p)] \\ &+ E[Q_c\{[\mu^2 e'^2(p)](\mathbf{r}(p) + \varphi(p))(\mathbf{r}(p) + \varphi(p)^T)\}/\hbar(p)]\end{aligned} \tag{3.79}$$

Using the techniques in [63] (see Appendix A) yields the solution of the coefficient' error covariance matrix:

$$\mathbf{M}_{\hbar(p+1)} = \mathbf{M}_{\hbar(p)} - 2\mu A\mathbf{V}\mathbf{M}_{\hbar(p)} + \mu^2\delta_c^2 B\mathbf{V}, \tag{3.80}$$

In the steady state, the following condition is valid:

$$\mathbf{M}_{\hbar(p+1)} \approx \mathbf{M}_{\hbar(p)}, \tag{3.81}$$

therefore, from (3.80) and (3.81):

$$2\mu A\mathbf{V}M_{\hbar(p)} = \mu^2\delta_c^2 B\mathbf{V}, \tag{3.82}$$

Finally, the solution of the coefficient error covariance for the finite precision LMS-MMSE MUD is given by:

$$\mathbf{M}_{\hbar(p)} = \frac{\mu\delta_c^2 B}{2A}, \tag{3.83}$$

where the variables in (3.83) are defined as follows:

$$A = \{1 + \sqrt{\frac{2}{\pi}} \frac{\Delta_C}{\mu\varepsilon_e} e^{\frac{-\Delta_c^2}{8\mu^2\delta_\varepsilon^2}} - erf(\frac{\Delta_c}{\sqrt{2}\varepsilon_e})\},$$

$$B = \left(\frac{\Delta_C}{\mu\varepsilon_e}\right)^2 \left[erf\left(\frac{\Delta_c}{\sqrt{2}\mu\varepsilon_e}\right) - erf\left(\frac{\Delta_c}{2\sqrt{2}\mu\varepsilon_e}\right)\right] + 1 + \sqrt{\frac{2}{\pi}}\left(\frac{\Delta_c}{\mu\varepsilon_e}\right) e^{\frac{-\Delta_c^2}{2\mu^2\varepsilon_e^2}} - erf\left(\frac{\Delta_c}{\sqrt{2}\mu\varepsilon_e}\right),$$

$$\varepsilon_e^2 = mse_{\min} + tr[\mathbf{V}M_{h(p)}].$$

and Δ_c, the granularity of the quantizers, is given by:

$$\Delta_c = 2^{-B_c}, \tag{3.84}$$

The coefficients' error covariance of the finite precision LMS-MMSE MUD is given above. If it is assumed that all the quantization error and granularity are zero, then the coefficients' error covariance of the finite precision LMS-MMSE MUD becomes:

$$\mathbf{M}_{h(p)} = \frac{\mu\delta_\varepsilon^2}{2}, \tag{3.85}$$

3.3.3.3 The Mean Square Error (MSE) of the Finite Precision LMS-MMSE MUD.

The mean square error (MSE) is the most important performance measure for adaptive detectors. The total MSE of the finite precision LMS-MMSE MUD is given by:

$$MSE_k = MSE_{\min,k} + MSE_{exc,k} + MSE_{exc,q}. \tag{3.86}$$

Where $MSE_{exc,q}$ is the excess MSE due to the quantization. From Fig. 3.3, the MSE is the mean square of the difference between the soft output $y'_{k,l}(p)$ and the reference signal $d_{k,l}(p)$. The soft output of the detector $y'_{k,l}(p)$ can be written as:

$$y'_{k,l}(p) = Q_{l}[w'^{T}_{k,l}(p)\mathbf{r}'(p)]. \tag{3.87}$$

Using (3.49), $y'_{k,l}(p)$ becomes:

$$\begin{aligned} y'_{k,l}(p) &= [(w^{T}_{k,l}(p) + \hbar^{T}_{k,l}(p))(\mathbf{r}(p) + \varphi(p))] + \eta_{k,l}(p) \\ &= w^{T}_{k,l}(p)\mathbf{r}(p) + w^{T}_{k,l}(p)\varphi(p) + \hbar^{T}_{k,l}(p)\mathbf{r}(p) + \eta_{k,l}(p) \end{aligned}, \tag{3.88}$$

where $\eta_{k,l}(p)$ is the quantization noise due to the inner product $Q_{l}[w'^{T}_{k,l}(p)\mathbf{r}'(p)]$ and has been defined in Section 3.3.2. The term $\hbar^{T}_{k,l}(p)\varphi(p)$ is ignored in (3.88).

Therefore, the total error is now:

$$\begin{aligned} e'_{k,l}(p) &= d_{k,l}(p) - y'_{k,l}(p) \\ &= \hat{b}_{k}(p)(c_{k,l}(p) + \phi_{k,l}(p)) - [w^{T}_{k,l}(p)\mathbf{r}(p) + w^{T}_{k,l}(p)\varphi(p) \\ &\quad + \hbar^{T}_{k,l}(p)\mathbf{r}(p) + \eta_{k,l}(p)] \\ &= [\hat{b}_{k}(p)c_{k,l}(p) - w^{T}_{k,l}(p)\mathbf{r}(p)] \\ &\quad + [w^{T}_{k,l}(p)\varphi(p) + \hbar^{T}_{k,l}(p)\mathbf{r}(p) + \hat{b}_{k}(p)\phi_{k,l}(p) + \eta_{k,l}(p)] \end{aligned}, \tag{3.89}$$

where the reference signal $d_{k,l}(p)$ is the product of the hard decision of the detector $\hat{b}_{k}(p)$ and the estimated channel coefficients $c_{k,l}(p)$. Squaring both sides of (3.89) and taking the expectation, using the assumptions made in Section 3.3.2, yields the total MSE of the finite precision LMS-MMSE MUD:

$$\begin{aligned} E[|e'_{k,l}(p)|^{2}] &= E[|\hat{b}_{k}(p)c_{k,l}(p) - w^{T}_{k,l}(p)\mathbf{r}(p)|^{2}] \\ &\quad + \mathrm{E}[|w^{T}_{k,l}(p)\varphi_{k,l}(p) + \hbar^{T}_{k,l}(p)\mathbf{r}(p) + \hat{b}_{k}(p)\phi_{k,l}(p) + \eta_{k,l}(p)|^{2}] \end{aligned} \tag{3.90}$$

It should be note that the first term on the right hand side of (3.90) represents the total MSE of the infinite precision LMS-MMSE MUD , which is given by:

$$MSE_{k} = MSE_{\min,k} + MSE_{exc,k}. \tag{3.91}$$

and the second term is the excess MSE due to the quantization.

Under the assumption made before, the quantization error $\varphi_{k,l}(p)$, $\hbar^{T}_{k,l}(p)$, $\phi_{k,l}(p)$ and $\eta_{k,l}(p)$ are independent of the corresponding input of the quantizers, as well as each other, so the terms $w^{T}_{k,l}(p)\varphi_{k,l}(p)$, $\hbar^{T}_{k,l}(p)\mathbf{r}(p)$, and $\eta_{k,l}(p)$ are independent of each other.

Therefore, the second term in (3.90), which is the excess MSE due to the quantization, can be mathematically written as:

$$E[|g'_{k,l}(p)|^2] = E[|w^T_{k,l}(p)\varphi(p)|^2] + E[|\hbar^T_{k,l}(p)\mathbf{r}(p)|^2] + E[|\hat{b}_k(p)\phi_{k,l}(p)|^2] + E[|\eta_{k,l}(p)|^2] \tag{3.92}$$

The MSE of the finite precision LMS-MMSE MUD is analyzed when the coefficients adaptation is in steady state, so it is assumed that the step-size μ is below the upper bound so that the adaptive processing is convergent. In the steady state, the first term on the right hand side of (3.92) has the solution [64]:

$$E[|w^T_{k,l}(p)\varphi(p)|^2] = E[|w^T_{k,l}(p)|^2]\delta^2_{ql} = (|w_{k,l}(opt)|^2 + \frac{1}{2}\mu * mse_{\min} * N)\delta^2_{ql} \tag{3.93}$$

with $\varphi(p)$ representing the quantization noise of input signal $\mathbf{r}(p)$, hence, (3.93) clearly shows how the quantization noise of the input signal affects the total MSE at the output of the adaptive filter.

The third term of (3.92) $E[|\hat{b}_k(p)\phi_{k,l}(p)|^2]$ is the additional noise in the total MSE due to the quantization of the channel coefficient:

$$E[|\hat{b}_k(p)\phi_{k,l}(p)|^2] = E[|\hat{b}_k(p)|^2]\delta^2_{ql} = \delta^2_{ql}. \tag{3.94}$$

The last term in (3.92), denotes the quantization error due to the computation of the inner product $Q_{ql}[w'^T_{k,l}(p)\mathbf{r}'(p)]$, and is always present whether or not the filter coefficients are in steady-state. It has the variance $N\delta^2_{ql}$, where N is an integer representing the number of taps of the adaptive detector.

$$E[|\eta_{k,l}(p)|^2] = N\delta^2_{ql}. \tag{3.95}$$

The second term in (3.92) can be written in a different form:

$$E[|\hbar^T_{k,l}(p)\mathbf{r}(p)|^2] = E\{\hbar_{k,l}(p)\hbar^T_{k,l}(p)|\mathbf{r}(p)|^2\}. \tag{3.96}$$

In the steady state, from (3.74), the above equation can be approximated to:

$$E[|\hbar^T_{k,l}(p)\mathbf{r}(p)|^2] = E\{\mathbf{M}_{h(p)}|\mathbf{r}(p)|^2\} = tr(\mathbf{M}_{h(p)}\mathbf{V}), \tag{3.97}$$

where $\mathbf{M}_{h(p)}$ is the coefficients' error covariance matrix that is given in the previous section (see (3.83)).

The excess MSE due to the quantization operation in the finite precision LMS-MMSE MUD now be written as:

$$MSE_{exc.q} = (|w_{k,l}(0)|^2 + \frac{1}{2}\mu * mse_{\min} * N + 1 + N)\delta_d^2 + tr(\mathbf{M}_{h(p)}\mathbf{V}) \tag{3.98}$$

Therefore, the total steady-state MSE of the finite precision LMS-MMSE MUD is:

$$\begin{aligned} MSE_k &= MSE_{\min,k} + MSE_{exc,k} + MSE_{exc,q} \\ &= MSE_{\min,k} + MSE_{exc,k} + (|w_{k,l}(0)|^2 + \frac{1}{2}\mu * mse_{\min} * N + 1 + N)\delta_d^2 \\ &\quad + tr(M_{h(p)}\mathbf{V}) \end{aligned} \tag{3.99}$$

where $MSE_{\min,k}$ is the optimal MSE of the Wiener filter for the known channel, and $MSE_{excess,k}$ is the excess MSE due to misadjustment, the steady-state value of $\mathbf{M}_{h(p)}$ is given by (3.83). From (3.99), the operation of quantization indeed degrades the performance of the MSE by the two quantization noise terms δ_d^2 and δ_c^2. In the latter part of this chapter, it will be shown from results that the degradation in the performance is caused mainly from the quantization of the coefficients. However, the implementation of the finite precision LMS-MMES MUD has the advantage of reducing the power consumption, therefore, in the next chapter, the relationship between the degradation of the performance and the power consumption in finite precision LMS-MMSE MUD will be investigated.

3.3.3.4 Bit Error Rate (BER) Analysis of the Finite Precision LMS MMSE MUD.

In this section, the BER performance of the finite precision LMS-MMSE MUD is analyzed, taking into account the quantized bit size of both the detector coefficients and data. In this

section, the BER is analyzed by finding out the ratio between the power E and noise variance ∂ in the decision variable of the detector. The BER of the detector can therefore be written as:

$$BER = Q(SNR). \tag{3.100}$$

The received signal of the detector is:

$$\mathbf{r} = \mathbf{SCAb} + \mathbf{n}. \tag{3.101}$$

The quantized received signal $\mathbf{r}'$ passes through the adaptive filter with quantized filter coefficients $w'_{k,l}(p)$, for which the optimal coefficients is (see chapter 3):

$$\mathbf{W}(opt) = \mathbf{S}\left\{\mathbf{SS}^T + E\left(\sigma^2\left(E[\mathbf{CAAC}^H]\right)^{-1}\right)\right\}^{-1}, \tag{3.102}$$

then the output is:

$$y_{k,l}(p) = w'^T{}_{k,l}(p)\mathbf{r}'. \tag{3.103}$$

From Fig. 3.3, the decision variable of the finite precision LMS-MMSE MUD for all the paths can be written as:

$$\begin{aligned} z'_{k,l}(p) &= Q_d[z_{k,l}(p)] \\ &= Q_d[c'_{k,l}(p)y'_{k,l}(p)] \\ &= Q_d\{c'_{k,l}(p)Q_d[w'^T{}_{k,l}(p)\mathbf{r}']\} \end{aligned} \tag{3.104}$$

In Section 3.3.2, the following relations have been defined (see 3.49):

$$\begin{aligned} c'_{k,l}(p) &= c_{k,l}(p) + \phi_{k,l}(p) \\ \mathbf{r}'(p) &= \mathbf{r}(p) + \varphi_{k,l}(p) \\ y'_{k,l}(p) &= y_{k,l}(p) + \kappa_{k,l}(p) \\ z'_{k,l}(p) &= z'_{k,l}(p) + \vartheta_{k,l}(p) \\ w'_{k,l}(p) &= w_{k,l}(opt) + \hbar_{k,l}(p) \end{aligned} \tag{3.105}$$

Therefore, in steady state, the decision variable for the k^{th} user and the l^{th} path of the finite precision LMS-MMSE MUD denoted by $z'_{k,l}(p)$ can be mathematically written as (on condition that $\mathbf{b} = 1$):

$$
\begin{aligned}
z'_{k,l}(p) = {} & c_{k,l}(p)(\mathbf{SCA})w^T_{k,l}(opt) + c_{k,l}(p)\mathbf{n}w^T_{k,l}(opt) \\
& + c_{k,l}(p)(\mathbf{SCA})\hbar^T_{k,l}(p) + c_{k,l}(p)\mathbf{n}\hbar^T_{k,l}(p) \\
& + c_{k,l}(p)\varphi_{k,l}(p)w^T_{k,l}(opt) + c_{k,l}(p)\varphi_{k,l}(p)\hbar^T_{k,l}(p) \\
& + c_{k,l}(p)\kappa_{k,l}(p) + (\mathbf{SCA})w^T_{k,l}(opt)\phi_{k,l}(p) + \phi_{k,l}(p)\mathbf{n}w^T_{k,l}(opt). \\
& + \phi_{k,l}(p)(\mathbf{SCA})\hbar^T_{k,l}(p) + \phi_{k,l}(p)\mathbf{n}\hbar^T_{k,l}(p) \\
& + \phi_{k,l}(p)\varphi_{k,l}(p)w^T_{k,l}(opt) + \phi_{k,l}(p)\varphi_{k,l}(p)\hbar^T_{k,l}(p) \\
& + \phi_{k,l}(p)\kappa_{k,l}(p) + \vartheta_{k,l}(p).
\end{aligned}
\tag{3.106}
$$

In (3.106), the second to last terms all consist of noises terms, and $\mathbf{n}$, $\hbar_{k,l}(p)$, $\varphi_{k,l}(p)$, $\kappa_{k,l}(p)$, $\phi_{k,l}(p)$ and $\vartheta_{k,l}(p)$ are zero mean, independent of each other, and also independent of the corresponding input, hence all the terms in (3.106) are uncorrelated with each other.

Therefore, the mean value of the decision variable is given by the following expression:

$$
\begin{aligned}
\bar{z}'_{k,l}(p) &= E[\bar{z}'_{k,l}(p) \mid \mathbf{b} = 1] \\
&= c_{k,l}(p)\mathbf{SCA}w_{k,l}(opt)
\end{aligned}
\tag{3.107}
$$

and the expression for noise variance of the decision variable is given by the following:

$$
\delta^2_{z'} = E[(z'_{k,l}(p) - \bar{z}'_{k,l}(p))^2 \mid \mathbf{b} = 1]. \tag{3.108}
$$

From appendix B, the noise variance of the decision variable has the solution:

$$
\begin{aligned}
\delta^2_{z'} = {} & c_{k,l}(p)c^T_{k,l}(p)\{M_{h(p)}[(\mathbf{SCA})(\mathbf{SCA})^{-1} + \delta^2_n + \delta^2_d] \\
& + w_{k,l}(opt)w^T_{k,l}(opt)[\delta^2_n + \delta^2_d] + \delta^2_d\} \\
& + M_{h(p)}[\delta^2_d(\mathbf{SCA})(\mathbf{SCA})^{-1} + \delta^2_d\delta^2_n + \delta^2_d\delta^2_d] \\
& + \delta^2_d\{w_{k,l}(opt)w^T_{k,l}(opt)[(\mathbf{SCA})(\mathbf{SCA})^{-1} + \delta^2_d + \delta^2_n] + \delta^2_d\} \\
& + \delta^2_d
\end{aligned}
\tag{3.109}
$$

Thus the signal-to-interference ratio of the decision variable is given by the following expression:

$$
SNR = \frac{\bar{z}'_{k,l}(p)^2}{\delta^2_{z'}}. \tag{3.110}
$$

Finally, the expression for the bit error rate of the finite precision LMS-MMSE MUD is given by the following:

$$BER = Q\{SNR\} = Q\{\frac{\overline{z}'_{k,l}(p)^2}{\delta^2_{z'}}\}. \quad (3.111)$$

3.4 Slowdown Phenomenon

In [59, 65, 66], it was shown that the finite precision LMS adaptive algorithm suffers from a potentially hazardous condition, in which the coefficient update will slowdown. The slowdown was believed to occur when the argument of the coefficient update quantizer in the equation fell into the quantizer's dead zone. Mathematically, this can be expressed as

$$\left|\mathrm{Re}\{\mu e'_{k,l}(p)\mathbf{r}'_{k,l}(p)\}\right| < \frac{\Delta_c}{2}. \quad (3.112)$$

This slowdown phenomenon of the finite precision LMS adaptive algorithm certainly affects the finite precision LMS-MMSE MUD too, since the coefficients update in the finite precision LMS-MMSE MUD is achieved by the LMS algorithm. For most practical case, in order to avoid the slowdown phenomenon, more bits should be allocated to coefficients than to the data [65, 66], this is also applicable to the finite precision LMS-MMSE MUD.

3.5 Results

The following results investigated the performance of the finite precision LMS-MMSE MUD, and the effects of reducing the wordlength that represent both the data and the coefficients. The simulation results are used to confirm the analysis results and techniques used. The performance of the infinite precision LMS-MMSE is also shown alongside the performance curves showing the effects of the quantization. The effects of the quantization of data and coefficients are also shown respectively.

3.5.1 Mean Filter Coefficients Error Covariance Matrix of the Finite Precision LMS-MMSE MUD.

In this simulation, an investigation is carried out into the effects of the finite precision on the mean coefficients error covariance. The step-size parameter u is set to $u = 0.03$. The transmitted signal has:

$$E[\mathbf{r}(p)\mathbf{r}^H(p)] = \mathbf{SCC}^H\mathbf{S}^H + \mathbf{I}\delta_n^2 \tag{3.113}$$

The additive white Gaussian noise (AWGN) has variance:

$$E[|n|^2] = \delta_n^2 = 10^{-8} \tag{3.114}$$

The optimal filter coefficients are given by:

$$\mathbf{W}(opt) = \mathbf{S}\left\{\mathbf{SS}^T + E\left(\sigma^2\left(E[\mathbf{CAAC}^H]\right)^{-1}\right)\right\}^{-1} \tag{3.115}$$

In this simulation, the detector is given 7000 iterations to converge. Fig. 3.4 shows the effects on the mean coefficients error covariance matrix, when the wordlength 8 bits to 16 bits. From this result, the relationship between the coefficients error covariance matrix of the finite precision LMS-MMSE MUD and the wordlength, can be found.

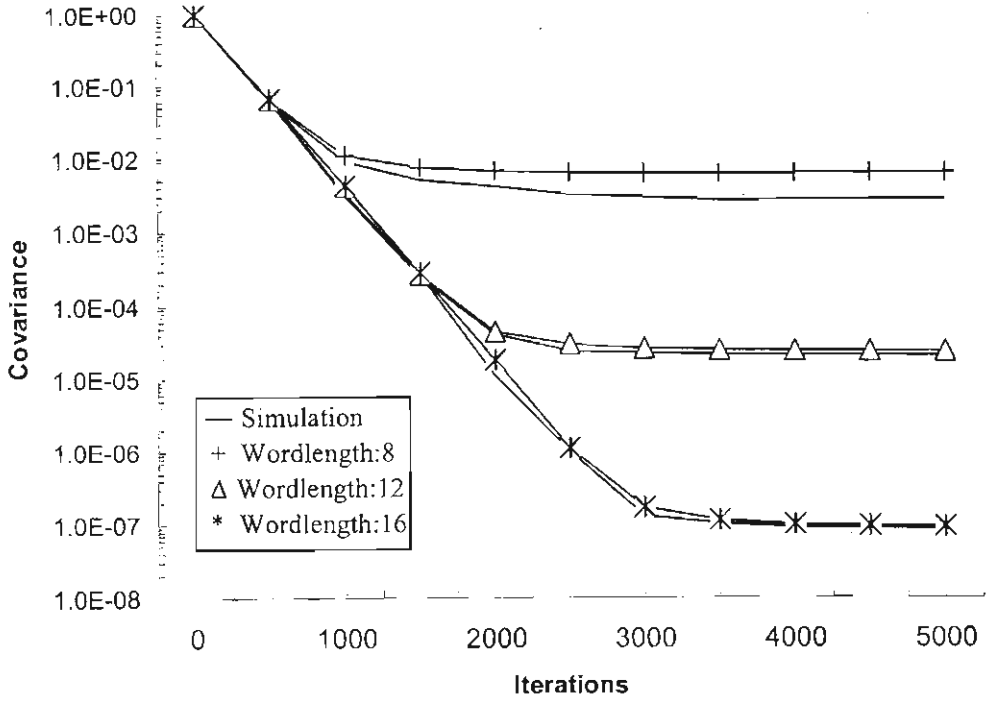

Figure 3.4. The Coefficients Error Covariance Matrix of the Finite Precision LMS MMSE MUD with the Different Wordlength of Bits.

Fig. 3.4 shows the coefficients error covariance matrix of the finite precision LMS-MMSE MUD, versus the different wordlength of data and coefficients. The analytical recursive curve of the covariance matrix is calculated from (3.80), and the analysis results and techniques are verified by comparison with the simulation results. In this simulation, more bits are assigned to the coefficients than to the data, in order to prevent the slowdown phenomenon, and the wordlength is varied from 8 to 16. It is clearly seen that the coefficients error covariance matrix of the finite precision LMS-MMSE MUD is inversely proportional to the wordlength. Also, the analysis results match the simulation results.

3.5.2 Steady-state, Mean Square Error Analysis of the Finite Precision LMS-MMSE MUD.

The MSE is the major performance measurement of the adaptive detector. In this section, the steady-state MSE is calculated using (3.99). It should be noted that when the MSE reaches its steady-state, it becomes a constant value over time. The results of the MSE of the finite precision LMS-MMSE MUD with different numbers of bits used to represent the data and coefficients, is given in Fig. 3.5. The slowdown phenomenon is assumed to not occur in order to investigate the effects of the finite precision of data and coefficients respectively. Fig. 3.6 shows the analysis results of steady-state MSE versus different wordlength of coefficients when the wordlength of data are fixed. In contrast, the analysis results of steady-state MSE versus different wordlength of data is given in Fig. 3.7 when the length of coefficients are fixed.

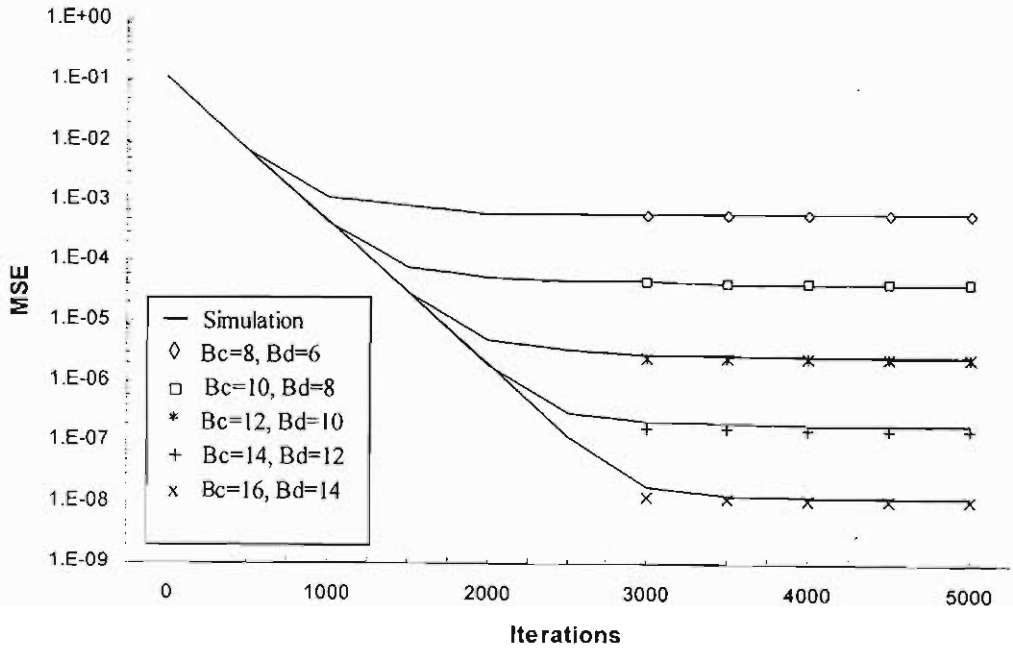

Figure 3.5. The mean square error of the finite precision LMS-MMSE MUD with different length of bits.

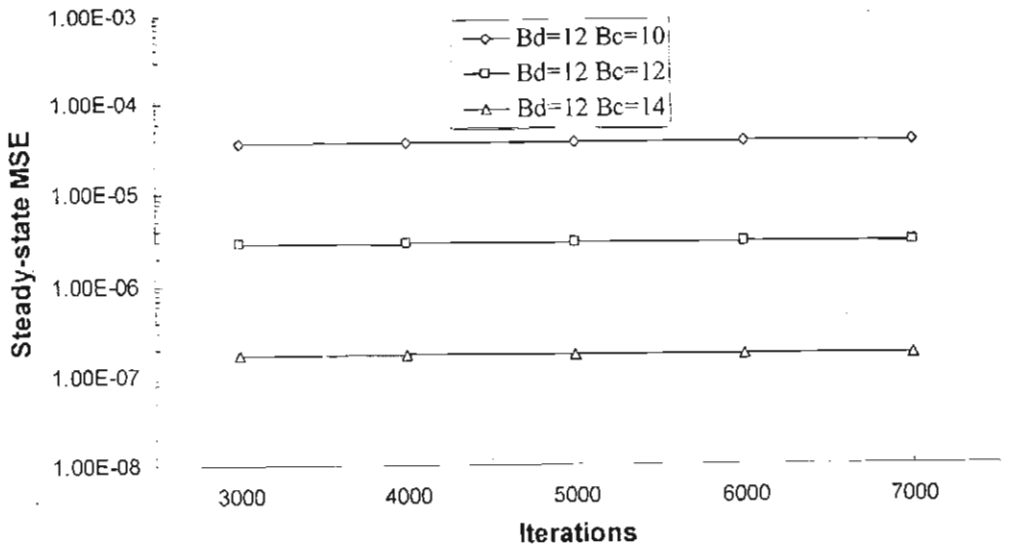

Figure 3.6. The steady-state mean square error with different length of the coefficients when the length of data is fixed.

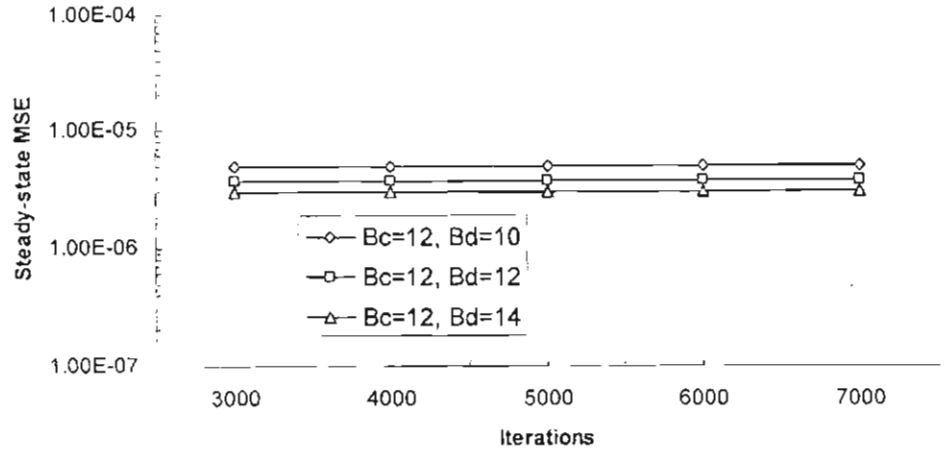

Figure 3.7 The steady-state mean square error with different length of data when the length of the coefficients are fixed.

Fig. 3.5 shows that the MSE of the finite precision LMS-MMSE MUD become worse as the number of bits used to represent the data and coefficients are reduced. The more the number of bits assigned to the data and coefficients, the smaller the MSE obtained. Therefore, from Fig. 3.5, it can be seen that, like the coefficients error covariance, the MSE of the finite

precision LMS-MMSE MUD is inversely proportional to the wordlength of the data and coefficients. In other words, the finite precision implementation degrades the performance of the detector.

In Fig. 3.6, the steady-state MSE performance is investigated when the length of data is fixed to 12 bits. It is clearly seen that as the wordlength of the coefficients increases form 10 to 14, the MSE decreased rapidly from 3.5e-05 to 1.7e-07. However, in contrast, from Fig. 3.7, when the wordlength of the coefficients is fixed to 12, and the wordlength of the data is increased from 10 to 14, the MSE performance is just slightly changed. In the analysis result that shown in Fig. 3.8, the total wordlength is fixed to 28 bits, with different wordlengths assigned to the data and coefficients. In the upper curve, although the wordlength of the data is greater than that in the lower curve, the steady-state MSE performance is still worse than that seen for the lower curve, because the wordlength of the coefficients in the upper curve are less than it in the lower curve. Therefore, it can be seen that the wordlength of the coefficients plays a major role in the MSE performance.

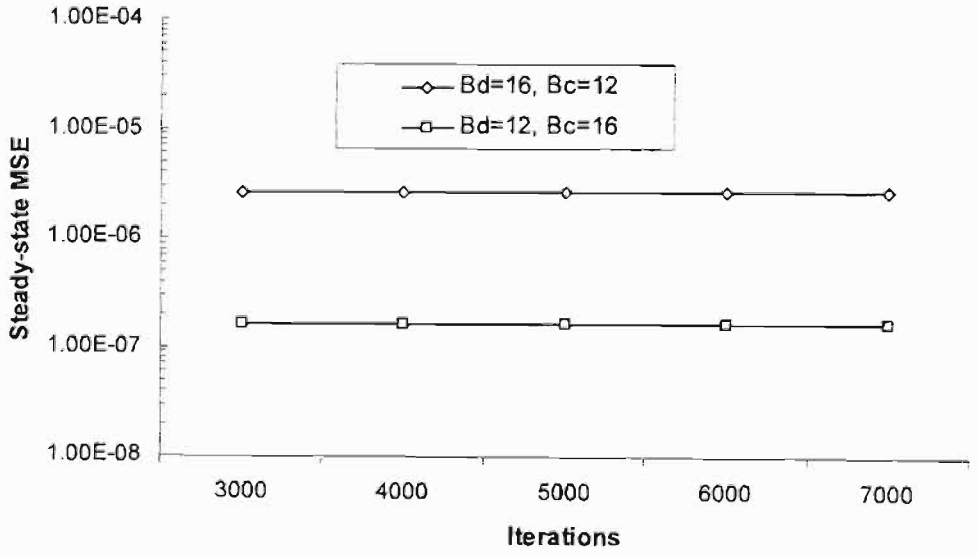

Figure 3.8 The steady-state MSE with the Different bits allocation.

3.5.3 The Bit Error Rate of the Finite precision LMS-MMSE MUD.

The section gives the BER results for the Finite precision LMS-MMSE MUD in both a 3 paths fading channel and non-fading channel. The analysis results are computed by:

$$BER = Q\{SNR\}$$
$$= Q\{\frac{\overline{z}'_{k,l}(p)^2}{\delta_z^2}\} \quad (3.116)$$

The important parameters that are involved in this simulation are given as:

Parameter	Value
Number of user	3
No of chips	31
No of paths	3(fading channel))
Step-size	0.03
Symbol rate	16kbits/s

Table 3.1. The parameters that are involved in the simulation.

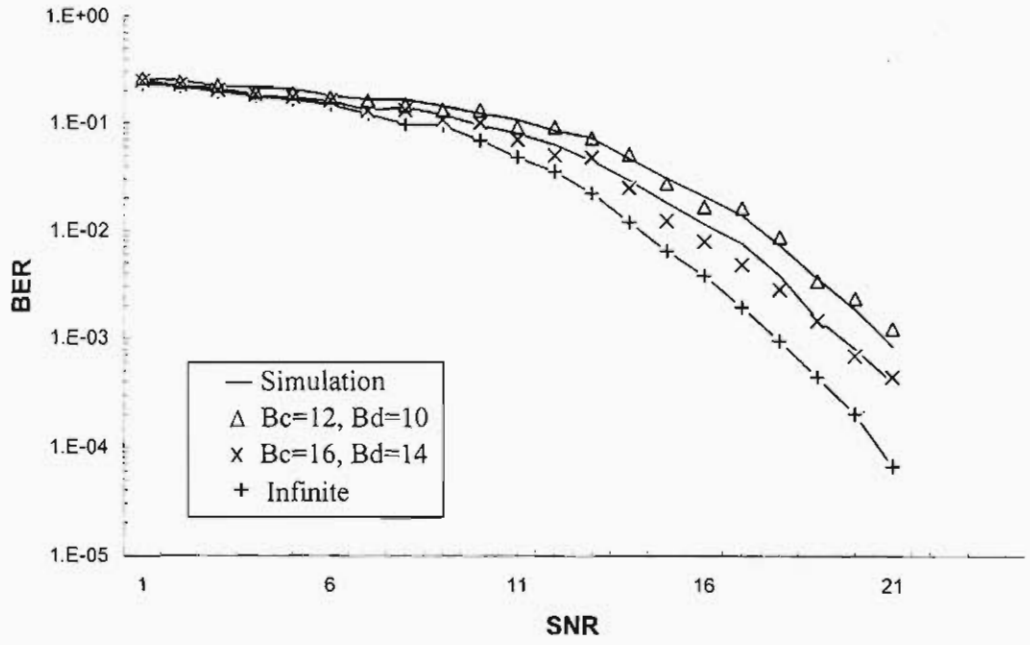

Figure 3.9 BRE for the Finite Precision LMS-MMSE MUD in 3-Path Fading Channel.

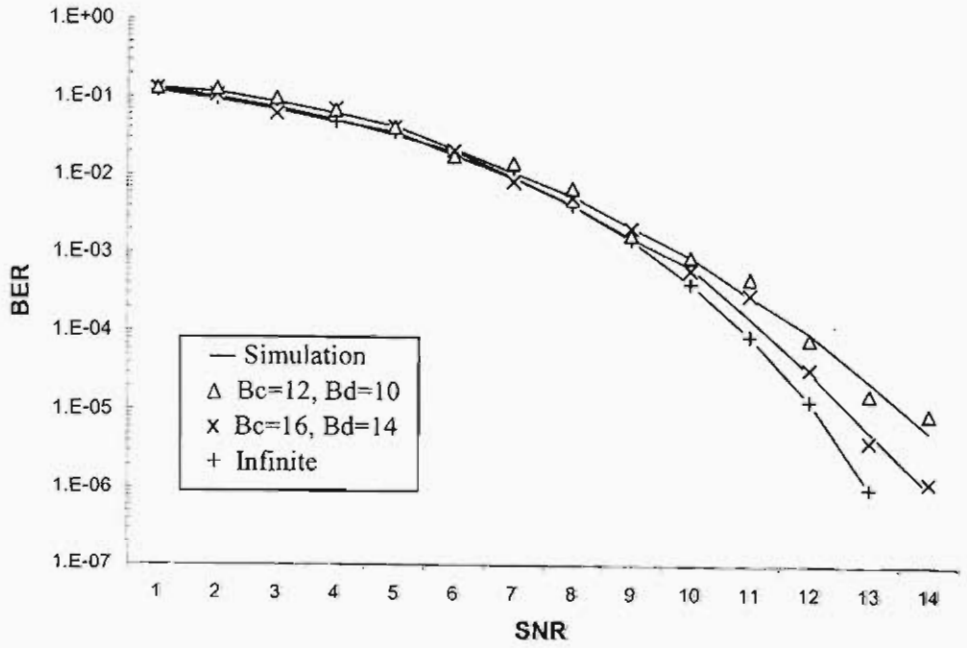

Figure 3.10 BRE for the Finite Precision LMS-MMSE MUD in a Non-fading Channel.

Fig. 3.9 shows the BER of the finite precision LMS-MMSE MUD in a 3 path fading channel with 3 users. As the wordlength increases, the BER performance becomes better, The BER of the infinite precision LMS-MMSE MUD is also presented in Fig. 3.9 to emphasize the effects of the finite precision implementation of the data and coefficients. Furthermore allowing all the non-zero fading coefficients to equal one, results in the BER of the finite precision LMS-MMSE MUD in a non-fading channel, shown in Fig. 3.10.

3.6 Summary

The low power implementation of the DS-CMDA receiver has become an increasingly important aspect in wireless communication system. This chapter presented a low power design technique based on the adaptive LMS-MMSE MUD, which is the finite precision LMS-MMSE MUD, together with the analysis of this detector. The results of analysis are verified by simulation results

In Section 3.2, a brief overview of the adaptive LMS-MMSE MUD is presented. When the detector is implemented in the multipath fading channel, the MMSE MUD can be divided into two categories: pre-combining and post-combining MMSE MUD. The post-combining MUD depends on the channel coefficients of all users and the reference signals have to be adapted as the channel changes, therefore, it has severe tracking problems in a fast fading channel. The pre-combining MMSE MUD assumes that the channel fading coefficients are either known or estimated, and so it only depends on the average channel profiles of the users, therefore, the adaptive implementation of the pre-combining MMSE MUD has significant advantages over that of the post-combining MMSE MUD.

Section 3.3 first presents the system model of the finite precision LMS-MMSE MUD. The finite precision LMS-MMSE MUD can be viewed as an infinite precision LMS-MMSE MUD, implemented with separate uniform scalar quantizers in the data path, and in the filter coefficient path. This obviously degrades the performance of the detector, therefore, in this chapter, the finite precision effects in the mean weight error, mean weight error covariance, the MSE and the BER of the finite precision LMS-MMSE MUD are presented. Finally, the analysis results are presented together with the simulation results.

Reducing the wordlength of bits can reduce the complexity of the detector, resulting in a reduction in power consumption. However through the analysis results, it is easily to seen that reducing the bits can also cause a degradation of the performance. Therefore, there is a tradeoff between the power consumption and performance. In the next chapter, the power consumption in the finite precision LMS-MMSE MUD is presented, furthermore, the optimal bit allocation is also presented through the relationship between the power consumption and the degradation of the performance.

Chapter 4
The Power Consumption in the Finite Precision LMS-MMSE MUD.

4.1 Introduction

Power consumption in the DS-CDMA system has been one of the most important considerations in both system design and implementation. In order to support wireless multimedia services, all CDMA-based systems for third generation systems have a large bandwidth and a high data rate. Therefore, power consumed by the digital signal processor (DSP) increases, because the CDMA receivers have to operate at a higher speed in order to satisfy the requirements of the large spread bandwidth and the high data rate, and this high power consumption leads to lower system capacity.

There have been many digital design strategies to reduce power consumption. Oliver Yuk [67] proposed the technique of using adaptive iteration with variable supply voltage to reduce the power consumption in a turbo code decoder as well as a technique [57] using transformation to reduce power consumption in CDMA receivers. Other design strategies include sign-magnitude arithmetic, reduction of the data rate, and differential encoding of data [57].

Chapter 3 has introduced another technique, that is, the finite precision implementation of the LMS-MMSE MUD, and the performance degradation by the finite precision effects in LMS-MMSE MUD also have been analyzed in chapter 3. In this chapter, the reduction of the power consumption in LMS-MMSE MUD due to finite precision effects is investigated, and the tradeoffs between the performances versus power consumption are also presented.

The rest of the chapter is organized as follows: Section 4.2 presents the derivation of the power consumption in the finite precision LMS-MMSE MUD. The results of the power consumption and power consumption versus performance are presented in Section 4.3. Finally Section 4.4 concludes of this chapter.

4.2 Power Consumption in the Finite Precision LMS-MMSE MUD

This chapter focuses on the power consumption per filter update in the finite precision LMS-MME MUD. The total power consumption per update of the finite precision LMS-MMSE MUD is determined by the power dissipation of the shift, add, multiply and memory store operation [69]. This depends on the specific circuit implementation of the FIR filter and control circuitry. In this chapter, the power is considered consumed by the operations of add, multiply.

Assume that the filter coefficients of the finite precision LMS-MMSE MUD will be updated per N_u bit iterations, where

$$0 < N_u < P. \tag{4.1}$$

and P is the total number of symbols transmitted by each user, as defined in chapter 2. The value of N_u depends on the channel's condition, so if the channel condition is changing quickly, the coefficients may be updated every bit iteration. In the rest of the chapter, we assume N_u =1 (i.e. the filter coefficients are updated per bit iteration).

Firstly, the analysis considered the power consumption by the adaptive filter. Recalling the filter coefficients update formula of the finite precision LMS-MMSE MUD:

$$w'_{k,l}(p+1) = w'_{k,l}(p) + Q_e\{\mu e'_{k,l}(p)\mathbf{r}'(p)\}, \tag{4.2}$$

and

$$e'_{k,l}(p) = d_{k,l}(p) - Q_{el}[w'_{k,l}{}^{T}(p)\mathbf{r}'(p)], \tag{4.3}$$

It can be seen that in (4.3), the computation of the inner product $Q_{el}[W'_{k,l}{}^{T}(p)\mathbf{r}'(p)]$ requires N complex multiplications of B_{el}+1 times, and N-1 complex addition of B_{el}+1 times [60].

The calculation of the error term $e'_{k,l}(p)$ needs a complex addition of B_d+1. Next, substituting the $e'_{k,l}(p)$ into (4.2), and multiply by $\mathbf{r}'(p)$ requires N complex multiplications of B_d+1 times. The addition with $W'_{k,l}(p)$ requires N complex additions of B_c+1 times. Secondly, the channel estimator will requires N complex multiplications of B_d+1 times and $N-1$ complex addition of B_d+1 times. Finally, the calculation of the decision variable $z'_{k,l}(p)=c'_{k,l}(p)y'_{k,l}(p)$ requires complex multiplications of B_d+1 times and complex additions of B_d+1 times. Therefore, in terms of multiplications and additions, there are $(3N+1)(B_d+1)$ complex multiplications, $2N(B_d+1)$ complex additions, and $N(B_c+1)$ complex additions per bit iteration.

In the real implementation of LMS-MMSE MUD, there are $(12N+4)$ multiplications of B_d+1 bits, $8N$ additions of B_d+1 bits, and $4N$ additions of B_c+1 bits per bit iteration. In the each multiplication of B_d+1 bits, the multipliers need three table lookups and one B_d addition. So in the filter coefficients update equation, we have $36N+12$ table lookups, $12N+4$ additions of B_d bits, $8N$ additions of B_d+1 bits, $4N$ additions of B_c+1 bits. In terms of addition, each addition of B bits requires $B-1$ full adders and one half adders, each full adder use 6 logic gates, each half adder use 2 logic gates.

Therefore in the real operation of filter update of the finite precision LMS-MMSE MUD, totally we need $36N+12$ table lookups per bit iteration, and $24[B_d(5N+1)+NB_c+9N+1]$ logic gates per bit iteration. Assume λ represents the power consumption per table lookup per bit, and ω is the power consumption per logic gate [60]. Then the total power consumption per bit iteration can be written as:

$$P_T = \{24[B_d(5N+1)+NB_c+9N+1]\}\omega+(36N+12)B_d\lambda\,. \qquad (4.4)$$

Equation (4.4) shows the relationship between the power consumption and the wordlength of both the data and coefficients, that is, the power consumption decreases when the wordlength is decreased. However, as discussed in the previous chapter, the performance is degraded when the wordlength is decreased. Therefore, in the finite precision LMS-MMSE MUD, low power consumption implementation takes place at the expense of the performance. There is a need for tradeoffs between the power consumption and performance when implementing the finite precision LMS-MMSE MUD, which is shown in the results of the next section.

4.3 Results of Power Consumption versus Performance for the Finite Precision LMS- MMSE MUD

The power consumption of the finite precision LMS-MMSE MUD has been investigated, and it has been show that the power consumption is linear with the number of bits used to represent the data and coefficients. Let the power consumption per table lookup per bit $\lambda = 0.8mW$, and the power consumption per logic gate $\omega = 5mW$. The next two results show how the number of bits that represent the data and coefficients will effect the power consumption respectively.

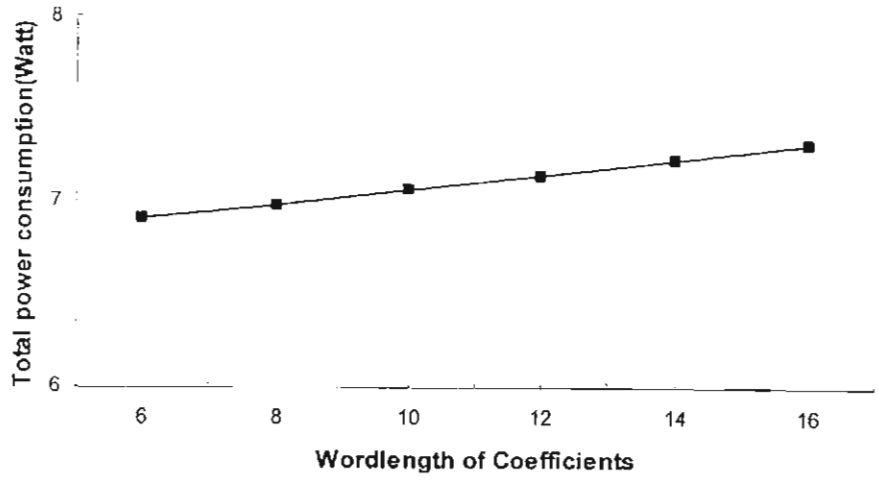

Figure 4.1 The total power consumption versus wordlength of the coefficients when the wordlength of the Data is Fixed (B_d =10).

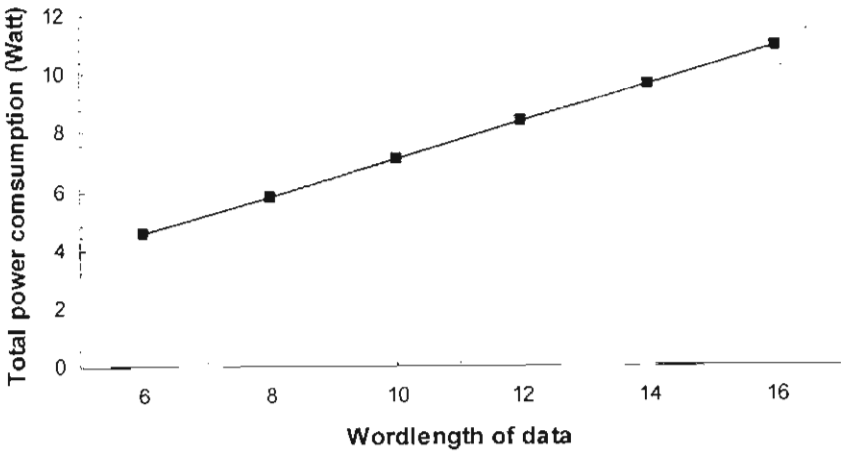

Figure 4.2, The total power consumption versus wordlength of data when the wordlength of the coefficients is fixed (B_c=10).

In Fig. 4.1, the power consumption of the finite precision LMS-MMSE MUD is investigated when the wordlength of data is fixed to 10 bits, and the wordlength of the coefficients are varied from 6 bits to 16 bits. The power consumption is only slightly varies around $7Watt$. In contrast, Fig. 4.2 shows the power consumption of this detector when the wordlength of coefficients are fixed to 10 bits and the wordlength of the data is varied from 6 bits to 16 bits. In this situation, the total power consumption varies from $4.5Watt$ to $10.8Watt$. By comparing the two results, it is easy to conclude that in the finite precision LMS-MMSE MUD, the wordlength of the data is decisive in determining the power consumptions.

As discussed in chapter 3, the reduction of power consumption takes place at the expense of the performance. Fig. 4.3 examines the relationship between power consumption and the MSE performance. The power consumption is investigated when the woldlength is varied from 6-16. We use equation (4.5) to calculate the MSE (see chapter 3). Fig. 4.3 shows the relationship between the power consumption and the steady-state MSE performance.

$$\begin{aligned} MSE_k &= MSE_{\min,k} + MSE_{exc,k} + MSE_{exc,q} \\ &= MSE_{\min,k} + MSE_{exc,k} + (|w_{k,l}(0)|^2 + \frac{1}{2}\mu * mse_{\min} * N + 1 + N)\delta_d^2 \\ &+ tr(M_{R(p)}\mathbf{V}) \end{aligned} \tag{4.5}$$

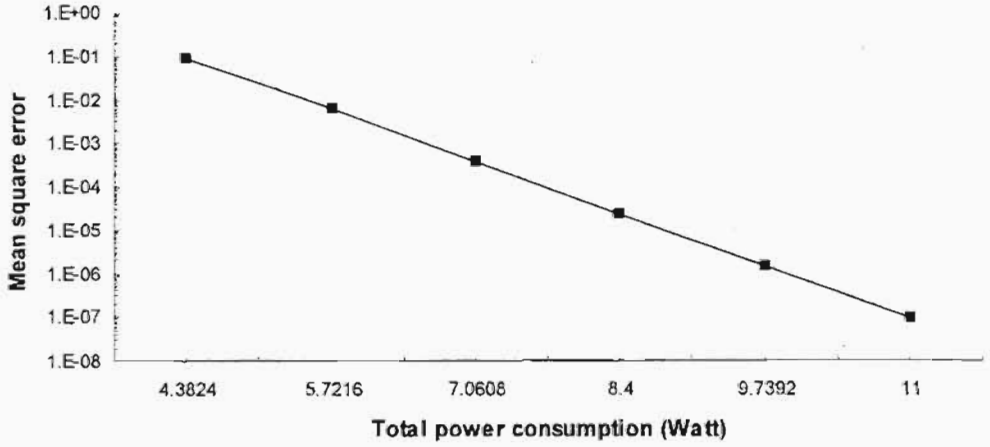

Figure 4.3. The power consumption versus the steady-state MSE performance

It is clearly to been seen that the power consumption is proportional to the performance. The better the MSE performance achieved, the more power is consumed, there is a need for the optimal bit allocation to provide the best performance as well as limit power consumption.

Again using equations (4.4) and (4.5), and the total power consumption in equation (4.4) is constant, it is possible to find the optimal bit allocation of the finite precision LMS-MMSE detector, as shown in Fig. 4.4.

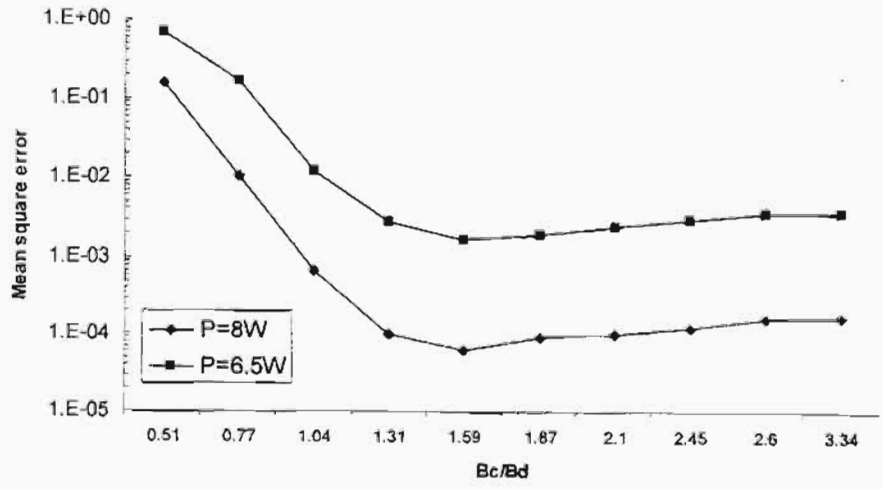

Figure 4.4 The steady-state MSE versus the ration of B_c / B_d under the power constrained.

The results shown in Fig. 4.4 are obtained when the total power consumption is constrained to $6.5Watt$ and $8Watt$. Different values are assigned to B_d and B_c under those constraint power consumptions, then the MSE is calculated using (4.5). When the power consumption is $8Watt$, the performance is better than that when the power consumption is $6.5Watt$. This once again verified the inversely proportional relationship between the power consumption and MSE. Obviously, from the graph, when the wordlength of the coefficient is less than that of data (i.e. the ratio<1), the MSE performance is always worse than when the ratio>1. In other words, in order to achieve better performance, more bits should always be assigned to the coefficients than to the data, and the best MSE performance is achieved when the ratio of B_d / B_c is approximately 1.6.

4.4 Summary

This chapter investigated the relationship between the total power consumption and the performance of the finite precision LMS-MMSE MUD. In section 4.1, a review is presented of the different techniques for the reduction of power consumption in the digital circuit. Section 4.2 presents a derivation of the expression for the total power consumption in the finite precision LMS-MMSE MUD. The results for Power consumption in the finite precision LMS-MMSE MUD, power consumption versus performance and the optimal bit allocation are presented in section 4.3.

Through the study of this chapter, a more general conclusion is that, in the finite precision LMS-MMSE MUD, most power is consumed by the processing of the data. In implementations of the finite precision LMS-MMSE MUD, it is optimal to allocate more bits to the coefficients than to the data, and this can also prevents the slowdown phenomenon that is introduced in the previous chapter.

Chapter 5

The Convergence Analysis of the Finite Precision FS-LMS-MMSE MUD.

5.1 Introduction

In chapter 3, the Finite precision LMS-MMSE MUD with sampling rate equal to chip rate is introduced, and its performance is analyzed. This chapter looks at the convergence analysis of the finite precision LMS-MMSE detector where the sampling rate is higher than the chip rate. This detector is called the finite precision fractionally spaced (FS) LMS-MMSE MUD.

In brief, this chapter consists of: Section 5.2 is an introduction to the FS-LMS-MMSE MUD. The system model of the finite precision FS-MMSE MUD is presented in Section 5.3, while the Section 5.4 presents the analysis of this detector. The results are shown in Section 5.5. Finally, Section 5.6 concludes the chapter.

5.2 The Fractionally Spaced LMS-MMSE Detector

Multiuser detection, especially in the context of the CDMA system, is now established and has become a very popular field of research. A detector that is robust against multiuse interference, by indirect or direct reduction of such interference, is desirable and leads directly to an increase in the system capacity [1].

It should be noted that for all the multiuser detectors discussed in the previous chapters where the sampling rate is equal to the chip rate, the detectors are referred to as "chip spaced (CS) detectors', and are optimal only if the detector is preceded by a filter matched to the channel distorted transmitted pulse [51]. However, when the channel characteristics are unknown, the detector cannot compensate for the channel distortion, therefore, the CS detectors become very sensitive to the choice of the sampling rate.

In contrast to the CS detector, the fractionally space (FS) detector has been developed, where the sampling rate is higher than the chip rate. Let the sampling rate of the FS detector be T_c/M , T_c has been defined before as the chip rate. M is a positive integer, normally M =2, so that the sampling rate of the FS detector is $T_c/2$. The FS detector has the advantage when compared with the CS detector, in that aliasing of the sampled signal is minimized. Another advantage is that the FS detector is less sensitive than the CS detector to the choice of sampling rate.

In the FS-LMS-MMSE detector, the detector coefficients are selected so as to minimize the MSE by the LMS adaptive algorithm, this optimization leads the filter coefficients to its optimal value:

$$\mathbf{W} = \mathbf{a}^{-1}\mathbf{V}, \tag{5.1}$$

where $\mathbf{V}$ is the covariance matrix of the input data:

$$\mathbf{V} = E\left[\mathbf{r}\mathbf{r}^T\right], \tag{5.2}$$

and $\mathbf{a}$ is the vector of the cross correlations of the transmitted data and corresponding input data:

$$\mathbf{a} = E[\mathbf{b}\mathbf{r}]. \tag{5.3}$$

It can be seen that these equations have exactly the same form as those for the CS detector, however there are some subtle differences. In the FS detector, some of the eigenvalues of the covariance matrix are nearly zero [62]. Long et al [71, 72] have made an attempt to exploit this property in the coefficients adjustment to reduce the excess mean square error.

The sampling rate of the FS-LMS-MMSE detector is T_c/M , which is much higher than the chip rate because M is defined as a positive integer. However, all the estimations of the

detector $\hat{b}_k(p)$ of the transmitted data $b_k(p)$ are computed at the symbol rate. Therefore, the detector coefficients must be adjusted at the symbol rate. A possible way to adjust the coefficients at the symbol rate, as well as increase the convergence speed, is investigated by Ling (1987). In this situation, it is necessary to perform the intersymbol interpolation at the receiver, so that a reference signal, from which the error signal is formed, is generated [73].

The focus of this chapter is on the convergence analysis of the finite precision LMS-MMSE tap-weight, when the received signal is sampled at a rate much higher than the chip rate. The results will show that in the FS-LMS-MMSE detector, the convergence performance is better if the initial filter coefficients lie in the signal subspace than that when the initial coefficients lie in the noise subspace.

5.3 The Signal Model of the Finite Precision FS-LMS-MMSE Detector

Once again the received signal can be expressed as (all the notation has been described in chapter 2):

$$\mathbf{r} = \mathbf{SCAB} + \mathbf{n}, \tag{5.4}$$

In the adaptive FS-LMS-MMSE receiver, the baseband received signal $\mathbf{r}(p)$ is sampled at the sampling rate f_s:

$$f_s = T_c / M . \tag{5.5}$$

The sampled received signal is then fed into the adaptive filter, with the optimal filter coefficients (see (3.7)):

$$\mathbf{W} = \mathbf{S}\left\{\mathbf{SS}^T + E\left(\sigma^2 \left(E[\mathbf{CAAC}^H]\right)^{-1}\right)\right\}^{-1} . \tag{5.6}$$

Then the output of the adaptive filter is sampled at the end of each symbol interval and fed into the decision device that yields the hard decisions.

It should be noted that in the finite precision FS-LMS-MMSE detector in practice, the additive noise process is no longer white, therefore, additive noise cannot be modeled as white when the received signal is sampled at a rate much higher than the chip-rate and the over-sampled signal cannot be directly split into the noise and signal subspaces.

In order to avoid this problem, the assumption is made that the matched filter has a magnitude response that is non-zero inside the range $-(1/2T_c) < f < (1/2T_c)$, and zero outside this range. This assumption ensures that the oversampling of the output of the chip-matched filter is equivalent to sampling the chip-matched filter at the chip-rate, followed by interpolation. Fig. 5.1 is a block diagram of the fractionally spaced detector signal model [74, 75].

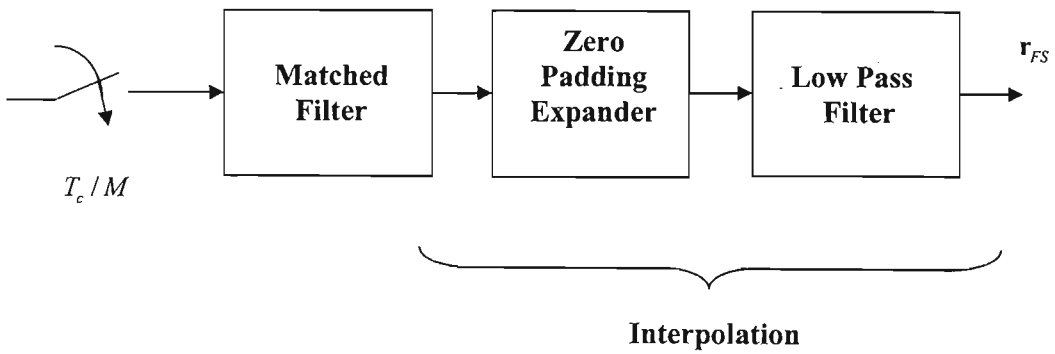

Figure 5.1 Block diagram of the fractionally spaced detector.

As discussed in pervious chapters, the eigenvalue of the input correlation matrix is a major factor affecting the convergence performance of the adaptive detector. For a finite precision LMS-MMSE detector, the correlation matrix of the input is:

$$\mathbf{V}_{r'(FS)} = E[\mathbf{r}_{FS}'(p)\mathbf{r}_{FS}'^{H}(p)], \tag{5.7}$$

where $\mathbf{r}'(p)$ represents the quantized detector input as defined in chapter 3. By using the fact that all the quantization noise terms have zero mean and are independent of each other and the corresponding input, together with the assumption that:

$$\mathbf{r}_{FS}'(p) = \mathbf{r}_{FS}(p) + \varphi(p), \tag{5.8}$$

then (5.7) can be written as:

$$\begin{aligned}\mathbf{V}_{r'(FS)} &= E[\mathbf{r}_{FS}'(p)\mathbf{r}_{FS}'^{H}(p)] \\ &= E[(\mathbf{r}_{FS}(p)+\varphi(p))(\mathbf{r}_{FS}(p)+\varphi(p))^{H}] \\ &= E[\mathbf{r}_{FS}(p)\mathbf{r}_{FS}^{H}(p)]+E[\mathbf{r}_{FS}(p)\varphi^{H}(p)]+E[\varphi(p)\mathbf{r}_{FS}^{H}(p)]+E[\varphi(p)\varphi^{H}(p)] \\ &= \mathbf{V}_{(FS)}+\delta_d^2\end{aligned} \tag{5.9}$$

Therefore, it be seen from (5.9), the input data correlation matrix of the finite precision FS-LMS-MMSE detector $\mathbf{V}_{r'(FS)}$ equal to the input data correlation matrix of the infinite precision FS-LMS-MMSE detector $\mathbf{V}_{(FS)}$ plus quantization noise. In the case of the chip-spaced LMS-MMSE (CS-LMS-MMSE) detector, the solution of the input data correlation matrix $\mathbf{V}$ is easier to derive, because in the CS case, the noise term at the output of the chip matched filter will be uncorrelated, therefore the noise term $\mathbf{n}(p)$ will have a covariance matrix $\delta_n^2\mathbf{I}$ (see chapter 2). The covariance matrix $\mathbf{V}$ for CS case can be written as:

$$\mathbf{V} = E[\mathbf{r}(p)\mathbf{r}^{H}(p)] = \mathbf{S}\mathbf{C}\mathbf{C}^{H}\mathbf{S}^{H}+\mathbf{I}\delta_n^2, \tag{5.10}$$

However, for the FS case, since the noise term is no longer white, the derivation of the $\mathbf{V}_{(FS)}$ become more complicate.

As can be seen from Fig. 5.1, the received signal is fed into a zero padding expander, where the expander adds zeros between consecutive pairs of input samples. Defining the length-$N_{\exp}$ coefficients of the expander as $\mathbf{F}_M$, When M =2, the length-$N_{\exp}$ coefficients of the expander $\mathbf{F}_M$ can be written as [75]:

$$\mathbf{F}_M = \begin{bmatrix} \vdots & & \\ & 1\ 0\ 0 & \\ & 0\ 0\ 0 & \\ \cdots & 0\ 1\ 0 & \cdots \\ & 0\ 0\ 0 & \\ & 0\ 0\ 1 & \\ & \vdots & \end{bmatrix}. \tag{5.11}$$

Then, it is able to write the output of the expander $\mathbf{y}_{\exp}$ is [74]:

$$\mathbf{y}_{\exp} = \mathbf{F}_M \mathbf{r}, \tag{5.12}$$

$\mathbf{y}_{\exp}$ is a vector of expander outputs. It should be noted that $\mathbf{F}_M$ can be infinite dimension if $N_{\exp}$ goes to infinte.

The output of the expander is passed through an ideal lowpass filter (LPF), which has a ideal magnitude response [76]:

$$\left|S(e^{j\omega})\right| = \begin{cases} M, & -\dfrac{\pi}{M} < \omega < \dfrac{\pi}{M} \\ 0, & \text{otherwise.} \end{cases}, \tag{5.13}$$

The resulting output of the lowpass filter, which is the input signal to the adaptive filter in the FS multiuser detector, is:

$$\begin{aligned} \mathbf{r}_{FS} &= \mathbf{S}_M \mathbf{y}_{\exp} \\ &= \mathbf{S}_M \mathbf{F}_M \mathbf{r} \end{aligned}, \tag{5.14}$$

where $\mathbf{S}_M$ is a symmetric Toeplitz matrix. It is clear seen from (5.14), that the input signal of the adaptive filter in the FS detector $\mathbf{r}_{FS}$ and the input signal of the adaptive filter in the CS detector $\mathbf{r}$ are different by a factor $\mathbf{S}_M \mathbf{F}_M$. This factor represents the function of the interpolation. In the rest of the chapter, the function of the interpolation will be denoted by $\mathbf{D}_M$.

Multiplying (5.14) by its transpose and taking the expectation on the product, yields the correlation matrix of $\mathbf{r}_{FS}$, given by:

$$\begin{aligned} \mathbf{V}_{(FS)} &= E[\mathbf{r}_{FS} \mathbf{r}_{FS}{}^H] \\ &= \mathrm{E}[\mathbf{D}_M \mathbf{r}\mathbf{r}^H \mathbf{D}_M{}^H]. \\ &= \mathbf{D}_M \mathbf{R}_{\mathbf{r}} \mathbf{D}_M{}^H \end{aligned} \tag{5.15}$$

It should be noted that $\mathbf{V}$ is Hermitian, and can be expressed as:

$$\mathbf{V} = \mathbf{\Gamma} \mathbf{\Lambda} \mathbf{\Gamma}^H, \tag{5.16}$$

where $\mathbf{\Gamma}$ is a unitary matrix of normalized eigenvectors and $\mathbf{\Lambda}$ is the diagonal matrix of the associated eigenvalues. Therefore, (5.15) can be rewritten as:

$$\begin{aligned}\mathbf{V}_{(FS)} &= \mathbf{D}_M \mathbf{R}_r \mathbf{D}_M{}^H \\ &= \mathbf{D}_M \boldsymbol{\Gamma}\boldsymbol{\Lambda}\boldsymbol{\Gamma}^H \mathbf{D}_M{}^H,\end{aligned} \tag{5.17}$$

In order to derive the complete solution of the correlation matrix $\mathbf{V}_{(FS)}$, the following two theories are introduced [74]:

1. **Theory:** If two vectors $\mathbf{c}_1$ and $\mathbf{c}_2$ are orthogonal (i.e., $\mathbf{c}_1^H \mathbf{c}_2 = \mathbf{c}_2^H \mathbf{c}_1 = 0$), then after interpolating, the result is also orthogonal (i.e. $(\mathbf{D}_M \mathbf{c}_1)^H (\mathbf{D}_M \mathbf{c}_2) = (\mathbf{D}_M \mathbf{c}_2)^H (\mathbf{D}_M \mathbf{c}_1) = 0$).

   Proof: assume that the n^{th} element of $\mathbf{c}_1$ and $\mathbf{c}_2$ be c_1 and c_2, respectively, using Parseval's theory [15] and the orthogonality of $\mathbf{c}_1$ and $\mathbf{c}_2$, yields:

$$\begin{aligned}\mathbf{c}_1^H \mathbf{c}_2 &= \sum_n c_1^*(n) c_2(n) \\ &= \frac{1}{2\pi} \int_{-\pi}^{\pi} C_1^*(e^{j\omega}) C_2(e^{j\omega}) d\omega, \\ &= 0\end{aligned} \tag{5.18}$$

   where $C_1(e^{j\omega})$ and $C_2(e^{j\omega})$ are the Fourier transforms of $c_1(n)$ and $c_1(n)$, respectively. Likewise, the Fourier transforms of $\mathbf{D}_M \mathbf{c}_1$ and $\mathbf{D}_M \mathbf{c}_2$ is:

$$\begin{aligned}\mathbf{D}_M \mathbf{c}_1 &= S(e^{j\omega}) C_1(e^{jM\omega}) \\ \mathbf{D}_M \mathbf{c}_2 &= S(e^{j\omega}) C_2(e^{jM\omega})\end{aligned} \tag{5.19}$$

   Therefore, by using Parseval's theory once again:

$$\begin{aligned}(\mathbf{D}_M \mathbf{c}_1)^H (\mathbf{D}_M \mathbf{c}_2) &= \frac{1}{2\pi} \int_{-\pi}^{\pi} \left|S(e^{j\omega})\right|^2 C_1^*(e^{j\omega}) C_2(e^{jM\omega}) d\omega \\ &= \frac{M^2}{2\pi} \int_{-\pi/M}^{\pi/M} C_1^*(e^{jM\omega}) C_2(e^{jM\omega}) d\omega \\ &= \frac{M}{2\pi} \int_{-\pi}^{\pi} C_1^*(e^{j\omega}) C_2(e^{j\omega}) d\omega \\ &= 0\end{aligned} \tag{5.20}$$

2. **Theory:** If the ideal LPF $S(e^{j\omega})$ has the magnitude response given in (5.13),

then $\|\mathbf{D}_M\mathbf{c}\|^2 = M\|\mathbf{c}\|^2$.

Proof: again using the Parseval's theory:

$$\begin{aligned}\|\mathbf{D}_M\mathbf{c}\|^2 &= \frac{1}{2\pi}\int_{-\pi}^{\pi}\left|S(e^{j\omega})\right|^2\left|C(e^{jM\omega})\right|^2 d\omega \\ &= \frac{M^2}{2\pi}\int_{-\pi/M}^{\pi/M}\left|C(e^{jM\omega})\right|^2 d\omega \\ &= \frac{M^2}{2\pi M}\int_{-\pi}^{\pi}\left|C(e^{jM\omega})\right|^2 d\omega \\ &= M\|\mathbf{c}\|^2\end{aligned} \tag{5.21}$$

In (5.16), the columns of $\mathbf{\Gamma}$ are orthogonal and have unit norm because they are the normalized eigenvalues of a Hermitiam matrix. Therefore, by applying theory 1, after interpolation, the columns of $\mathbf{D}_M\mathbf{\Gamma}$ are also orthogonal.

Theory 2 reveals that the squared norm of each column of $\mathbf{D}_M\mathbf{\Gamma}$ is M. If the $\mathbf{X}$ is selected to be orthogonal to $\mathbf{D}_M\mathbf{\Gamma}$, and satisfy:

$$\mathbf{X}^H\mathbf{X} = \mathbf{I}, \tag{5.22}$$

then the unitary transform of the correlation matrix of the input signal of the adaptive filter in the FS-LMS-MMSE detector is given by the following expression:

$$\mathbf{V}_{(FS)} = [M^{-(1/2)}\mathbf{D}_M\mathbf{\Gamma}\mathbf{X}]\begin{bmatrix} M\mathbf{\Lambda} & 0 \\ 0 & 0 \end{bmatrix}\begin{bmatrix} M^{-(1/2)}\mathbf{\Gamma}^H\mathbf{D}_M^H \\ \mathbf{X}^H \end{bmatrix}, \tag{5.23}$$

Equation (5.23) represents the correlation over-sample matrix of the FS-LMS-MMSE detector. Substituting (5.23) into (5.9) yields the input correlation matrix of the finite precision FS-LMS-MMSE detector:

$$\mathbf{V}_{r(FS)} = [M^{-(1/2)}\mathbf{D}_M\mathbf{\Gamma}\mathbf{X}]\begin{bmatrix} M\mathbf{\Lambda} & 0 \\ 0 & 0 \end{bmatrix}\begin{bmatrix} M^{-(1/2)}\mathbf{\Gamma}^H\mathbf{D}_M^H \\ \mathbf{X}^H \end{bmatrix} + \delta_d^2. \tag{5.24}$$

Expression (5.24) applies to the received signal vector $\mathbf{r}$ spanning all symbols transmitted. However, in practical implementation, the received signal vector is processed in windows, therefore, only an approximate relation can be obtained, given by [71]:

$$\mathbf{y}_{Low} = \bar{D}_M\mathbf{r}, \tag{5.25}$$

where $\bar{D}_M$ is the symmetric Toeplitz matrix, representing the interpolation with finite dimensions.

In order to distinguish the filter coefficient of the FS detector from the filter coefficients of the CS detector, the notation q is defined to represent the filter coefficients of the FS detector. Therefore, the coefficients update equation of the finite precision FS-LMS-MMSE may now be approximately written as:

$$q'_{k,l}(p+1) = q'_{k,l}(p) + Q_c\{\mu e'_{k,l}(p)\mathbf{r}'_{FS}(p)\}, \tag{5.26}$$

where:

$$e'_{k,l}(p) = d_{k,l}(p) - Q_u[q'^{T}_{k,l}(p)\mathbf{r}'_{FS}(p)]. \tag{5.27}$$

5.4 The Analysis of the Finite Precision FS-LMS-MMSE Detector

The analysis of the finite precision LMS-MMSE detector is presented in chapter 3 when the sampling rate is equal to the chip rate. This section presents the analysis of the finite precision LMS-MMSE detector when the sampling rate is higher than the chip rate. The analysis includes the mean coefficients convergence behavior, the steady status coefficients error covariance, and the steady state mean square error.

5.4.1 An Analysis of Mean Coefficients Convergence Behavior the Finite Precision FS-LMS-MMSE Detector

As done in the chapter 3, it can be shown that the mean of the difference between the coefficients computed using the LMS adaptive algorithm and their optimal value, is given by the following equation (see chapter 3):

$$E[\Delta q'_{k,l}(p+1)] = (\mathrm{I}-\mu\mathbf{V}_{r(FS)})E[\Delta q'_{k,l}(p)] \tag{5.28}$$

Substituting (5.24) into (5.28), yields the complete recursive for the mean filter coefficients error of the finite precision FS-LMS-MMSE detector:

$$E[\Delta q'_{k,l}(p+1)] = \left\{ \text{I-}\mu[M^{-(1/2)}\mathbf{D}_M\boldsymbol{\Gamma}\mathbf{X}] \begin{bmatrix} M\boldsymbol{\Lambda} & 0 \\ 0 & 0 \end{bmatrix} \begin{bmatrix} M^{-(1/2)}\boldsymbol{\Gamma}^H\mathbf{D}_M^H \\ \mathbf{X}^H \end{bmatrix} + \delta_n^2 \right\} E[\Delta q'_{k,l}(p)] \quad (5.29)$$

Equation (5.29) can be simplified to [74]:

$$\begin{aligned} E[\Delta q'_{k,l}(p+1)] = {} & M^{-1}\bar{D}_M\boldsymbol{\Gamma}(1-\mu M\boldsymbol{\Lambda})^{p+1}\boldsymbol{\Gamma}^H\bar{D}_M^H\Delta q'_{k,l}(p) \\ & + \mathbf{X}\mathbf{X}^H\Delta q'_{k,l}(p) + \delta_n^2\Delta q'_{k,l}(p) \end{aligned} \quad (5.30)$$

The matrix of the eigenvectors $\boldsymbol{\Gamma}$ can be written as a sum of two orthogonal matrices , which are the signal subspace (denoted by $\mathbf{E}_S$) and the noise subspace (denoted by $\mathbf{E}_n$) matrices, respectively. Therefore, splitting the matrix $\boldsymbol{\Gamma}$ into the signal subspace $\mathbf{E}_S$ and the noise subspace $\mathbf{E}_n$, and assuming that the vector $\Delta q'_{k,l}$ was initially in the signal subspace, (5.30) becomes:

$$\begin{aligned} E[\Delta q'_{k,l}(p+1)] = {} & M^{-1}\bar{D}_M\mathbf{E}_s(1-\mu M\boldsymbol{\Lambda}_s - \mu\delta_n^2 S\mathbf{I})^{p+1}\mathbf{E}_s{}^H\bar{D}_M^H\Delta q'_{k,l}(p) \\ & + \mathbf{X}\mathbf{X}^H\Delta q'_{k,l}(p) + \delta_n^2\Delta q'_{k,l}(p) \end{aligned} \quad (5.31)$$

Where matrix $\boldsymbol{\Lambda}_s$ is defined as:

$$\boldsymbol{\Lambda}_s = diag[s_{k,l}(p)c_{k,l}(p)c_{k,l}^H(p)s_{k,l}^T(p)]. \quad (5.32)$$

From (5.30) and (5.31), the following conclusion about the convergence of the finite precision FS-LMS-MMSE detector can be made:

- If $p \to \infty$, and $|1-\mu M(\lambda_{k,l}+\delta_n^2)| < 1$, then the limit of equation (5.30) as p approaches infinity is:

$$\lim_{p\to\infty} E[\Delta q'_{k,l}(p+1)] = \mathbf{X}\mathbf{X}^H\Delta q'_{k,l}(0). \quad (5.33)$$

  where $\lambda_{k,l}$ is the k^{th} user's l^{th} path's element of the matrix $\mathbf{V}_{\mathbf{r}'(FS)}$. The zero eigenvalues of $\mathbf{V}_{\mathbf{r}'(FS)}$ do not affect the convergence speed of the finite precision FS-LMS-MMSE detector.

- For the MSE of the adaptive filter to converge to it's minimum value, $\Delta q_{k,l}(p)$ should be in the subspace spanned by $\mathbf{X}$.

- The eigenvalues of $\mathbf{V}_{r'(FS)}$ is M times the eigenvalues of matrix $\mathbf{V}_r$. This can be shown as:

$$tr(\mathbf{V}_{r'(FS)}) = Mtr(\mathbf{V}). \tag{5.34}$$

5.4.2 An Analysis of Mean Coefficients Error Covariance of the Finite Precision FS-LMS-MMSE Detector

The coefficient update equation of the finite precision FS-LMS-MMSE detector is given by (5.26). Post-multiplying (5.26) and averaging on the data, yields the mean coefficients error covariance of the finite precision FS-LMS-MMSE detector, which is denoted by $\mathbf{M}_{\Delta q'(P)}$:

$$\begin{aligned}\mathbf{M}_{\Delta q'(P+1)} = E\{&[\Delta q'_{k,l}(p) + Q_c\{\mu e'_{k,l}(p)\mathbf{r}'_{FS}(p)\}] \\ &[\Delta q'_{k,l}(p) + Q_c\{\mu e'_{k,l}(p)\mathbf{r}'_{FS}(p)\}]^T / \Delta q'(p)\}\end{aligned} \tag{5.35}$$

Following the same procedure as in chapter 3, (5.35) can be rewritten as the following expression:

$$\begin{aligned}\mathbf{M}_{\Delta q'(P+1)} = \mathbf{M}_{\Delta q'(P)} &+ E\{\Delta\mathbf{q}'(p)Q_c\{[\mu e'(p)](\mathbf{r}_{FS}(p)+\varphi(p))^T(p)/\Delta\mathbf{q}'(p)\} \\ &+ E[Q_c\{[\mu e'(p)](\mathbf{r}_{FS}(p)+\varphi(p))\}\Delta\mathbf{q}'^T(p)/\Delta\mathbf{q}'(p)] \\ &+ E[Q_c\{[\mu^2 e'^2(p)](\mathbf{r}_{FS}(p)+\varphi(p))(\mathbf{r}_{FS}(p)+\varphi(p)^T)\}/\Delta\mathbf{q}'(p)]\end{aligned} \tag{5.36}$$

Finally, the solution of the detector coefficients error covariance matrix of the finite precision FS-LMS-MMSE detector is (chapter 3):

$$\mathbf{M}_{\Delta q'(P+1)} = \mathbf{M}_{\Delta q'(P)} - 2\mu A\mathbf{V}_{(FS)}\mathbf{M}_{h(P)} + \mu^2\delta_\varepsilon^2 B\mathbf{V}_{(FS)}, \tag{5.37}$$

It should be noted that in steady state, the following condition is valid:

$$\mathbf{M}_{\Delta q'(p+1)} \approx \mathbf{M}_{\Delta q'(p)}, \tag{5.38}$$

Therefore the solution of the coefficient error covariance for the finite precision FS-LMS-MMSE detector is given by:

$$\mathbf{M}_{\Delta q'(p)} = \frac{\mu \delta_\varepsilon^2 B}{2A}, \tag{5.39}$$

where the notations A and B are as defined in chapter 3. Assuming all the quantization error and granularity are zero, the mean coefficients error covariance of the finite precision FS-LMS-MMSE detector can written as follows:

$$\mathbf{M}_{\Delta q'(p)} = \frac{\mu \delta_\varepsilon^2}{2}, \tag{5.40}$$

5.4.3 An Analysis of Mean Square Error of the Finite Precision FS-LMS-MMSE Detector

In the finite precision FS-LMS-MMSE detector, the MSE is the mean square of the difference between the soft output $y'_{k,l}(p)$ and the reference signal $d_{k,l}(p)$. The soft output of the detector $y'_{k,l}(p)$ can be written as:

$$y'_{k,l}(p) = Q_d[q'^T_{k,l}(p)\mathbf{r}'_{FS}(p)]. \tag{5.41}$$

Assuming:

$$\begin{aligned} q'_{k,l}(p) &= q_{k,l}(p) + \hbar_{k,l}(p) \\ \mathbf{r}'_{FS}(p) &= \mathbf{r}_{FS}(p) + \varphi(p) \\ c'_{k,l}(p) &= c_{k,l}(p) + \phi_{k,l}(p) \end{aligned} \tag{5.42}$$

where $\hbar_{k,l}(p)$, $\phi_{k,l}(p)$ and $\varphi(p)$, as defined in chapter 3, are the quantization noise terms due to the quantization of data and coefficients, respectively. Then (5.41) becomes:

$$\begin{aligned} y'_{k,l}(p) &= [(q^T_{k,l}(p) + \hbar^T_{k,l}(p))(\mathbf{r}_{FS}(p) + \varphi(p))] + \eta_{k,l}(p) \\ &= q^T_{k,l}(p)\mathbf{r}_{FS}(p) + q^T_{k,l}(p)\varphi(p) + \hbar^T_{k,l}(p)\mathbf{r}_{FS}(p) + \eta_{k,l}(p) \end{aligned}, \tag{5.43}$$

where $\eta_{k,l}(p)$ is the quantization noise due to the inner product $Q_d[q'^T_{k,l}(p)\mathbf{y}_{low}'(p)]$. The term $\hbar^T_{k,l}(p)\varphi(p)$ is ignored in (5.43). Therefore, the total error now is:

$$\begin{aligned} e'_{k,l}(p) &= d_{k,l}(p) - y'_{k,l}(p) \\ &= \hat{b}_k(p)(c_{k,l}(p) + \phi_{k,l}(p)) - [q^T{}_{k,l}(p)\mathbf{r}_{FS}(p) + q^T{}_{k,l}(p)\varphi(p) \\ &\quad + \hbar^T{}_{k,l}(p)\mathbf{r}_{FS}(p) + \eta_{k,l}(p)] \\ &= [\hat{b}_k(p)c_{k,l}(p) - q^T{}_{k,l}(p)\mathbf{r}_{FS}(p)] \\ &\quad + [q^T{}_{k,l}(p)\varphi(p) + \hbar^T{}_{k,l}(p)\mathbf{r}_{FS}(p) + \hat{b}_k(p)\phi_{k,l}(p) + \eta_{k,l}(p)] \end{aligned} \quad (5.44)$$

where the reference signal $d_{k,l}(p)$ is the product of the hard decision of the detector $\hat{b}_k(p)$ and the estimated channel coefficients $c'_{k,l}(p)$. Squaring both sides of (5.44), and taking the expectation whilst using the fact that all the quantization noise are zero mean, yields the total MSE of the finite precision FS-LMS-MMSE MUD:

$$\begin{aligned} E[|e'_{k,l}(p)|^2] &= E[|\hat{b}_k(p)c_{k,l}(p) - q^T{}_{k,l}(p)\mathbf{r}_{FS}(p)|^2] \\ &\quad + E[|q^T{}_{k,l}(p)\varphi_{k,l}(p) + \hbar^T{}_{k,l}(p)\mathbf{r}_{FS}(p) + \hat{b}_k(p)\phi_{k,l}(p) + \eta_{k,l}(p)|^2] \end{aligned} \quad (5.45)$$

It should be noted that the first term at the right hand side of (5.45) represents the total MSE of the infinite precision FS-LMS-MMSE MUD [56], and the second term is the excess MSE due to the quantization.

Under the assumptions made before, the quantization errors $\varphi_{k,l}(p)$, $\hbar^T{}_{k,l}(p)$ $\phi_{k,l}(p)$ and $\eta_{k,l}(p)$ all have zero mean and are independent of the corresponding input of the quantizers, and each other. So the terms $w^T{}_{k,l}(p)\varphi_{k,l}(p)$, $\hbar^T{}_{k,l}(p)\mathbf{r}(p)$, and $\eta_{k,l}(p)$ are independent of each other. Therefore, the second term in (5.45), which is the excess MSE due to the quantization , can be mathematically written as:

$$\begin{aligned} E[|g'_{k,l}(p)|^2] &= E[|q^T{}_{k,l}(p)\varphi(p)|^2] + E[|\hbar^T{}_{k,l}(p)\mathbf{r}_{FS}(p)|^2] \\ &\quad + E[|\hat{b}_k(p)\phi_{k,l}(p)|^2] + E[|\eta_{k,l}(p)|^2] \end{aligned} \quad (5.46)$$

The MSE of the finite precision FS-LMS-MMSE detector is analyzed when the coefficients adaptation is in steady state, the first term on the right hand side of (5.46) has the solution (see chapter 3):

$$\begin{aligned} E[|q^T{}_{k,l}(p)\varphi(p)|^2] &= E[|q^T{}_{k,l}(p)|^2]\delta_d^2 \\ &= (|q_{k,l}(opt)|^2 + \frac{1}{2}\mu * mse_{\min} * N)\delta_d^2 \end{aligned} \quad (5.47)$$

The third term, $E[|\hat{b}_k(p)\phi_{k,l}(p)|^2]$ of (5.46) is the additional noise in the total MSE, due to the quantization of the channel coefficient:

$$E[|\hat{b}_k(p)\phi_{k,l}(p)|^2] = E[|\hat{b}_k(p)|^2]\delta_d^2 = \delta_d^2 . \tag{5.48}$$

the last term in (5.46) has the solution:

$$E[|\eta_{k,l}(p)|^2] = N\delta_d^2 . \tag{5.49}$$

The second term in (5.46) can be written in a different form:

$$E[|\hbar^T{}_{k,l}(p)\mathbf{r}_{FS}(p)|^2] = E\{[(q'_{k,l}(p) - q_{k,l}(p)]^T[(q'_{k,l}(p) - q_{k,l}(p)]\,|\,\mathbf{r}_{FS}(p)|^2\} . \tag{5.50}$$

In steady state, the above equation can be written as::

$$\begin{aligned} E[|\hbar^T{}_{k,l}(p)\mathbf{r}_{FS}(p)|^2] &= E\{\mathbf{M}_{\Delta q'(p)}\,|\,\mathbf{r}_{FS}(p)|^2\} \\ &= tr(\mathbf{M}_{\Delta q'(p)}\mathbf{V}_{(FS)}) \end{aligned} , \tag{5.51}$$

where $\mathbf{M}_{\Delta q'(p)}$ is the coefficients error covariance matrix, it is given in (5.39).

Now we can write the excess MSE due to the quantization in the finite precision FS-LMS-MMSE MUD with two quantizers from (5.47), (5.48), (5.49) and (5.51):

$$\begin{aligned} MSE_{exc,q} &= E[|g'_{k,l}(p)|^2] \\ &= (|q_{k,l}(0)|^2 + \frac{1}{2}\mu * mse_{\min} * N + 1 + N)\delta_d^2 + tr(\mathbf{M}_{\Delta q'(p)}\mathbf{V}_{(FS)}) \end{aligned} \tag{5.52}$$

where $\mathbf{M}_{\Delta q'(p)}$ and $\mathbf{V}_{(FS)}$ are given by (5.39) and (5.23) respectively. Therefore, the total MSE at the output of the finite precision FS-LMS-MMSE detector can be expressed as:

$$\begin{aligned} MSE_k &= MSE_{\min,k} + MSE_{exc,k} + MSE_{exc,q} \\ &= MSE_{\min,k} + MSE_{exc,k} + (|q_{k,l}(0)|^2 + \frac{1}{2}\mu * mse_{\min} * N + 1 + N)\delta_d^2 \\ &\quad + tr(\frac{\mu\delta_\varepsilon^2 B\mathbf{V}_{(FS)}}{2A}) \end{aligned} \tag{5.53}$$

5.5 Results

In this section, the results of the MSE performance and convergence behavior of the finite precision FS-LMS-MMSE detector are presented. The simulation runs 5000 iterations to allow the coefficient to converge, and asynchronous systems are used with each user transmitting over a single-path non-fading channel, and all other parameters are identical with those in chapter 3.

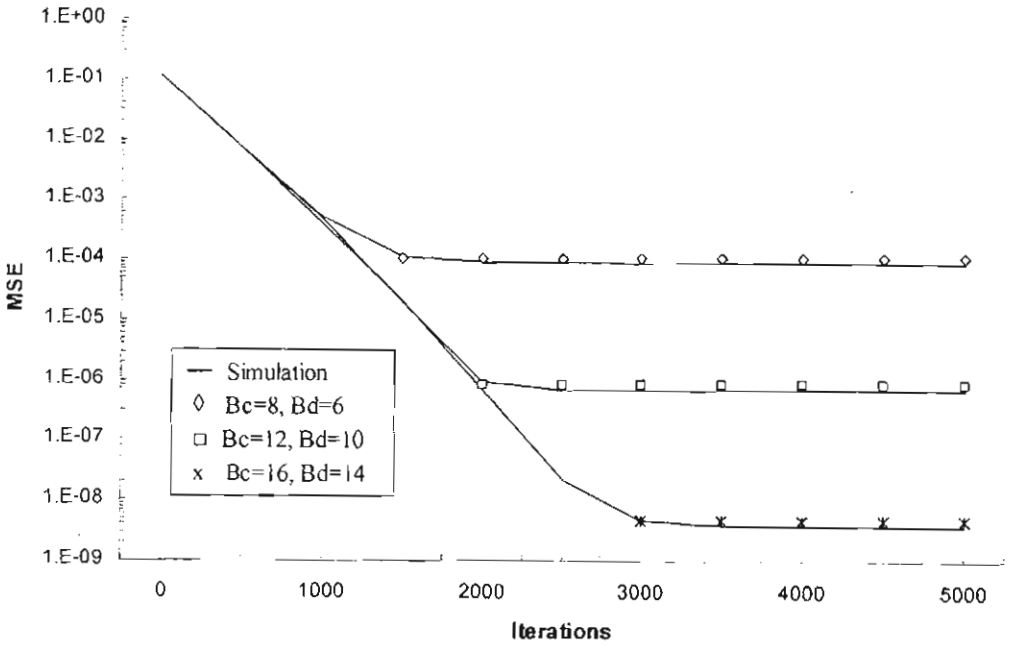

Figure 5.2. The mean square error of the finite precision FS-LMS -MMSE MUD with the different wordlength of bits.

The results of the MSE performance of the finite precision FS-LMS-MMSE detector are shown in Fig. 5.3. Once again, the results show that the performance of the detector is degraded as the wordlengths of the data and coefficients decrease, this is identical to the case of the infinite precision CS-LMS-MMSE detector. However, after comparing the above results with those presented in chapter 3, it is clearly seen that the finite precision FS-LMS-

MMSE detector provides superior performance to that of the finite precision CS-LMS-MMSE detector.

The following results show the convergence behavior of the finite precision FS-LMS-MMSE detector when the initial detector coefficients are initialized into the signal sub-space and when they are randomly initialized. The wordlength of the data and coefficients are set as 10 and 12 respectively. The LMS adaptive algorithm runs 5000 iterations. It can be seen that when the intial coefficients are initialized into the signal sub-space, the convergence speed of the finite precision FS-LMS-MMSE detector is faster than that of the detector where the intial coefficients are randomly selected.

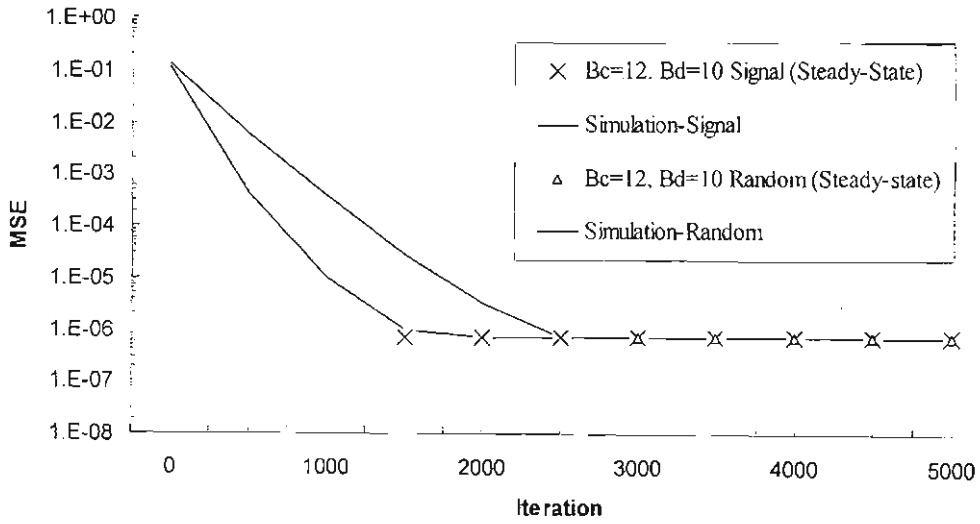

Figure 5.3. The convergence behavior of the finite precision FS-LMS-MMSE detector when the initial detector coefficients are initialized into the signal sub-space and when they are randomly initialized.

5.6 Summary

The chapter analyzed the convergence and performance of the finite precision FS-LMS-MMSE detector. The general conclusion of this chapter is that the finite precision FS-LMS-MMSE detector can achieve better performance than the finite precision CS-LMS-MMSE

detector. Also, when the initial coefficients are initialized into the signal sub-space, the convergence speed of the finite precision FS-LMS-MMSE detector is faster than the convergence speed of the detector that is initialized randomly.

Chapter 6

Summary and Conclusion

6.1 Summary

This thesis considered low power implementation of CDMA receivers, with special focus on the adaptive MMSE detector. The finite precision implementation of the LMS-MMSE multiuser detector is analysed. Its performance and power consumption have been analyzed, and a tradeoff between performance and power consumption of the finite precision LMS-MMSE detector is presented. Chapter 1, which is a briefly introduction of DS-CDMA systems, summarized the thesis layout, motivation and original contribution.

Chapter 2 presents a review of DS-CDMA multiuser detectors. The signal model that is used for DS-CDMA systems was presented, followed by the descriptions of the conventional detector and optimal multiuser detector. Then a family of suboptimal mutliuser detectors in both non-fading and fading channels was reviewed. Those detectors were divided into two classes: linear multiuser detectors and non-linear multiuser detectors. Linear multiuser detectors include the decorrelating detector, the minimum mean square error detector and the polynomial expansion detector. Nonlinear multiuser detectors, which were reviewed in this chapter, are the successive interference cancellation detector, the parallel interference cancellation detector and the decision feedback detector. The adaptive implementation of the multiuser detectors are also presented in this chapter, and the reviews of two most widely used adaptive algorithms, the least mean square algorithm and the recursive least squares algorithm, are also presented.

Chapter 3 focused on the finite precision effects in the LMS-MMSE adaptive multiuser detector. Firstly, the adaptive LMS-MMSE multiuser detector is presented with sampling rate equals to chip rate. Following this, a system model of the finite precision LMS-MMSE multiuser detector was proposed, which is the modified LMS-MMSE multiuser detector with insertion of quantizers into both the data and the coefficients path. The performance of this

detector was analyzed, including the mean coefficients convergence, mean coefficients error covariance, mean square error and bit error rate. The analysis results were presented and verified by the simulation results. The results showed how the finite wordlength affect the mean coefficients error covariance, mean square error and bit error rate, respectively. From the results, it can be seen that the finite wordlength degrade the performance of the detector, the less the wordlength assigned to the data and the coefficients, the poor the performance achieved by the finite precision LMS-MMSE detector. The results also showed that in the finite precision LMS-MMSE multiuse detector, the wordlength of the coefficients plays a major role in determining the performance of the detector.

Chapter 4 investigated the power consumption of the finite precision LMS-MME multiuser detector. The expression of total power consumption was derived and showed that the power consumption is linear with the wordlength. Through the results presented in this chapter, the following conclusions were made: 1) In the finite precision LMS-MMSE multiuser detector, the wordlength of the data is decisive in determining the power consumptions. 2) The performance is proportional to the power consumption. 3) In the implementation of the finite precision LMS-MMSE detector, in order to achieve better performance, more bits should always be assigned to the coefficients than to the data.

Chapter 5 presented the finite precision fractionally spaced (FS) LMS-MMSE multiuser detector, in which the sampling rate is higher than the chip rate. The system model of the finite precision FS-MMSE MUD is presented. Then the performance of this detector is analyzed. The results showed that the finite precision FS-LMS-MMSE detector provides superior performance to that of the finite precision CS-LMS-MMSE detector, in addition to this, when the intial coefficients are initialized into the signal sub-space, the convergence speed of the finite precision FS-LMS-MMSE detector is faster than that of the detector where the intial coefficients are randomly selected.

6.2 Conclusions

Multiuser detectors are currently being researched further, in order to develop a system that can provide good performance as well as low cost. This has drawn more and more attention from researchers and holds much promise for improving the DS-CDMA system and capacity, the research to commercialize multiuser detectors is expecting in the future while DS-

CDMA systems are more widely deployed. In this thesis, the LMS-MMSE multiuser detector implemented with finite wordlength was proposed. The performance and power consumption of the detector due to the finite wordlenth affect have been investigated. The performance measurements used in this thesis includes:

- Mean coefficients convergence.
- Mean coefficients error covariance.
- Mean square error.
- Bit error rate.

From the analysis, the following conclusions were made. 1) The finite wordlength implementation degrades the performance, however, it greatly reduces the power consumption, and performance is proportional to power consumption. 2) In the finite precision LMS-MMSE multiuser detector, the wordlength of the data and coefficients are decisive in determining power consumption and performance. From 1) and 2), it can be seen that there is a need to find the optimal bits combination of the finite precision LMS-MMSE multiuser detector. The thesis showed that the optimal bits combination is that the ratio of B_c to B_d approximate to 1.6.

6.3 Future Works

The further works in low power implementation of CDMA receivers may involve following aspects:

- Performance analysis of the multiuser detectors with the software radio when the finite wordlength effects are present.
- Implement and analyze the lattice based multiuser detectors in the presence of quantization error.
- The comparison of different low power implementation strategies for CDMA systems.